AD-A118 609 PRINCETON UNIV NJ DEPT OF MECHANICAL AND AEROSPACE --ETC F/G 20/4
ROTOR AERODYNAMICS IN GROUND EFFECT AT LOW ADVANCE RATIOS.(U)
JUL 82 H C CURTISS, W F PUTMAN, E J HANKER DAAG29-80-K-0098
UNCLASSIFIED MAE-1571 ARO-16061.2-EG NL

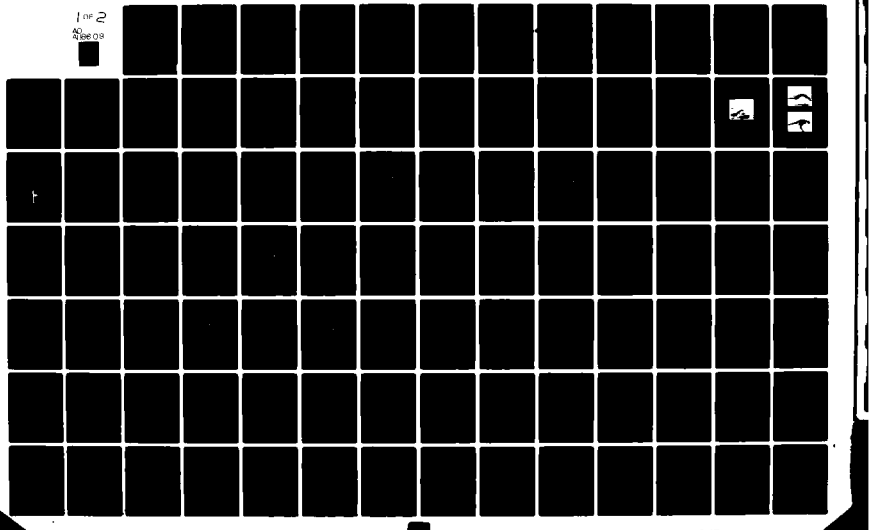

ROTOR AERODYNAMICS IN GROUND EFFECT AT LOW ADVANCE RATIOS

FINAL REPORT

H. C. CURTISS, JR.
W. F. PUTMAN
E. J. HANKER, JR.

JULY 27, 1982

U. S. ARMY RESEARCH OFFICE
GRANT DAAG 29-78-G-0194
CONTRACT DAAG 29-80-K-0098

DEPARTMENT OF MECHANICAL AND AEROSPACE ENGINEERING
PRINCETON UNIVERSITY
PRINCETON, NJ 08544

REPORT NO. 1571-MAE

THE FINDINGS IN THIS REPORT ARE NOT TO BE CONSTRUED AS AN OFFICIAL DEPARTMENT OF THE ARMY POSITION, UNLESS SO DESIGNATED BY OTHER AUTHORIZED DOCUMENTS.

SECURITY CLASSIFICATION OF THIS PAGE (When Data Entered)

REPORT DOCUMENTATION PAGE		READ INSTRUCTIONS BEFORE COMPLETING FORM
1. REPORT NUMBER 1571-MAE	2. GOVT ACCESSION NO. AD-A118609	3. RECIPIENT'S CATALOG NUMBER
4. TITLE (and Subtitle) Rotor Aerodynamics in Ground Effect at Low Advance Ratios		5. TYPE OF REPORT & PERIOD COVERED Final Report 9/10/78 - 2/28/82 6. PERFORMING ORG. REPORT NUMBER 1571-MAE
7. AUTHOR(s) H. C. Curtiss, Jr. W. F. Putman E. J. Hanker, Jr.		8. CONTRACT OR GRANT NUMBER(s) Grant DAAG 29-78-G-0194 Contract DAAG 29-80-K-0098
9. PERFORMING ORGANIZATION NAME AND ADDRESS Department of Mechanical & Aerospace Engineering Princeton University Princeton, NJ 08544		10. PROGRAM ELEMENT, PROJECT, TASK AREA & WORK UNIT NUMBERS N/A
11. CONTROLLING OFFICE NAME AND ADDRESS U. S. Army Research Office Post Office Box 12211 Research Triangle Park, NC 27709		12. REPORT DATE July 27, 1982 13. NUMBER OF PAGES
14. MONITORING AGENCY NAME & ADDRESS(if different from Controlling Office)		15. SECURITY CLASS. (of this report) Unclassified 15a. DECLASSIFICATION/DOWNGRADING SCHEDULE NA

16. DISTRIBUTION STATEMENT (of this Report)

Approved for public release; distribution unlimited.

17. DISTRIBUTION STATEMENT (of the abstract entered in Block 20, if different from Report)

NA

18. SUPPLEMENTARY NOTES

The findings in this report are not to be construed as an official Department of the Army position, unless so designated by other authorized documents.

19. KEY WORDS (Continue on reverse side if necessary and identify by block number)

Helicopters, Helicopter Rotors, Ground Effect, Low Speed Aerodynamics

20. ABSTRACT (Continue on reverse side if necessary and identify by block number)

The results of an experimental study of the aerodynamic characteristics of a helicopter rotor operating in ground effect at low advance ratios are presented. Flow visualization studies were conducted along with measurement of the forces and moments acting on the rotor as a function of advance ratio, height above ground and collective pitch. Steady state experiments as well as non-steady experiments involving translational acceleration were conducted Three distinct flow regimes were noted from the flow visualization studies. At the low end of the advance ratio range a recirculating flow was present,

DD FORM 1 JAN 73 1473 EDITION OF 1 NOV 65 IS OBSOLETE

Unclassified

SECURITY CLASSIFICATION OF THIS PAGE (When Data Entered)

at intermediate advance ratios a horseshoe shaped vortex formed under the rotor, and at the high end of the advance ratio range studied, the rotor wake flows entirely downstream. At test conditions were the recirculating flow or ground vortex is present there are marked departures from classical ground effect theory. Translational acceleration was found to have a significant effect on the rotor forces and moments indicating that some appreciable time is required for the establishment of the ground effect flow field when a recirculating flow or ground vortex exists in the steady state. The results indicate that magnitude of the ground effects experienced by a helicopter are sensitive to the flight path of the helicopter.

FOREWORD

This report presents the results of an experimental investigation of the aerodynamic characteristics of an isolated rotor operating in ground effect at low advance ratios. Rotor forces and moments were measured as a function of height-to-diameter ratio, advance ratio, collective pitch and horizontal acceleration. In addition, flow visualization studies were conducted to assist in understanding the complex flow field that was found to exist under the rotor at these low forward speeds.

These experiments were conducted in a unique facility, the Princeton Dynamic Model Track in which the model is mounted on a carriage/track system and moved through still air. Proper simulation of the flow boundary conditions equivalent to helicopter flight over the ground is thus achieved in this facility. Furthermore, the influence of acceleration and deceleration on the rotor forces and moments can be studied.

This final report presents all of the experimental data taken in the course of the investigation along with a discussion of some of the important experimental results.

TABLE OF CONTENTS

LIST OF ILLUSTRATIONS

LIST OF TABLES

NOMENCLATURE

a	rotor blade two-dimensional lift curve slope
a_x	translational acceleration, g
b	number of blades
c	blade chord, ft
C_m, C_l, C_Q	hub moment coefficients, torque coefficient, $\frac{M_H,\ L_H,\ Q}{\rho\pi R^2(\Omega R)^2 R}$
C_Y, C_H, C_T	rotor force coefficients $\frac{H,T,Y}{\rho\pi R^2(\Omega R)^2}$
$\bar{h}$	height of rotor above ground divided by rotor diamet
H	rotor in-plane force, shaft axes, positive downstream
I_b	blade flapping moment of inertia, slug ft^2
L_H	rotor hub rolling moment, positive right roll, ft-lb
M_H	rotor hub pitching moment, positive nose-up, ft-lb
p	ratio of lowest natural frequency of blade in flapping to rotor angular velocity at operating RPM
Q	rotor torque, ft-lb
R	rotor radius, ft
T	rotor thrust, shaft axes, lb
V	rotor translational velocity, fps
Y	rotor side force, shaft axes, positive to the right
γ	Lock number, $\frac{\rho acR^4}{I_b}$
θ_c	rotor collective pitch at three-quarters radius, deg

μ	rotor advance ratio, $\frac{V}{\Omega R}$
μ^*	normalized advance ratio, $\mu/\sqrt{\frac{C_T}{2}}$
ρ	air density, slugs per cubic ft
σ	rotor solidity, $\frac{bc}{\pi R}$
Ω	rotor angular velocity, rad per sec

INTRODUCTION

It has been known for some time that when a lifting rotor is operated close to the ground at low speeds, the rotor wake is highly distorted by the presence of the ground. Close to the ground, the rotor wake rather than entirely flowing downstream splits and a portion of the rotor wake flows forward (upstream) and then recirculates through the rotor or forms a vortex or roughly horseshoe shape under the rotor depending upon the rotor operating condition. This experimental investigation was undertaken with the objective of providing experimental data on the forces and moments on a rotor operation in conditions where the recirculating flow or ground vortex is present. Previous investigations have shown that the presence of this complex flow field can have a significant influence on the behavior of helicopters flying near the ground.[1,2]

The investigations performed included extensive flow visualization studies over the advance ratio range from 0 to 0.1 at height-to-diameter ratios of 0.23, 0.34, and 0.45, at two collective pitch settings. The six rotor forces and moments were measured through this range of test variables. It was expected that horizontal acceleration might also influence the rotor forces and moments and so experiments were also conducted to examine the influence of low levels of translational acceleration and deceleration.

This report presents all of the experimental data taken during the course of the program. Reference 3 describes some of the results of the investigation.

The model rotor characteristics are listed in Table I. A four-bladed hingless rotor with an eight-foot diameter was used for the experiments. The cross section of the test facility is shown in Figure 1 and a photograph of the model installed in the test facility is shown in Figure 2. The building enclosing the carriage/track system is 30 feet by 30 feet in cross section so there should be little effect of the enclosure on the experimental results.

Test conditions investigated are listed in Table II. Rotor collective pitch was chosen such that nominal thrust coefficient-solidity ratios are characteristic of contemporary helicopters. Rotor cyclic pitch was maintained constant at a value such that the rotor hub pitching moment was zero in the middle of the advance ratio range investigated.

The method of conducting the tests involved first setting the rotor collective pitch, cyclic pitch and angular velocity to desired values. Then the model velocity was set by controls on the carriage. Two types of experiments were conducted. One series involved running the model at constant translational velocity and in the other set the carriage was programmed to accelerate or decelerate the model at various rates from some selected initial velocity to a selected final velocity. This latter method is considerably more efficient in terms of data production than the former method since one run produces a continuous trace showing the dependence of the forces and moments on velocity. Preliminary experiments in this program as well as past experience in related experiments conducted in this facility indicated that the acceleration method of testing produces essentially quasi-static

data if the acceleration values are small enough. That is, at a given velocity during a run with a low level of acceleration it was expected that the forces and moments would be the same as obtained during a constant velocity run. However, in the course of this test program it was discovered that even very low values of acceleration of the order of 0.01g's produced significant changes in the rotor forces and moments compared to the forces and moments at the same steady velocity without acceleration. Note that the shaft angle of attack is zero so that the effects shown are directly the influence of translational acceleration.

The effect of acceleration is discussed more fully later in this report. In examining the data presented it should be kept in mind that acceleration is shown to be an important parameter in determining the magnitude of the ground effect.

This result implies that the nature of the ground effect experienced by a helicopter will depend upon the flight path and not just on the instantaneous values of the motion variables.

The dependence of the results on low values of acceleration in general indicates that some appreciable time is associated with the development of a fully established ground effect flow field.

RESULTS

Flow Visualization

Smoke was emitted from a series of probes located upstream of the rotor as shown in Figures 1 and 2. The flow patterns were recorded with a movie camera and a video camera. Detailed examination of video tapes of the flow field indicated the presence of three distinct flow regimes. At the highest advance ratios investigated the entire rotor wake moved downstream. At intermediate advance ratios a ground vortex was present under the rotor as illustrated by the photograph in Figure 3. In the low advance ratio range the flow field is better described as a recirculating flow. Figure 4 shows a typical flow pattern in this regime. The recirculating regime was characterized by considerable unsteadiness at times appearing somewhat like the vortex ring state encountered in vertical descent over the upstream half of the rotor. There were only small lateral flow components in this regime with the smoke tending to remain in the vertical plane in which it was emitted. Moving the probe off the centerline of the rotor indicated little or no recirculation in vertical planes away from the centerline.

In the advance ratio range where the ground vortex was present the flow appeared to be considerably steadier and there was significant lateral flow with a well defined horseshoe vortex under the rotor similar to that shown in Reference 2. Based on analysis of the flow visualization data, the occurrance of these flow regimes chould be characterized by the parameter

$$\mu^* = \mu/\sqrt{\frac{C_T}{2}}$$

as shown in Figure 5. The physical significance of the parameter μ^* is that it determines the ratio of the forward speed to the momentum value of the induced velocity and also can be thought of as characterizing the rotor wake angle out of ground effect.

Note that the gound vortex flow regime only exists over a rather narrow speed range and in the large part of the range, a recirculating flow is present. The shaded area in the low speed portion of the graph indicates that there always appeared to be some amount of recirculation present at the low speeds, however the recirculating flow was well-defined as shown for example in Figure 4 only in the rather narrow regime indicated.

Rotor Forces and Moments

The experimental results are presented in Appendix A for the majority of parameters investigated. Rotor force and moment coefficients are presented as functions of height-to-diameter ratio, collective pitch, and translational acceleration. Selected data comparisons are presented and discussed in this section. Only the hub moment coefficients, thrust and torque are discussed. The rotor inplane and axial force measurements are presented in Appendix A. These forces are small and not particularly influenced by the presence of the ground. This discussion concentrates on the effects of acceleration which were only briefly described in Reference 3. Initial experiments indicated that if the translational acceleration of the model was low enough then the experimental results were not dependent

upon acceleration. However careful examination of the data upon completion of the experimental test program indicated that even the lowest value of acceleration ($\approx$ 0.01g's) investigated had a significant effect on the rotor forces and moments in ground effect. The effects of acceleration are largest at the lowest height-to-diameter ratio and largest collective pitch and diminish with reduced collective pitch and increased height-to-diameter ratio.

First consider the effects of acceleration. The largest effect of acceleration and deceleration was measured at the lowest height to diameter ratio. Figure 6 shows the effect of a low level of acceleration and deceleration on the pitching moment, rolling moment, thrust and torque variation with advance ratio. The effect of acceleration is particularly significant in the pitching moment and thrust variations. A large hysteresis loop appears in the pitching moment curves and the minimum value of the thrust occurs at quite different advance ratios depending upon whether the rotor was accelerated or decelerated through the speed range. The torque and rolling moment show less sensitivity to acceleration due in part to the fact that they do not vary appreciably with advance ratio.

The decelerating case involves starting the run at an advance ratio $\mu \approx 0.065$. The translational velocity is reduced at the rate of 0.01g's to an advance ratio of $\mu \approx 0.02$. The accelerating run is just the reverse starting at $\mu = 0.02$ and increasing to $\mu = 0.065$ at an acceleration of 0.01g's. In the decelerating case, the *minimum* thrust occurs at an advance ratio of $\mu \approx 0.035$ while in the accelerating case it occurs at $\mu \approx 0.047$.

The measured decrease in thrust physically must be due to increased downward flow through the rotor due to the recirculation/ground vortex flow and the trends shown in the data indicate that some time is involved in

establishing this downward flow due to the ground vortex. This does not seem surprising since it appears physically that the ground vortex flow must represent a piling up of the rotor tip vortices. Order of magnitude considerations presented in Reference 3 indicates that the strength of the ground vortex is the order of the sum of all of the vorticity in the rotor wake from the rotor to the ground. The establishment of this strong vortex requires a time of the order of the rotor height divided by the average induced velocity.

The process by which the flow field is established is undoubtedly more complex since the forward moving portion of the wake passing over the ground will produce vortices of opposite sign. In fact, preliminary theoretical calculations indicate that some mechanism such as the presence of a ground boundary layer produced by the upstream flow is required to produce a flow-field such as observed from the flow visualization experiments.

Note that at a given acceleration level the experimental results are very repeatible. Figures A-7 and A-8 (Appendix A) show the comparison of a number of runs in this test condition with the same values of translational acceleration and deceleration.

The effects of this low value of acceleration become weaker as the collective pitch is reduced and the height-to-diameter ratio is increased as shown in Figure 7 for example. Also included in this figure are data points taken at constant speed indicating only that the effects of translational acceleration have become small in this case.

Figures 8 through 10 show the effects of increasing levels of acceleration and deceleration at the intermediate height-to-diameter ratio. Again the effects are particularly evident in pitching moment and thrust. An increasing size hysteresis loop is noted in pitching moment. Comparing the thrust variations with advance ratio in these three cases it can be seen that as the acceleration level is increased, the average thrust is increased indicating less down flow through the rotor showing that the ground vortex/recirculating flow does not have time to become fully established.

Figures 11 through 14 show comparisons of the effect of acceleration and deceleration directly. The largest effects are seen in Figure 12. Note in particular the thrust variation. At the lowest acceleration (.007g's) there is a sharp decrease in thrust at an advance ratio $\mu \cong 0.047$. This decrease must be due to a strong downflow through the rotor. As the acceleration level is increased the decrease becomes smaller and smaller. Similar effects can be seen in the other figures.

These results indicate that in conditions where the effect of the presence of the ground on a helicopter rotor is strong and in the steady state where there would be a ground vortex or recirculating flow present, if the helicopter is accelerating or decelerating the full severity of the effect may not be felt.

These data also indicate that rather sudden changes in pitching moment occur at advance ratios of the order of 0.05 indicating that sudden control motions will be required to keep the helicopter in equilibrium flight. Similar effects were noted in Reference I although they appeared primarily in the rolling moment. In the experiments reported here the sudden change occurs in the pitching moment characteristic rather than the rolling moment due to the higher flapping stiffness of this rotor.

We now consider some of the other effects shown in the experimental data. All of these comparisons are made at the same value of translational acceleration.

Reducing height-to-diameter ratio of course increases the influence of the presence of the ground resulting in reduced pitching moments and smaller changes in rolling moment. Whether the effects of the presence of the ground show up primarily in pitching moment or rolling moment depend largely on the rotor blade flap stiffness. It would be expected that the presence of the ground would primarily cause a variation in induced velocity along the longitudinal axis of the rotor, so that rolling moment changes would be most significant on low stiffness rotors. As the flap stiffness is increased the effects would tend to show up in the pitching moment. A method is given in Reference 3 for interpreting experimental results at other values of rotor stiffness.

The thrust increases with reduced height to diameter ratio at advance ratios above $\mu \approx 0.04$. Below this advance ratio the general trends are less clear and the effect of height-to-diameter becomes weaker. There are generally small effect on torque coefficient, which does not vary strongly either with advance ratio or height-to-diameter ratio. Recall that these data are presented for a given collective pitch so that a decreasing thrust coefficient at approximately constant torque coefficient would imply that for a helicopter in flight power would have to be increased to maintain equilibrium flight.

Now consider the effects of collective pitch as shown in Figures 15 through 17. At a given height-to-diameter ratio increasing the collective

pitch clearly increases the severity of the ground effect except at the highest height-to-diameter ratio. The irregular variation of the pitching moment and the decrease in thrust occur at lower advance ratios when the collective pitch is reduced indicating that the data is roughly scaling like

$$\mu/\sqrt{\frac{C_T}{2}}$$

It should be noted that these experimental results indicate clearly that the severe effects of ground proximity as caused by the ground vortex/ recirculating flow are fundamentally dependent upon collective pitch and not disc loading as indicated for example in Reference 1. Note that in fact in Reference 1 variations in disc loading are obtained by varying collective pitch. The nominal disc loading of the rotor employed in these experiments is 0.7 psf. Very similar phenomena to that noted in Reference 1 are found in these experimental results. Direct quantitative comparison are difficult to make due to differences in the rotor characteristics.

Table I. Model Rotor Characteristics

R	Radius	4 ft
b	Number of Blades	4
σ	Solidity	.066
γ	Lock Number	6.63
p	Flap Frequency Ratio	1.33 per rev
ΩR	Tip Speed	189 fps
ϕ_B	Flap/Cyclic Phase Lag	35^o
	Twist (linear)	-8^o

Table II. Test Conditions

μ	Advance Ratio	0 to 0.1
$\bar{h}$	Rotor Height to Diameter	.23, .34, .45
θ_c	Collective Pitch at .75 Radius	8^o, 10^o
α_s	Shaft Angle of Attack	0^o
a_x	Translational Acceleration	.01, .05, 0.1(g)

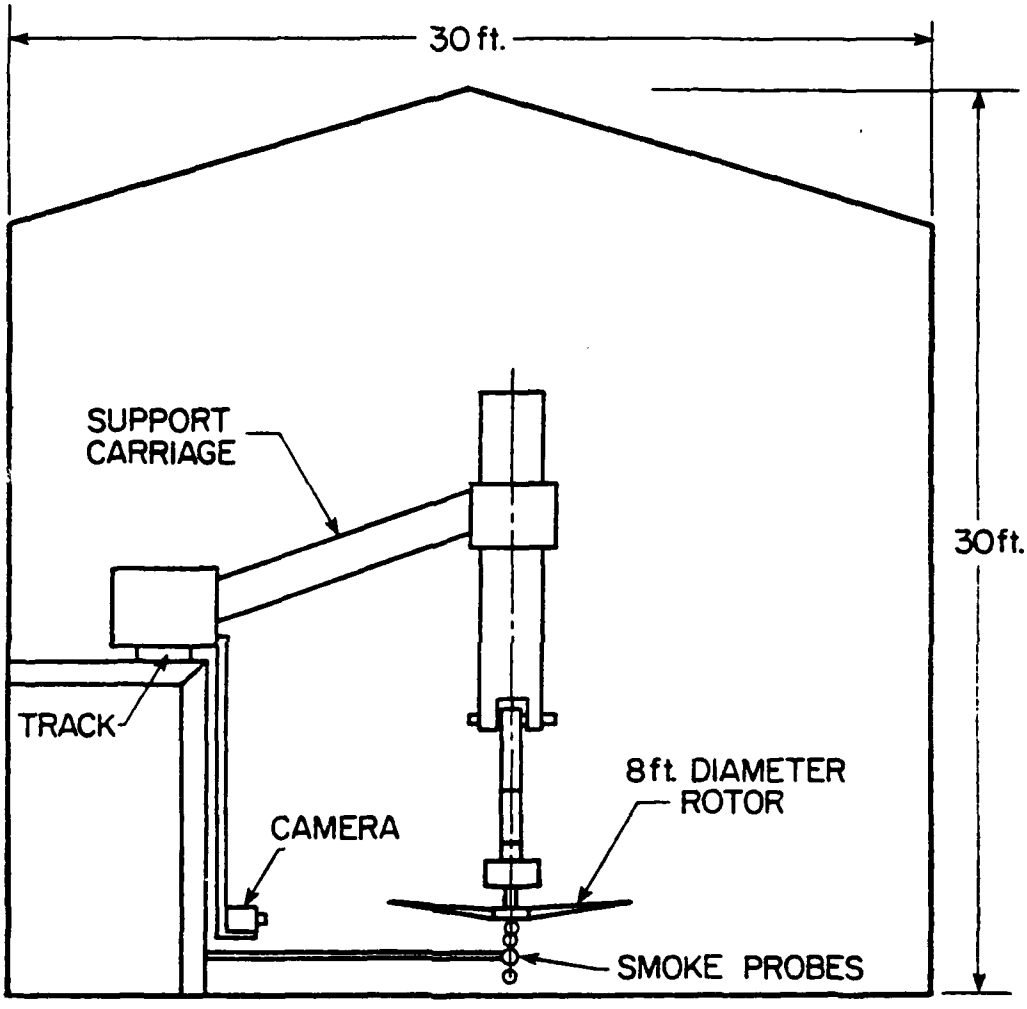

Figure 1. Cross Section of Test Facility.

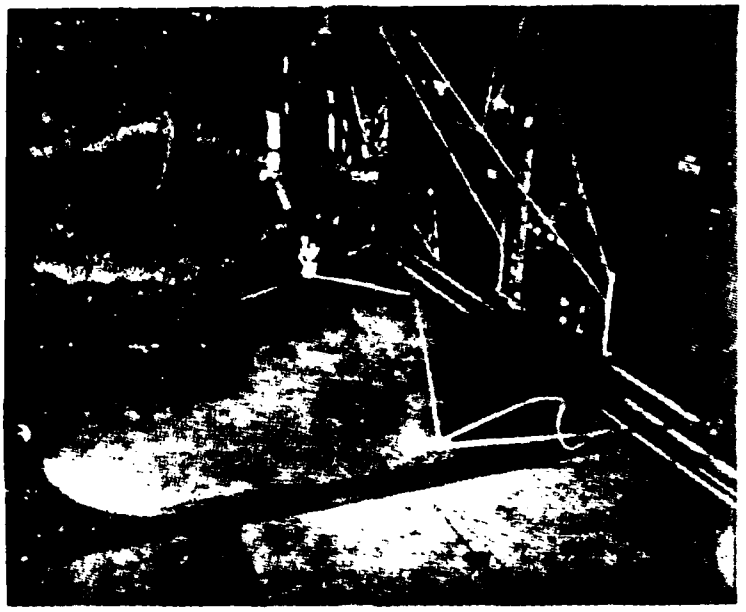

Figure 2. Overall View of Test Facility and Rotor Model.

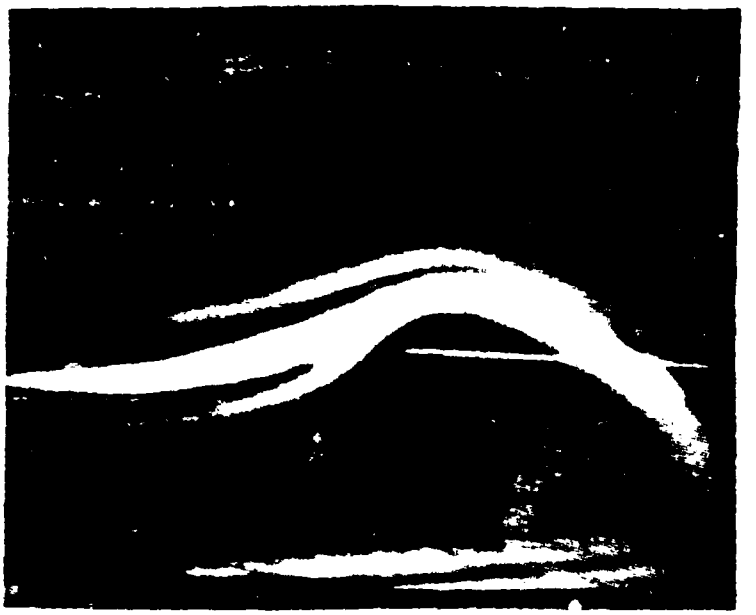

Figure 3. Flow Pattern in Ground Vortex Regime, (μ = .043.).

Figure 4. Flow Pattern in Recirculation Regime, (μ = .034).

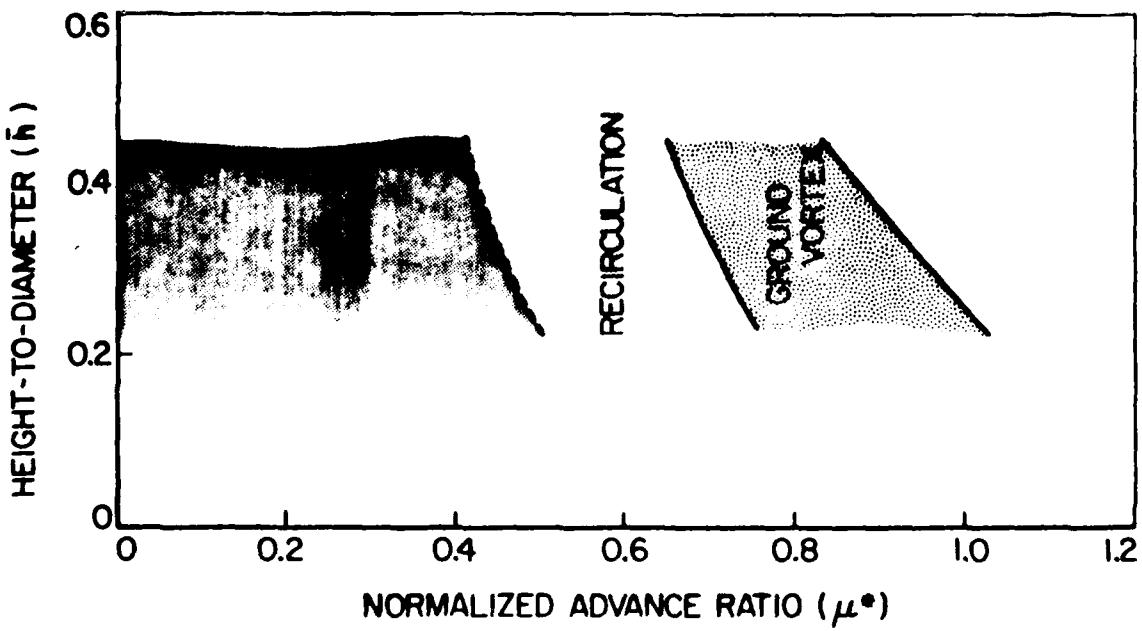

Figure 5. Boundaries for Recirculation and Ground Vortex Flow Determined From Flow Visualization Studies.

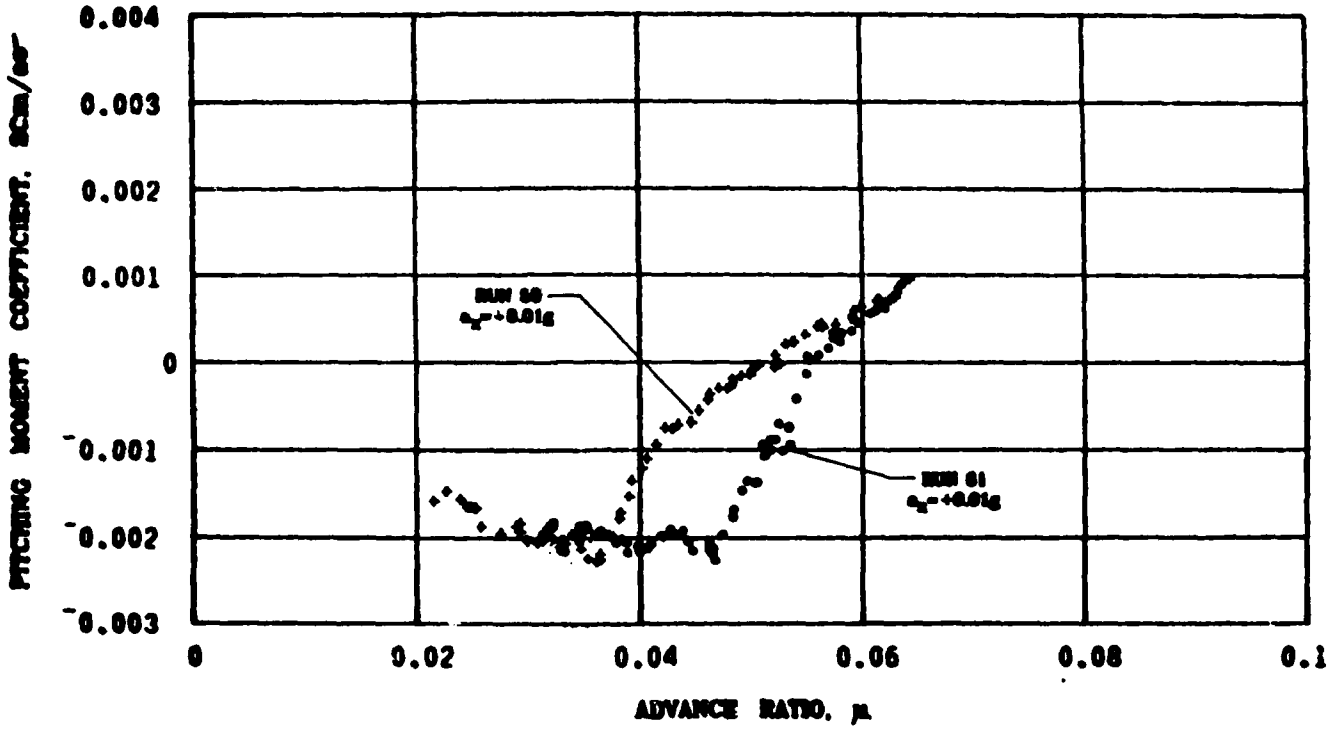

Figure 6. Variation of Rotor Force and Moment Coefficients with Advance Ratio and Translational Acceleration and Deceleration, $\theta_c = 9.8^{\circ}$, $\bar{h} = 0.23$, $a_x = \pm 0.01g$.

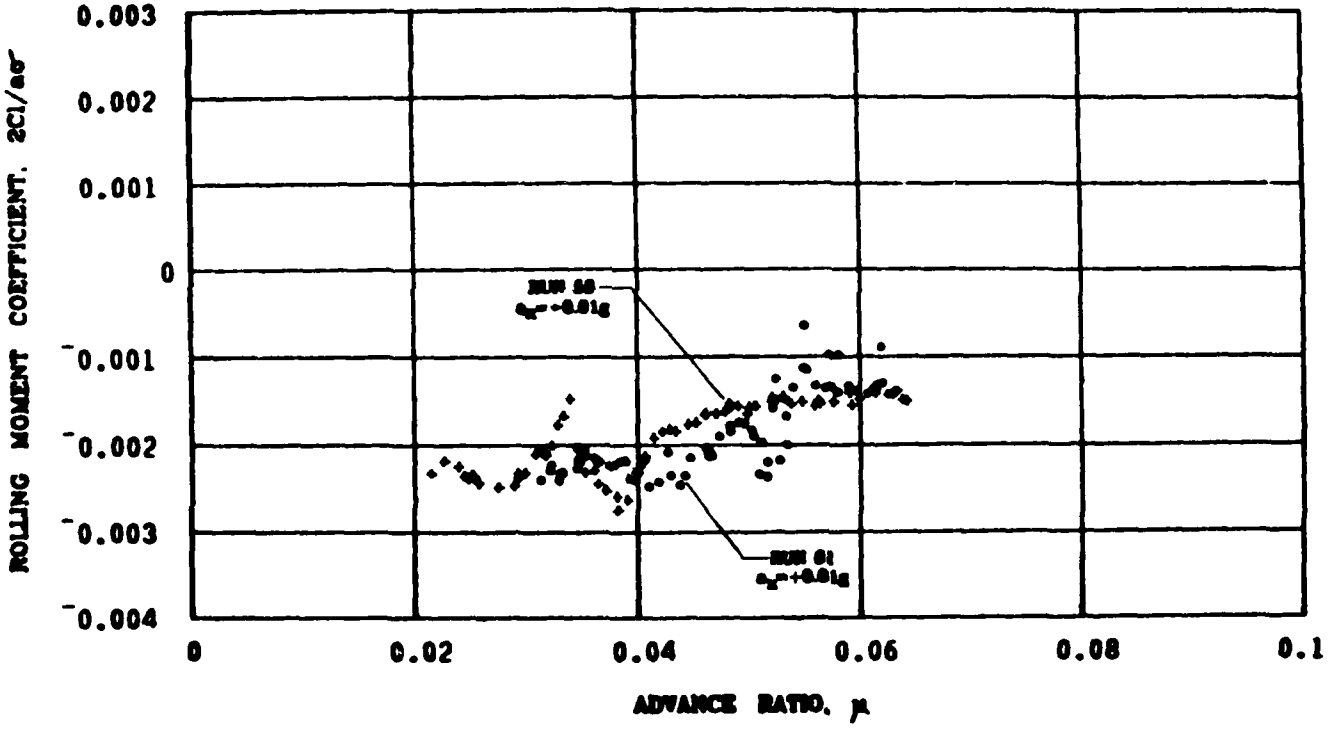

Figure 6. Continued.

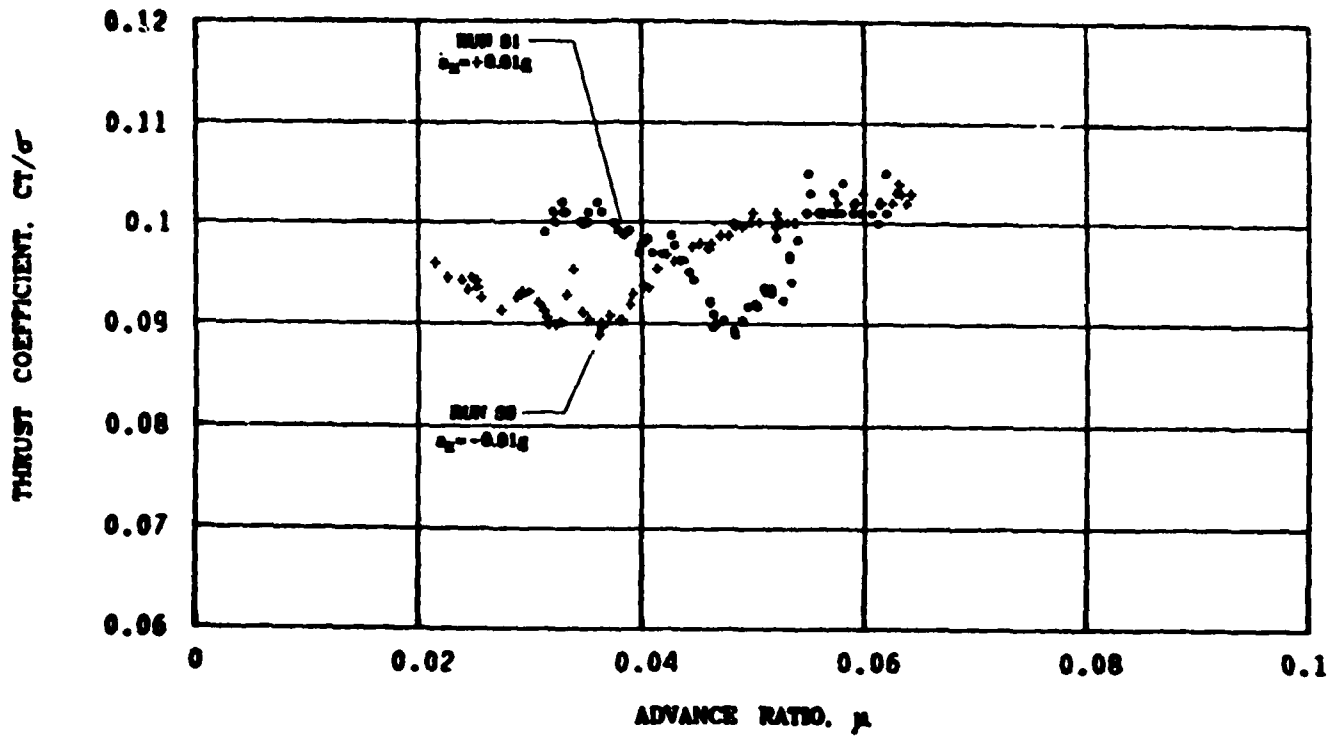

Figure 6. Continued.

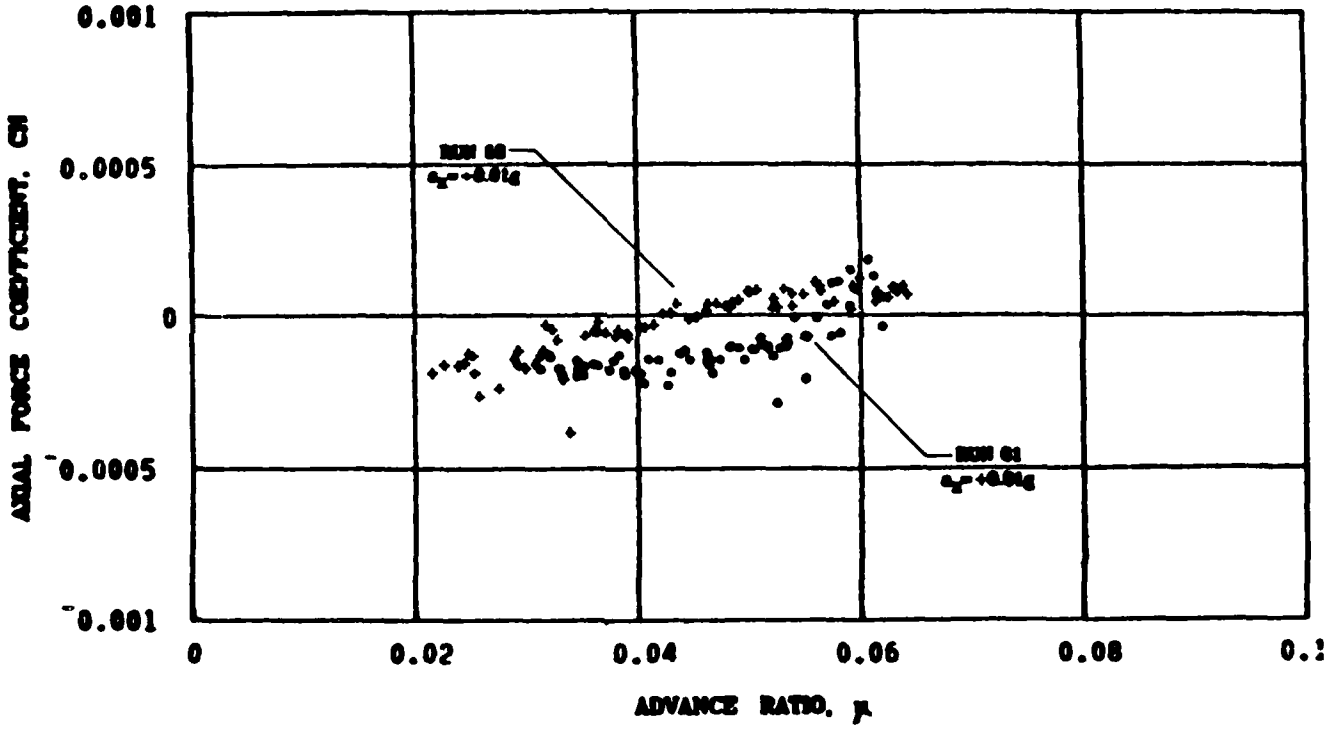

Figure 6. Continued.

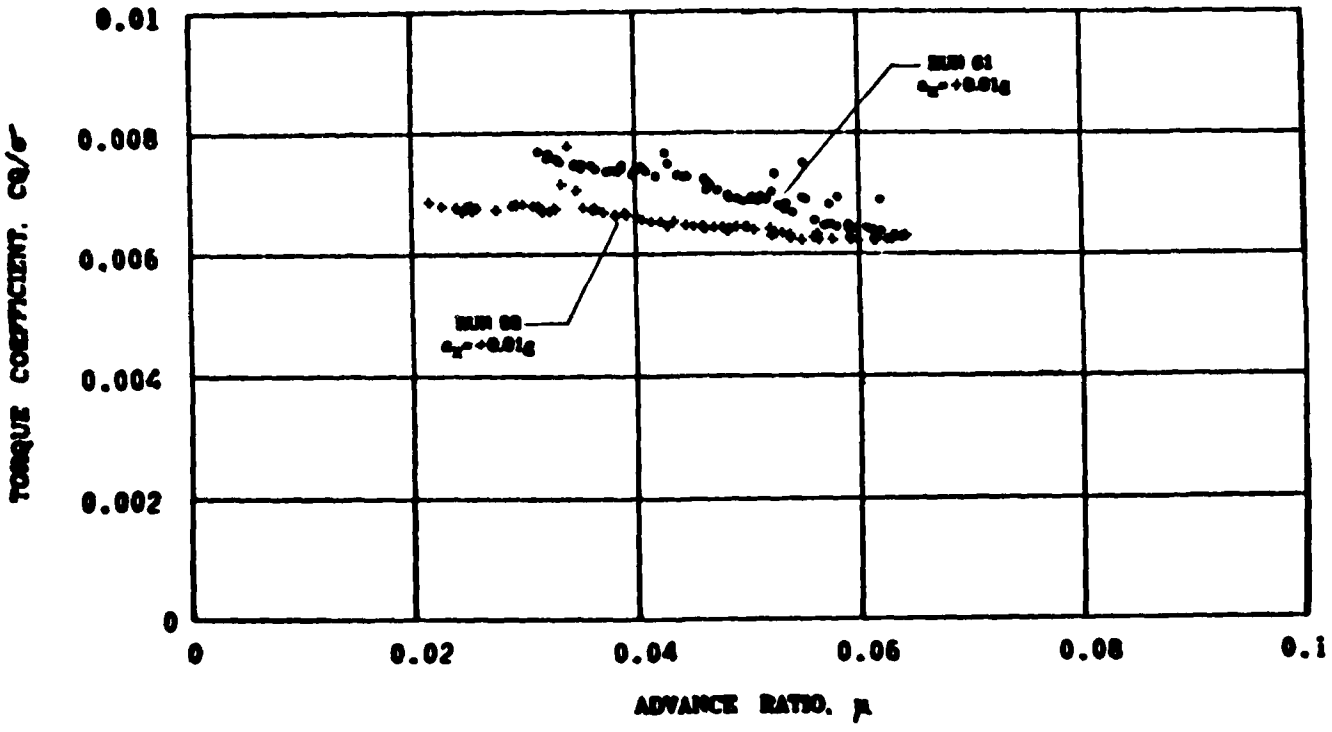

Figure 6. Continued.

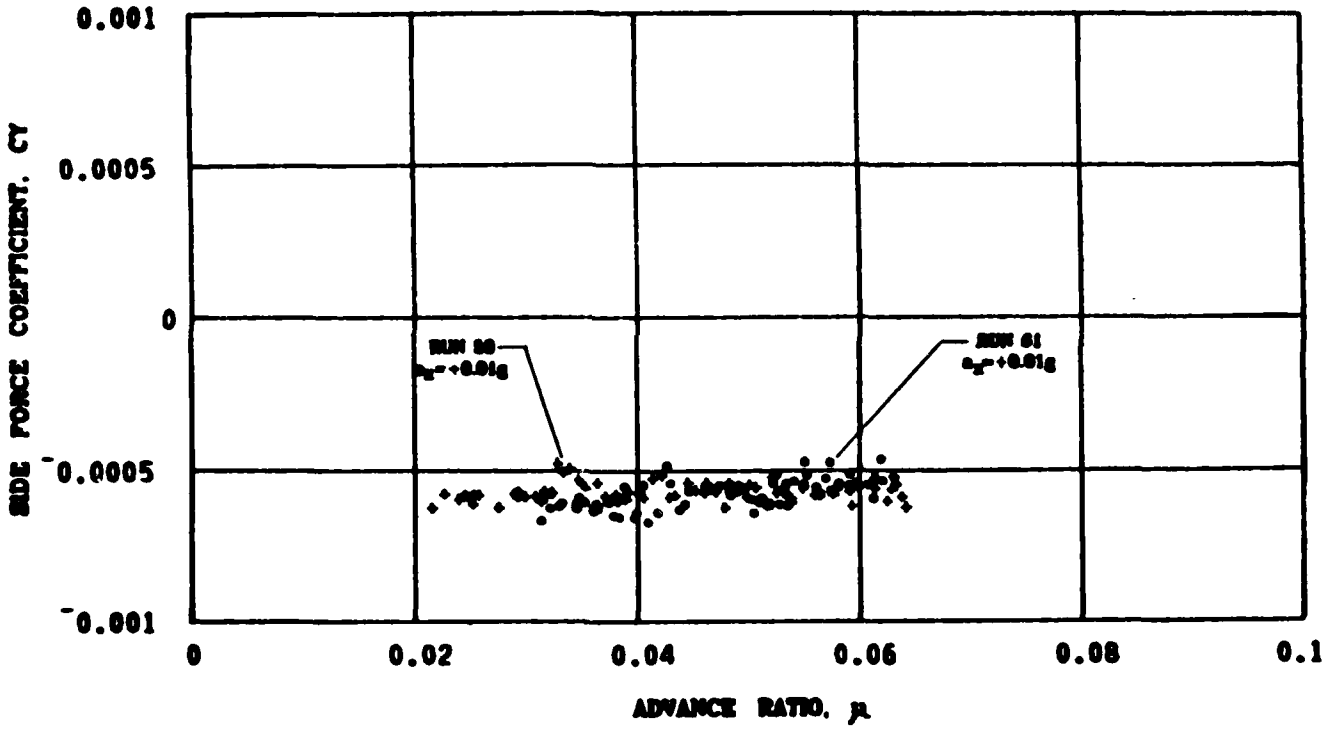

Figure 6. Continued.

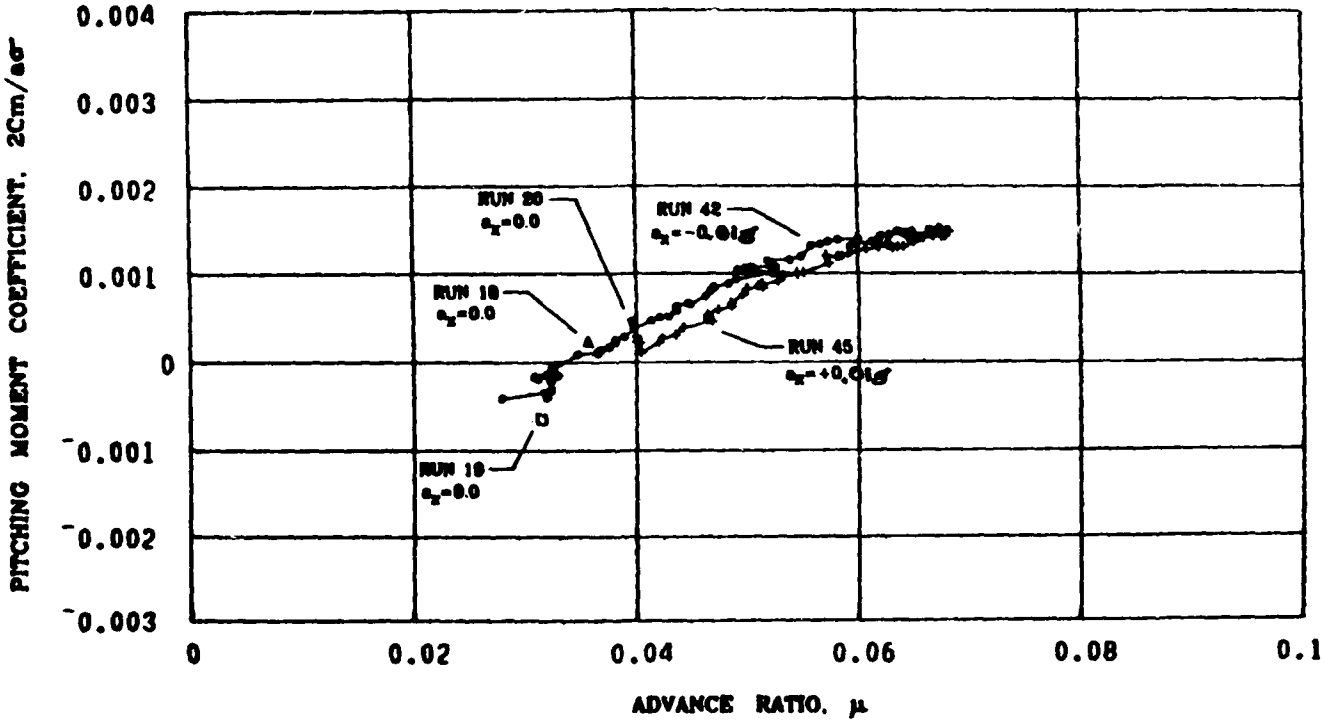

Figure 7. Variation of Rotor Force and Moment Coefficients with Advance Ratio and Translational Acceleration and Deceleration, $\theta_c = 8.4^o$, $\bar{h} = 0.45$, $a_x = 0, \pm 0.01g$.

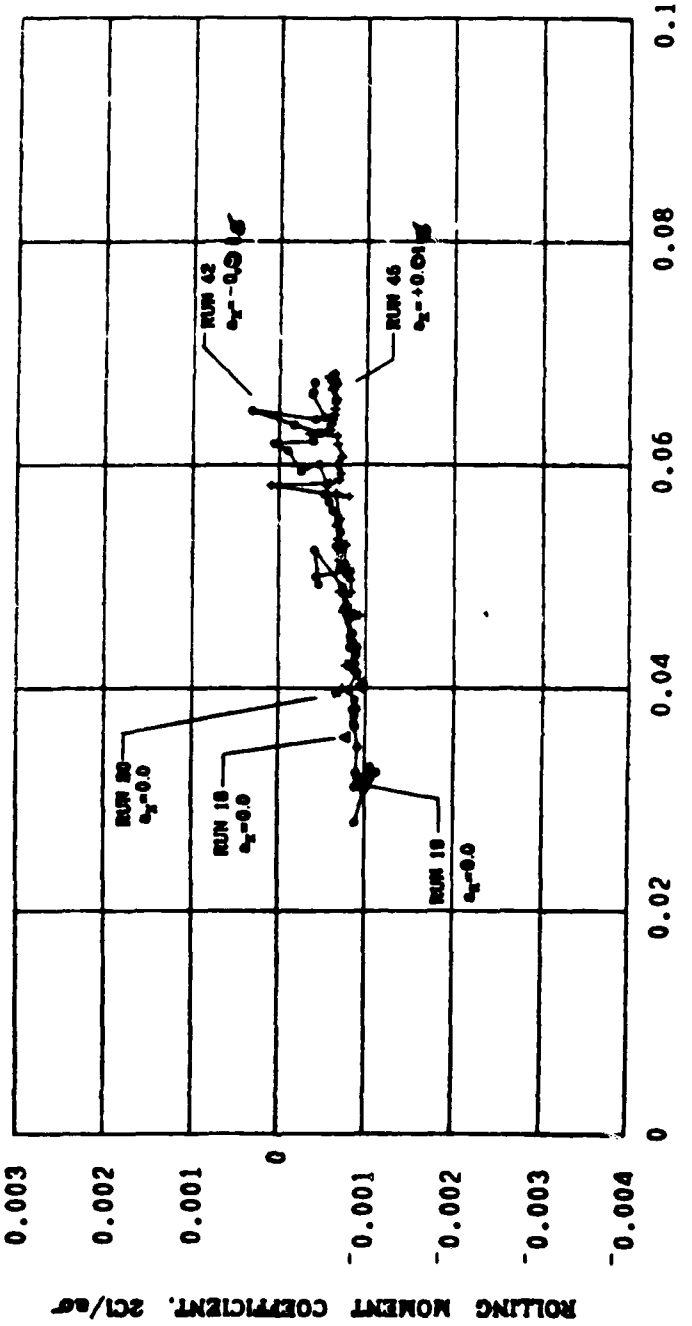

Figure 7. Continued

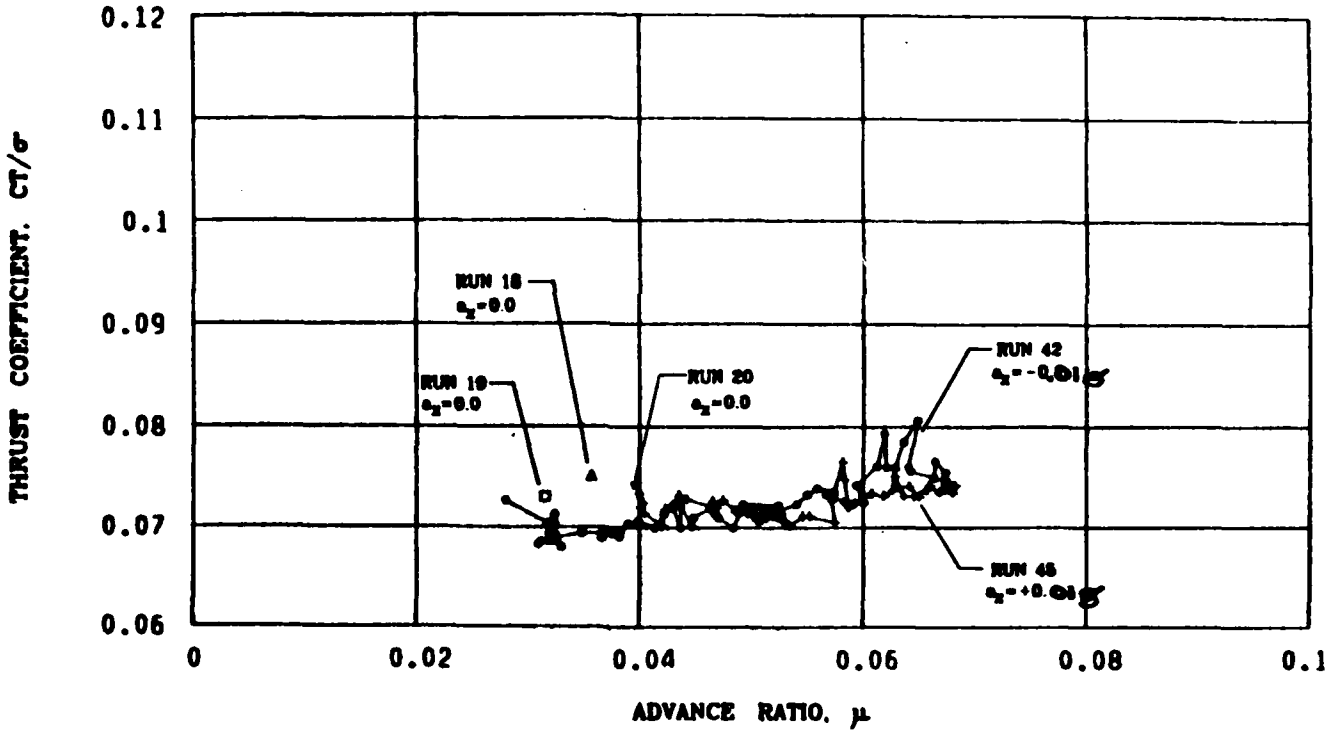

Figure 7. Continued

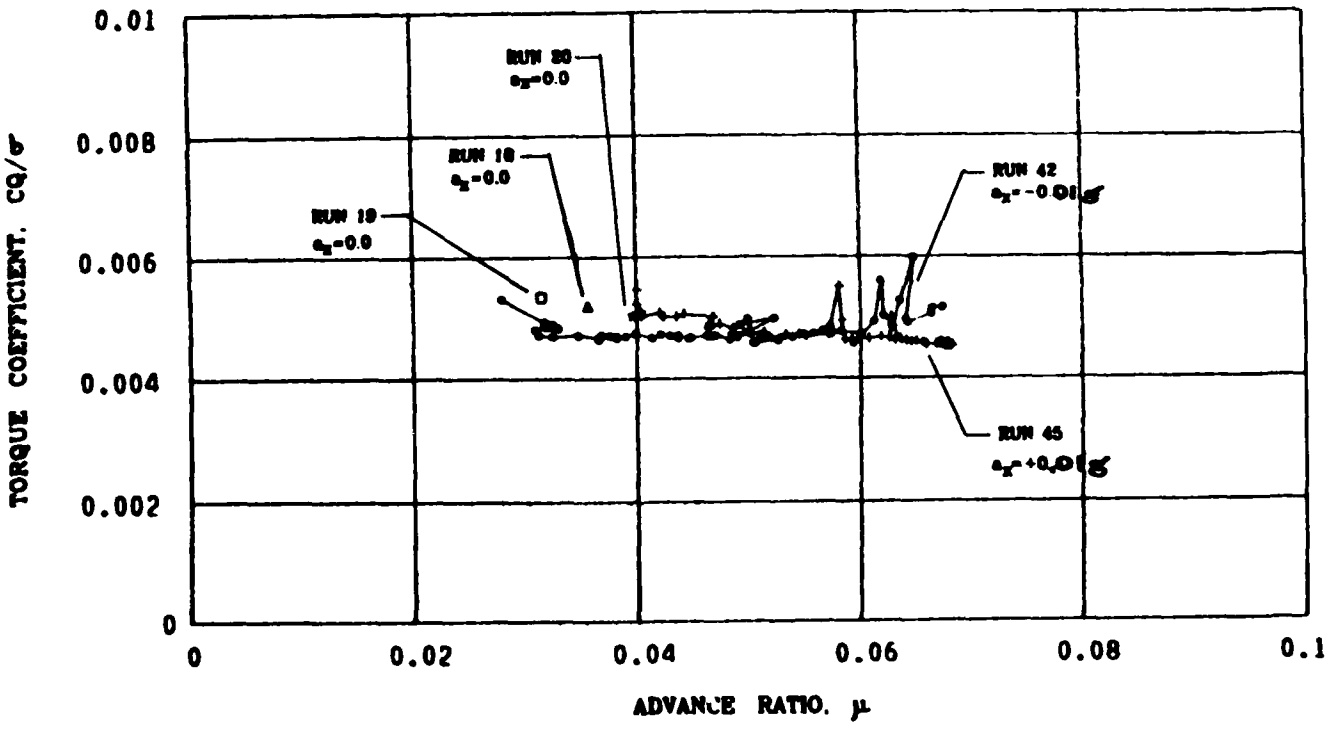

Figure 7. Continued

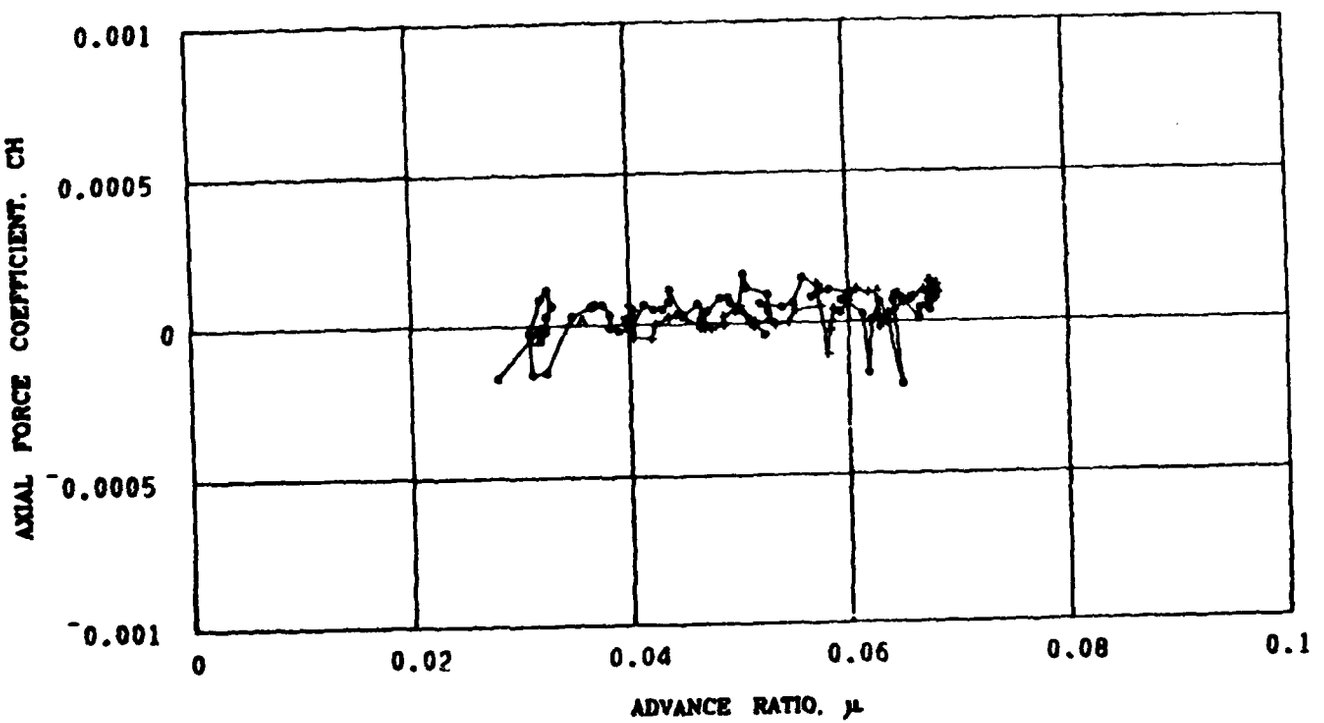

Figure 7. Continued

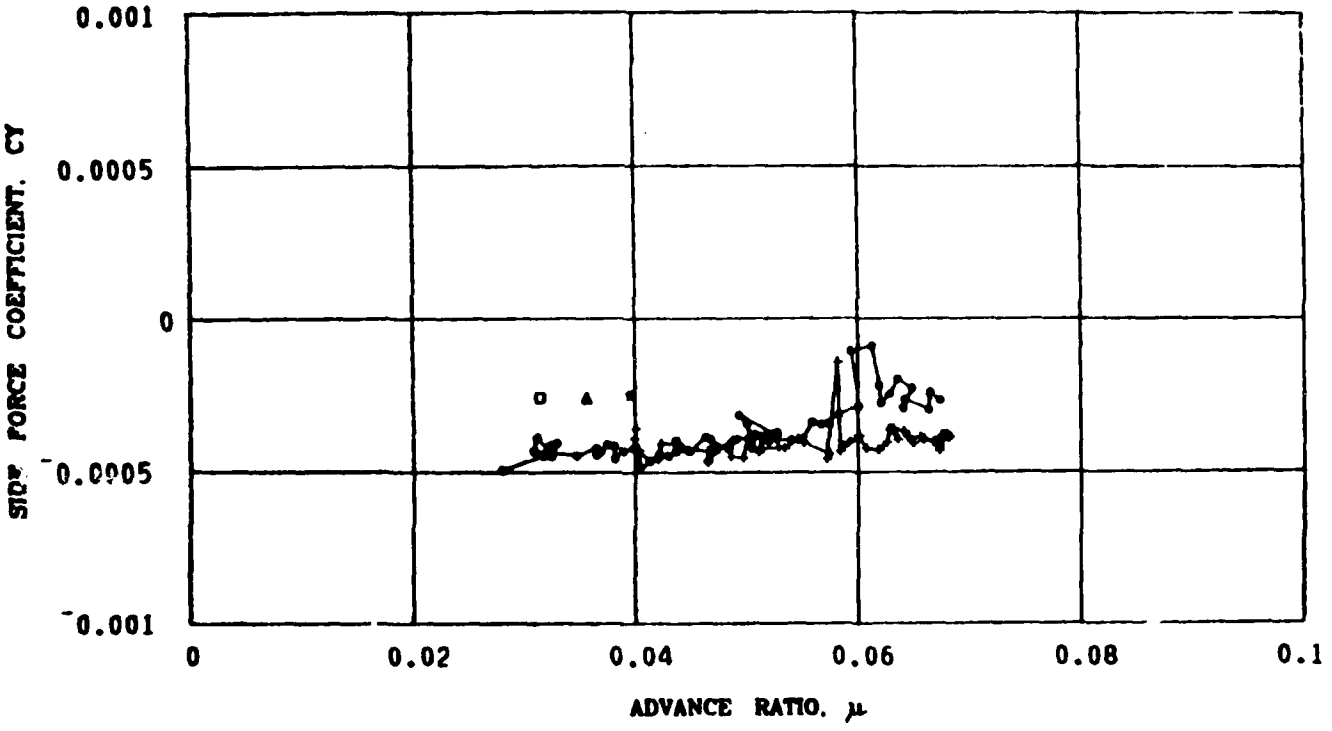

Figure 7. Continued

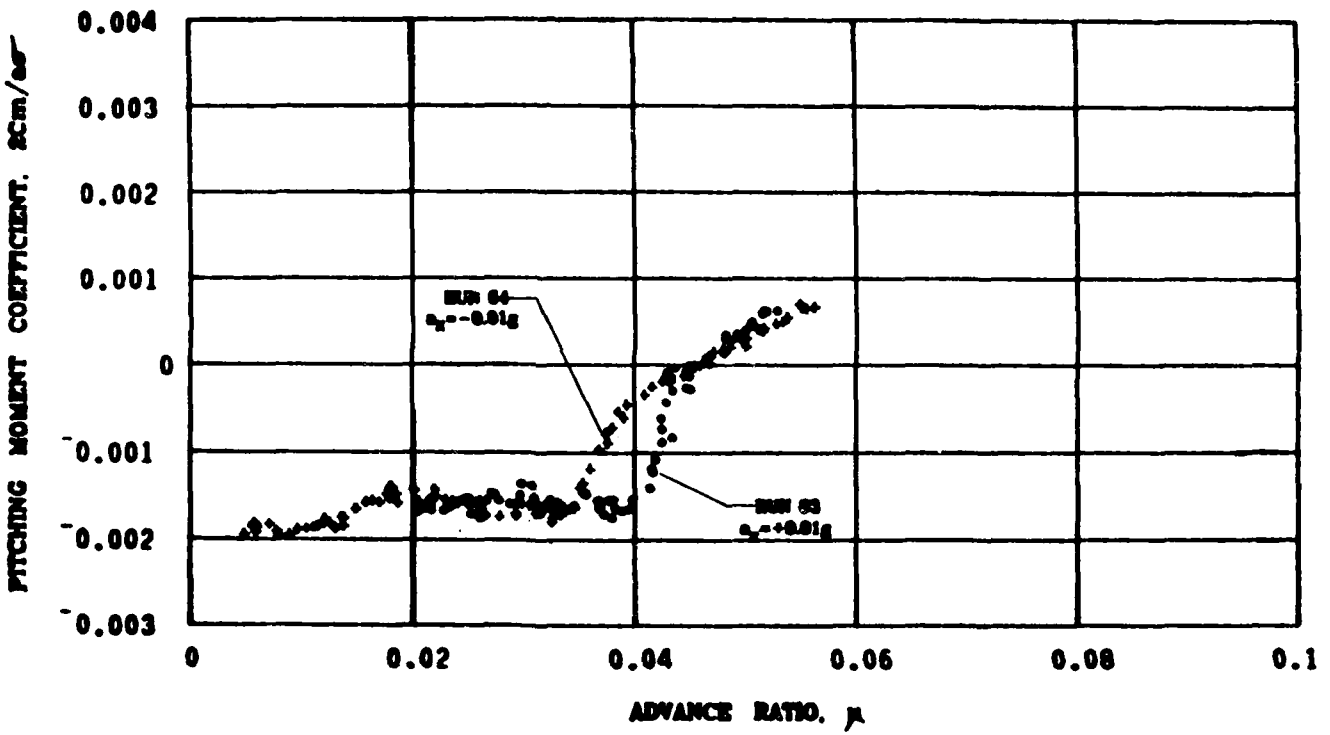

Figure 8. Variation of Rotor Force and Moment Coefficients with Advance Ratio and Translational Acceleration and Deceleration, $\theta_c = 9.8^o$, $\bar{h} = 0.34$, $a_x = \pm 0.01g$.

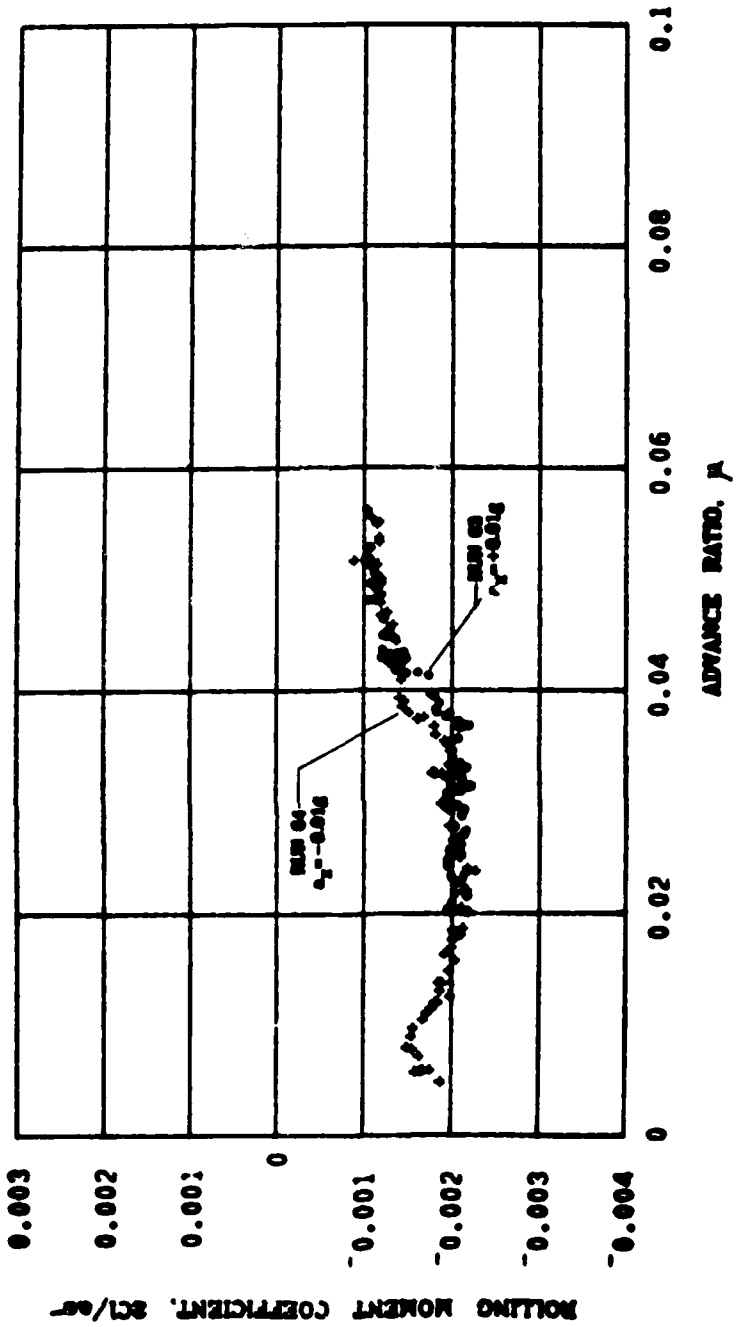

Figure 8. Continued.

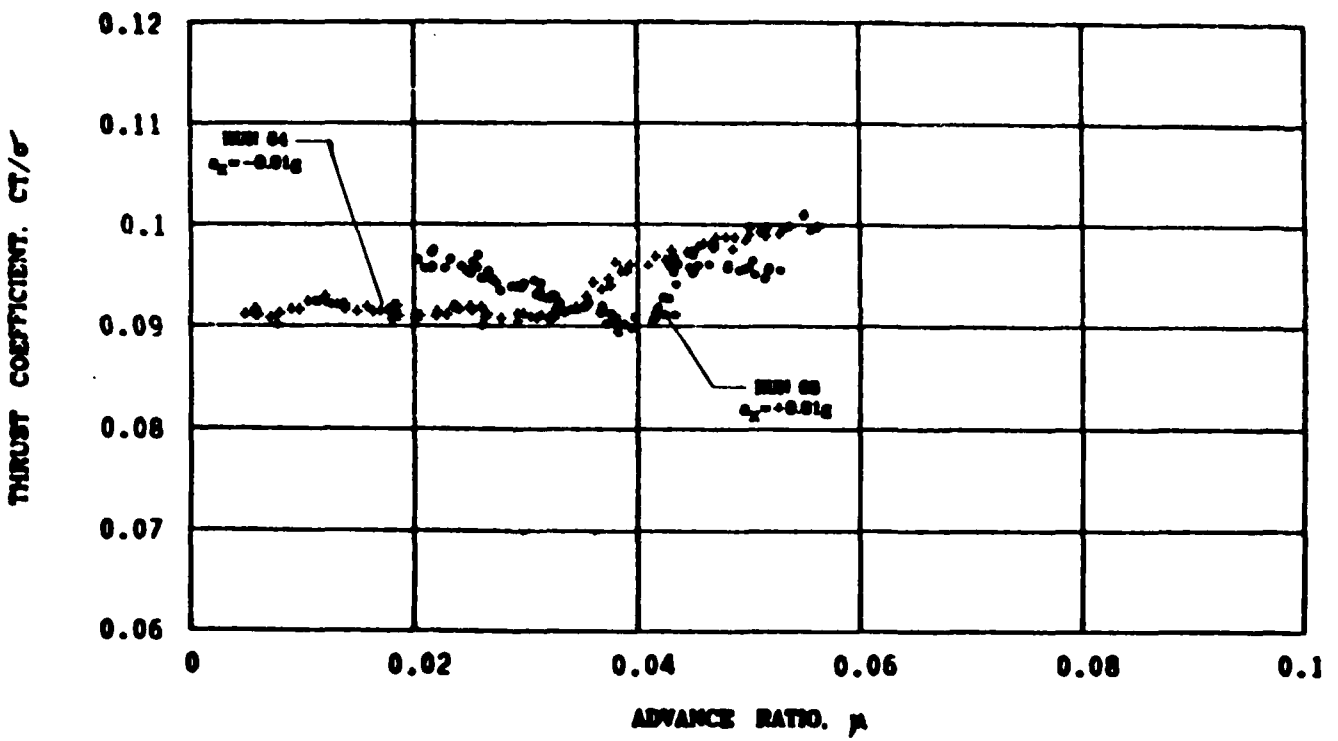

Figure 8. Continued.

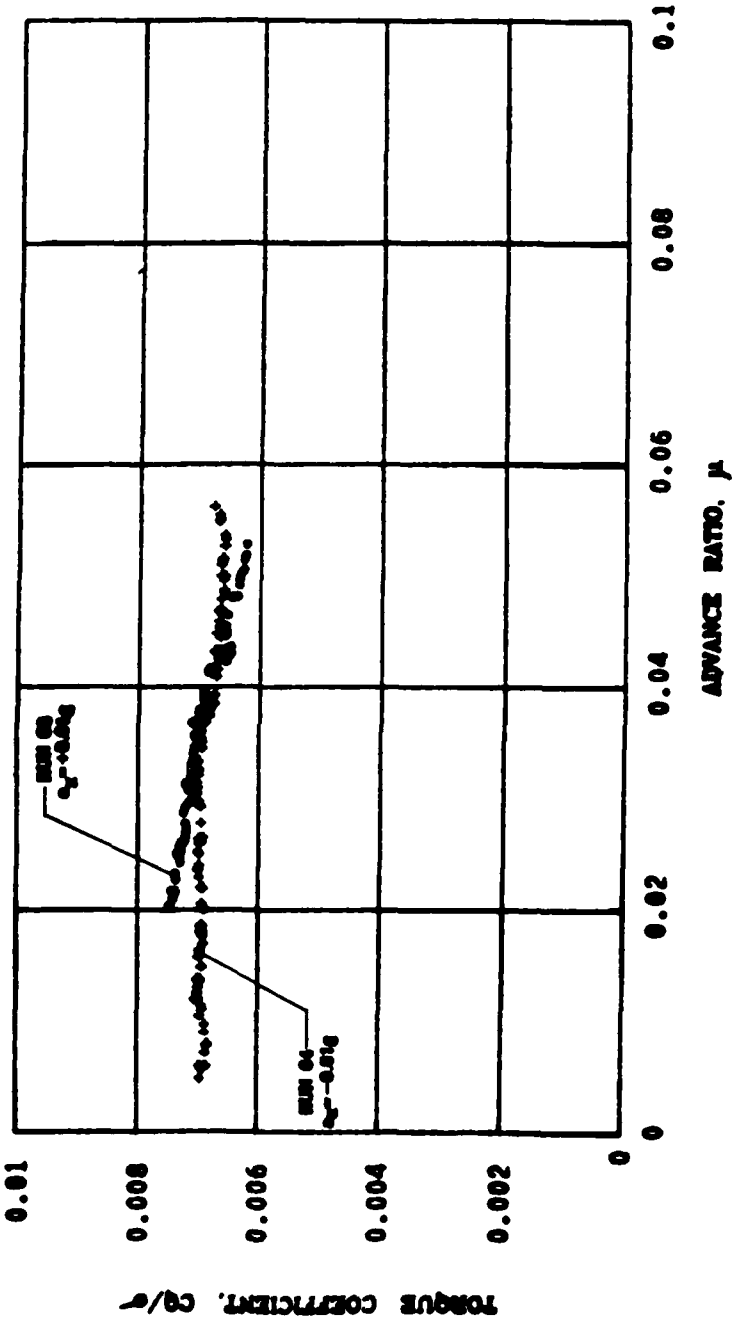

Figure 8. Continued.

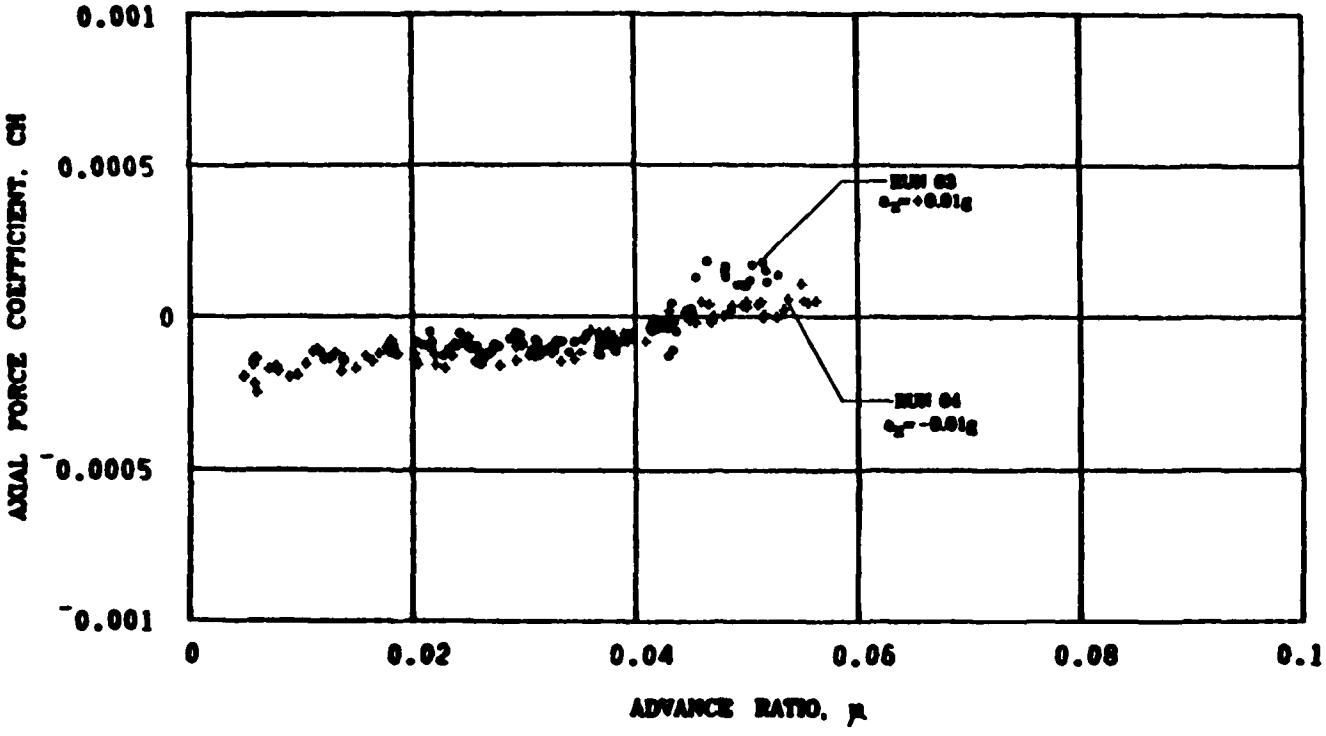

Figure 8. Continued.

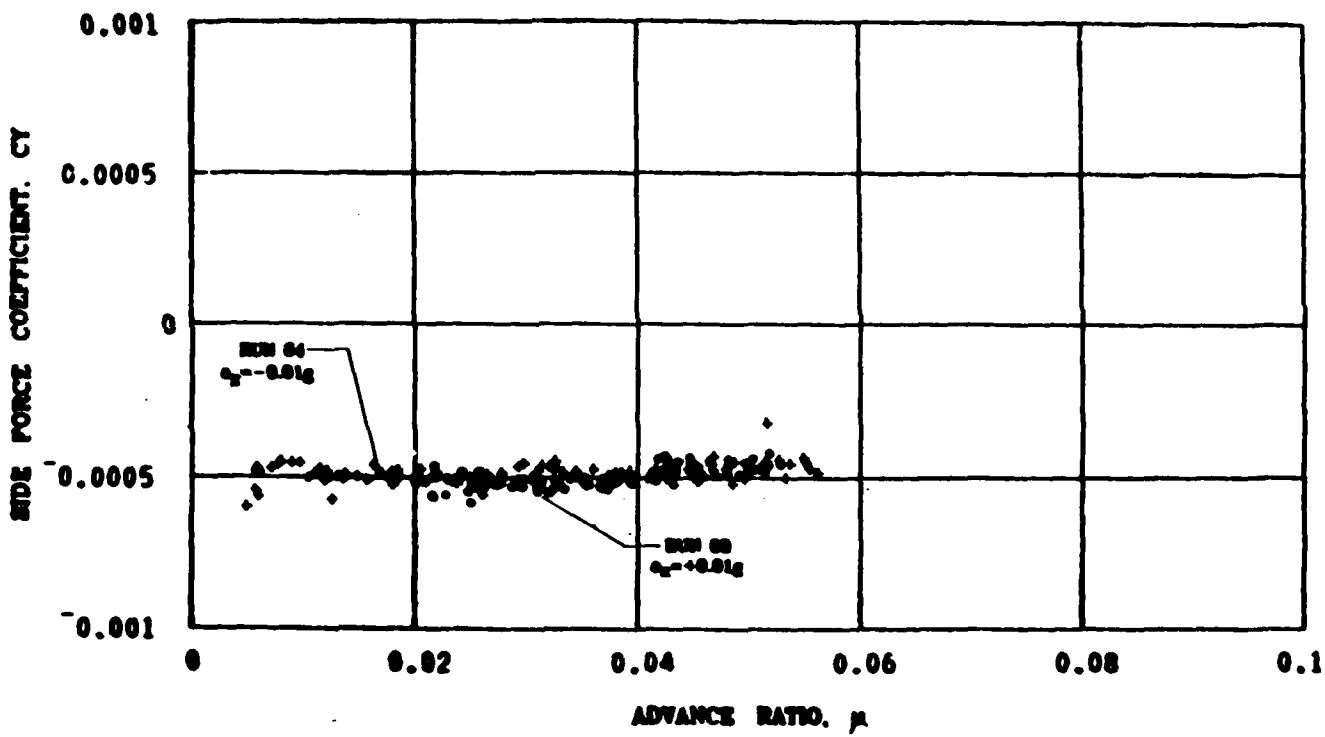

Figure 8. Continued.

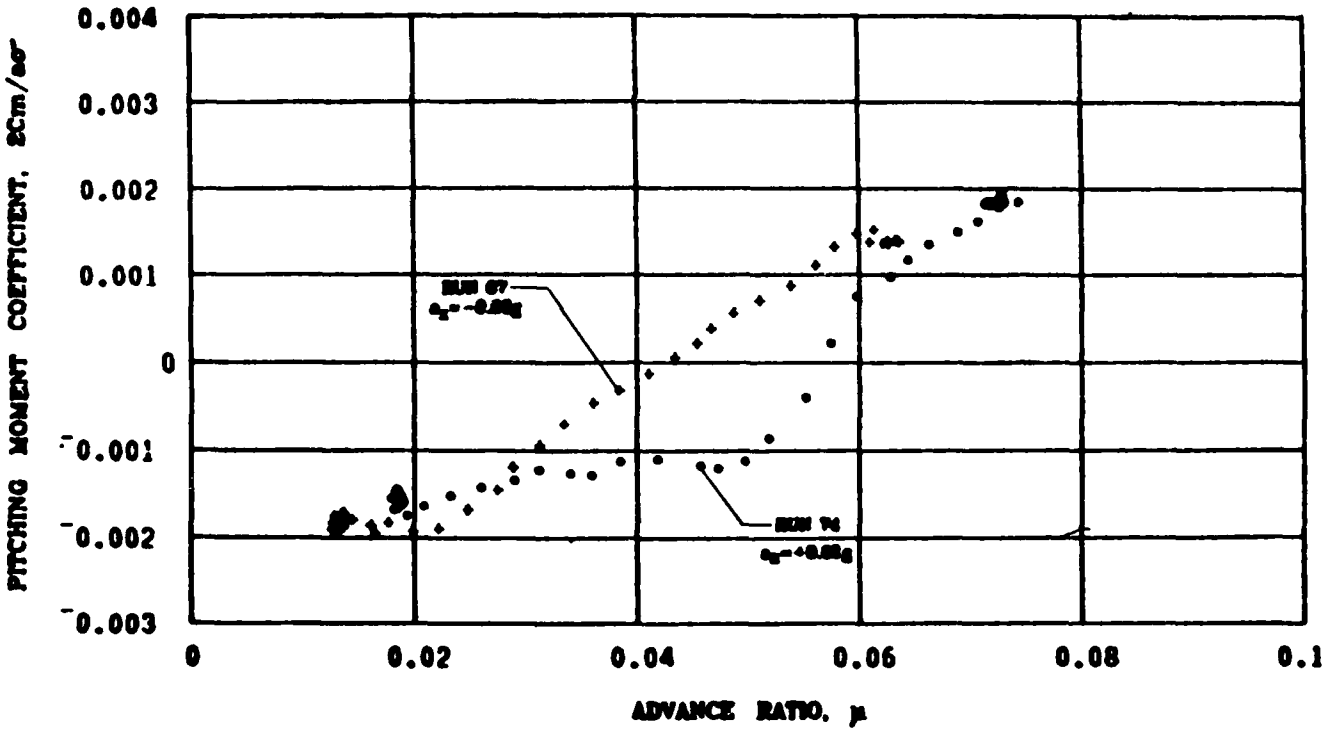

Figure 9. Variation of Rotor Force and Moment Coefficient with Advance Ratio and Translational Acceleration and Deceleration, $\theta_c = 9.8^{\circ}$, $\bar{h} = 0.34$, $a_x = \pm 0.03g$.

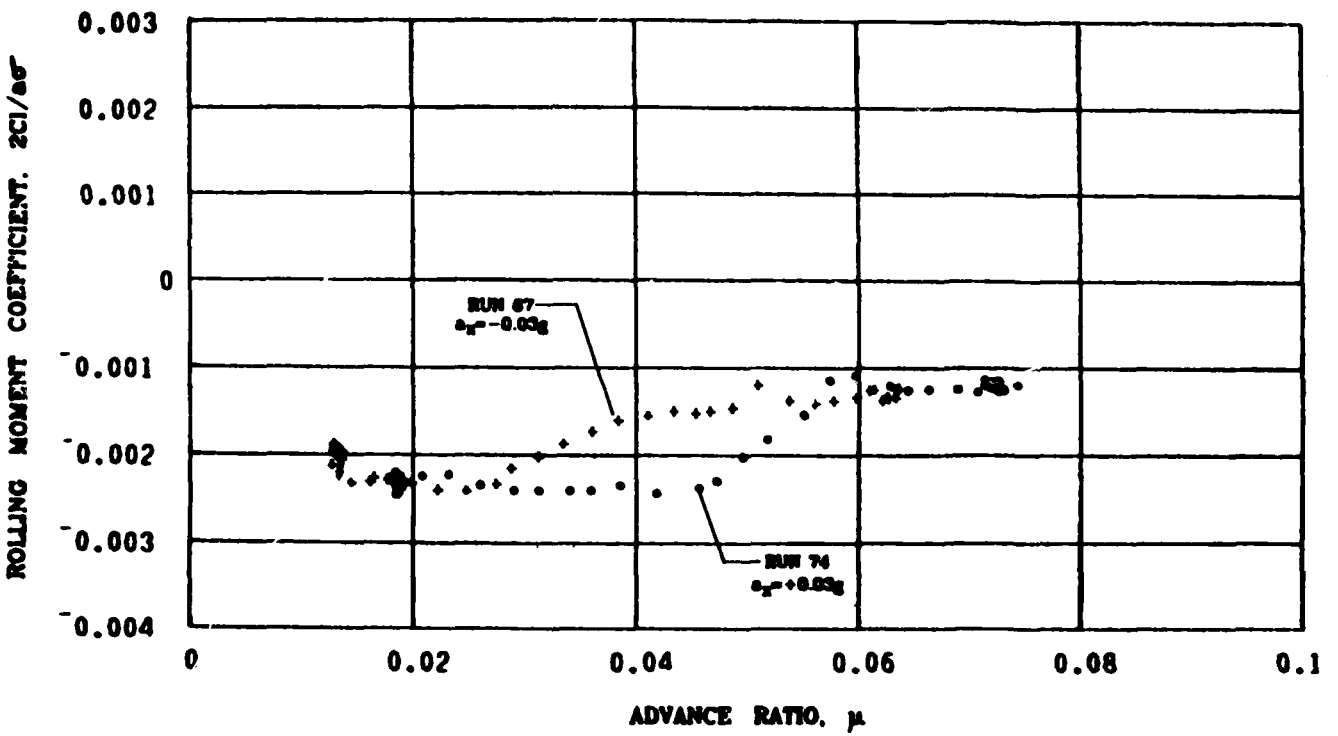

Figure 9. Continued.

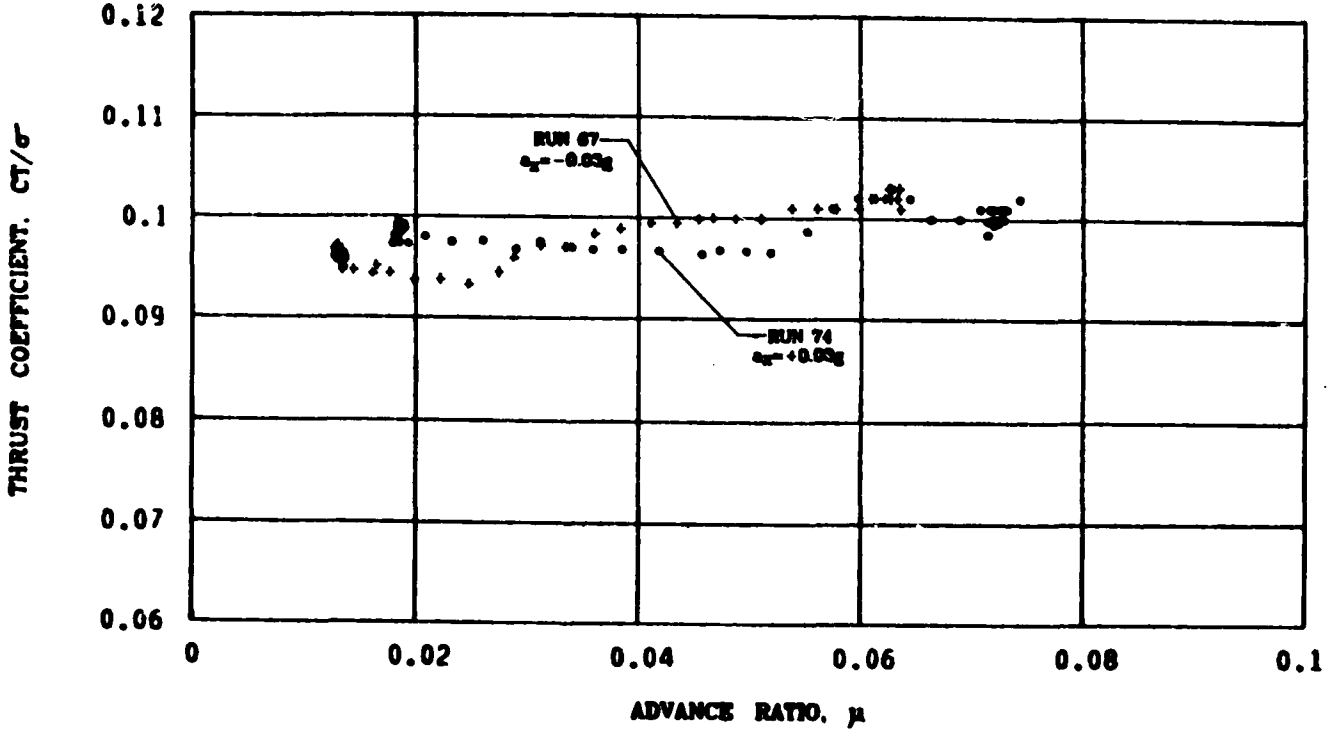

Figure 9. Continued.

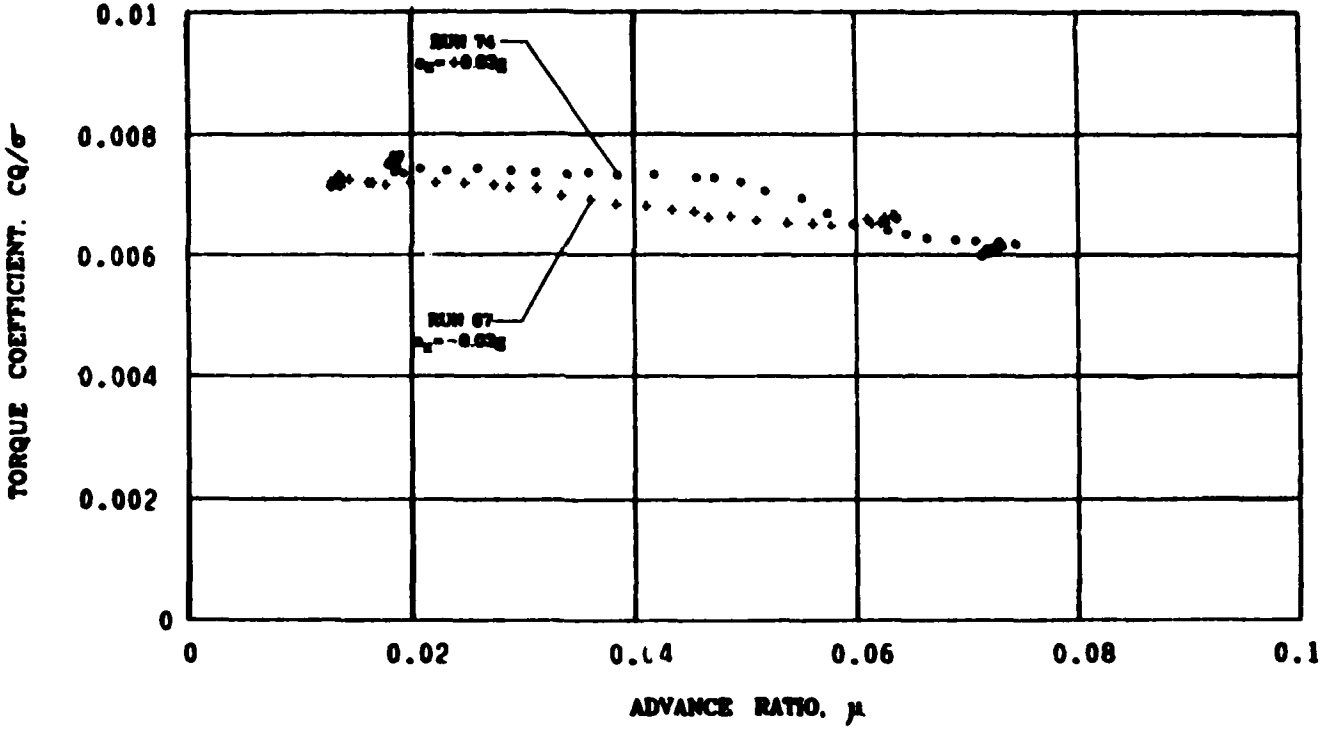

Figure 9. Continued.

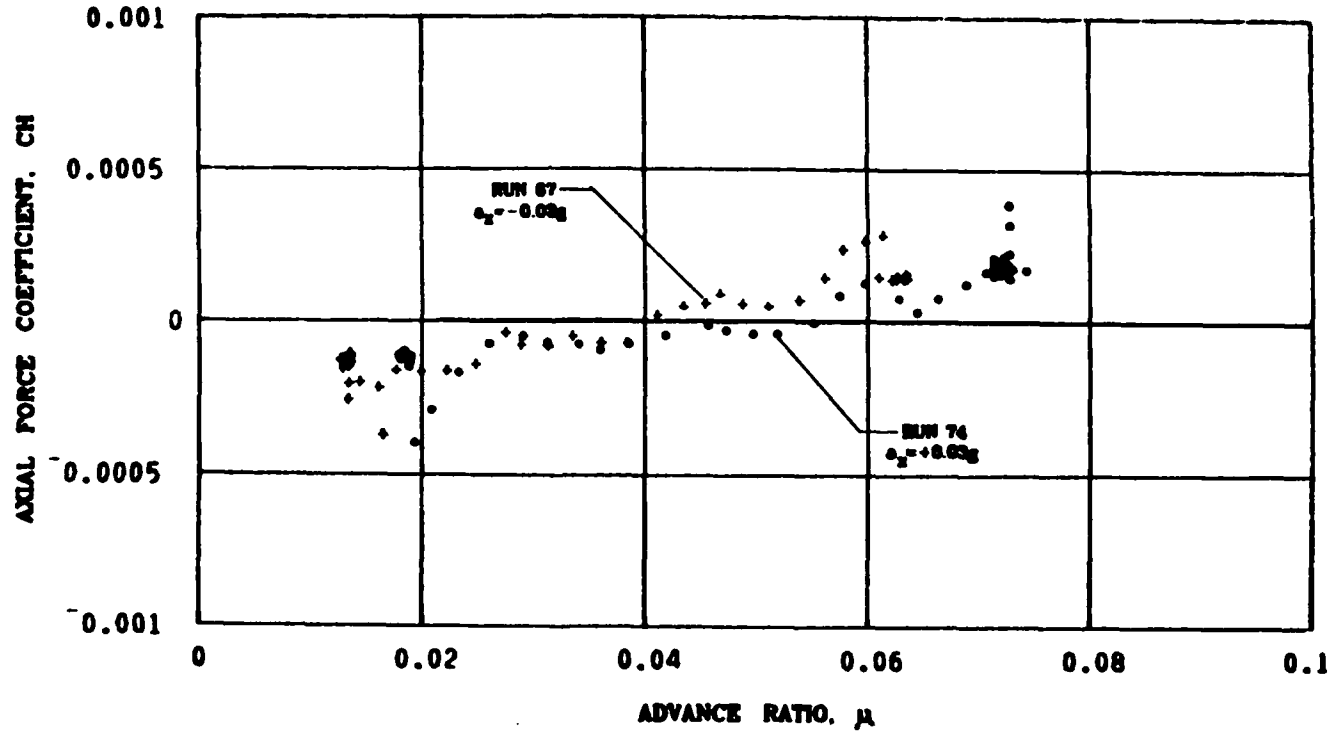

Figure 9. Continued.

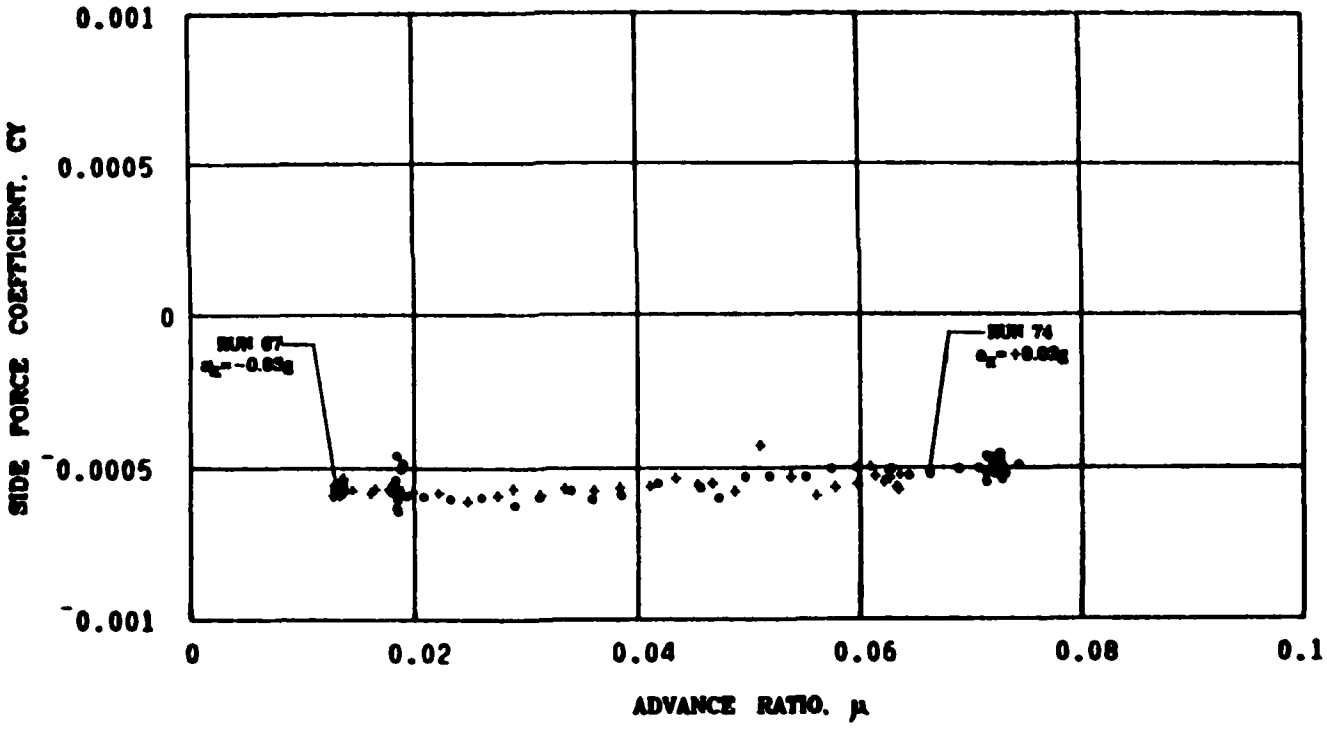

Figure 9. Continued.

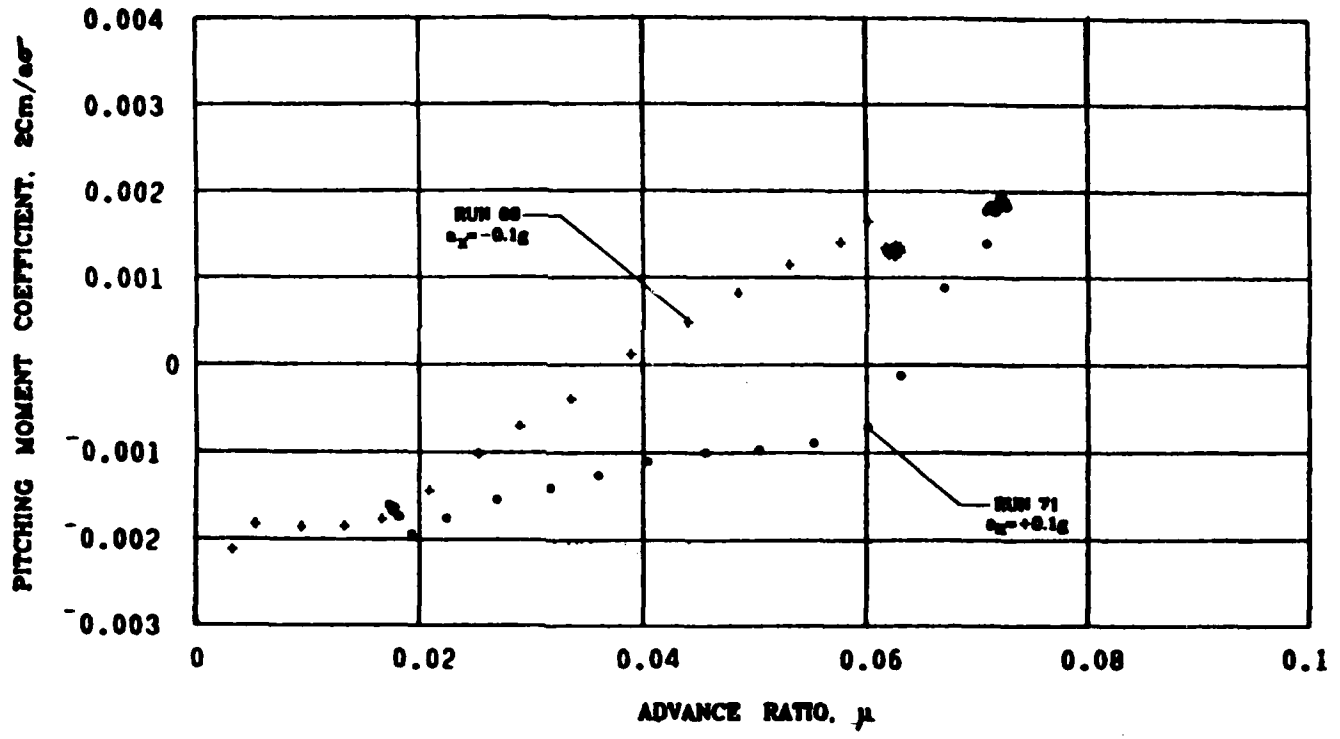

Figure 10. Variation of Rotor Force and Moment Coefficients with Advance Ratio and Translational Acceleration and Deceleration, $\theta_c = 9.8^o$, $\bar{h} = 0.34$, $a_x = \pm 0.1g$.

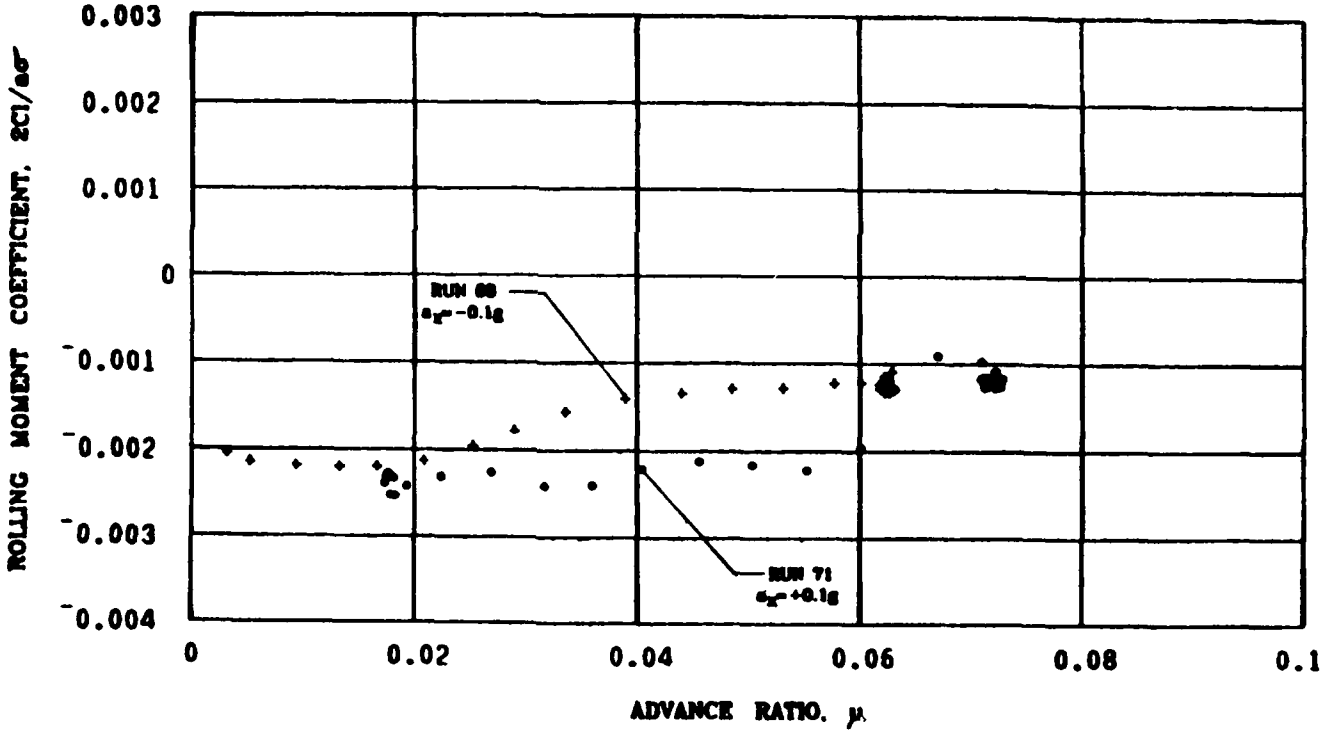

Figure 10. Continued.

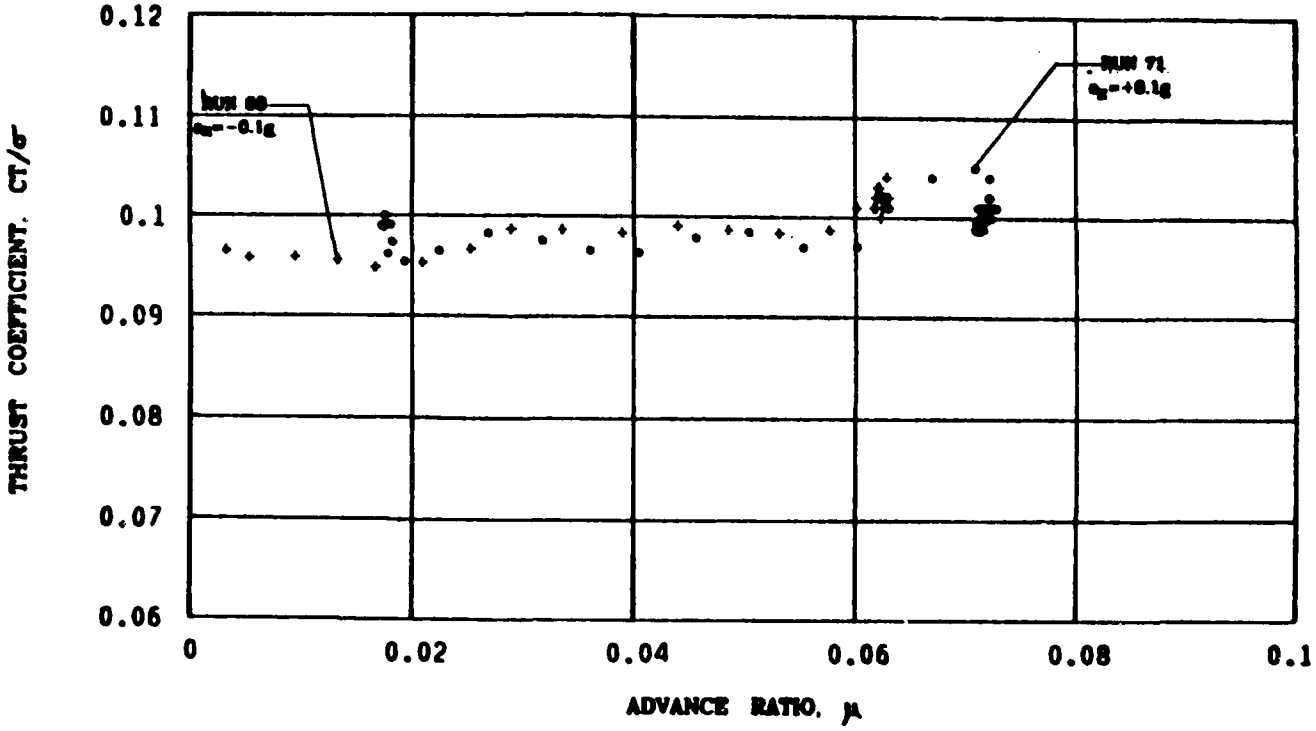

Figure 10. Continued.

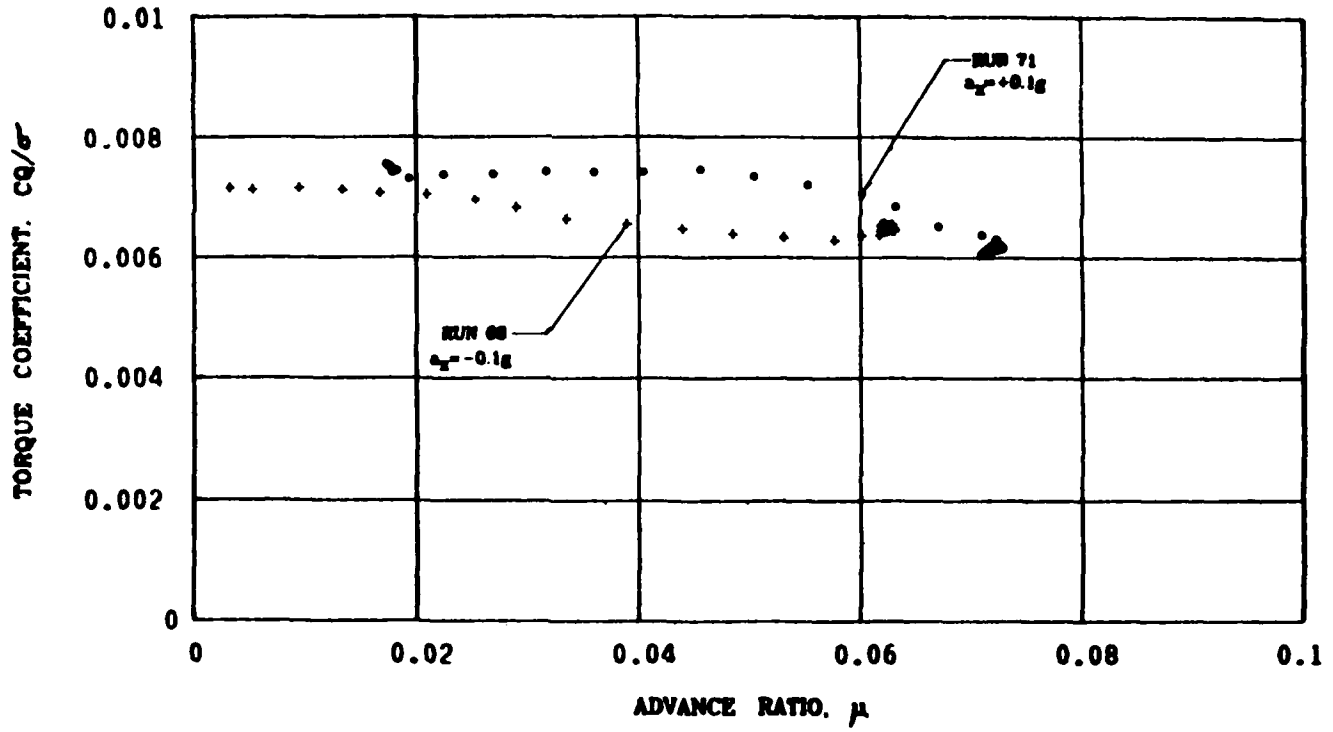

Figure 10. Continued.

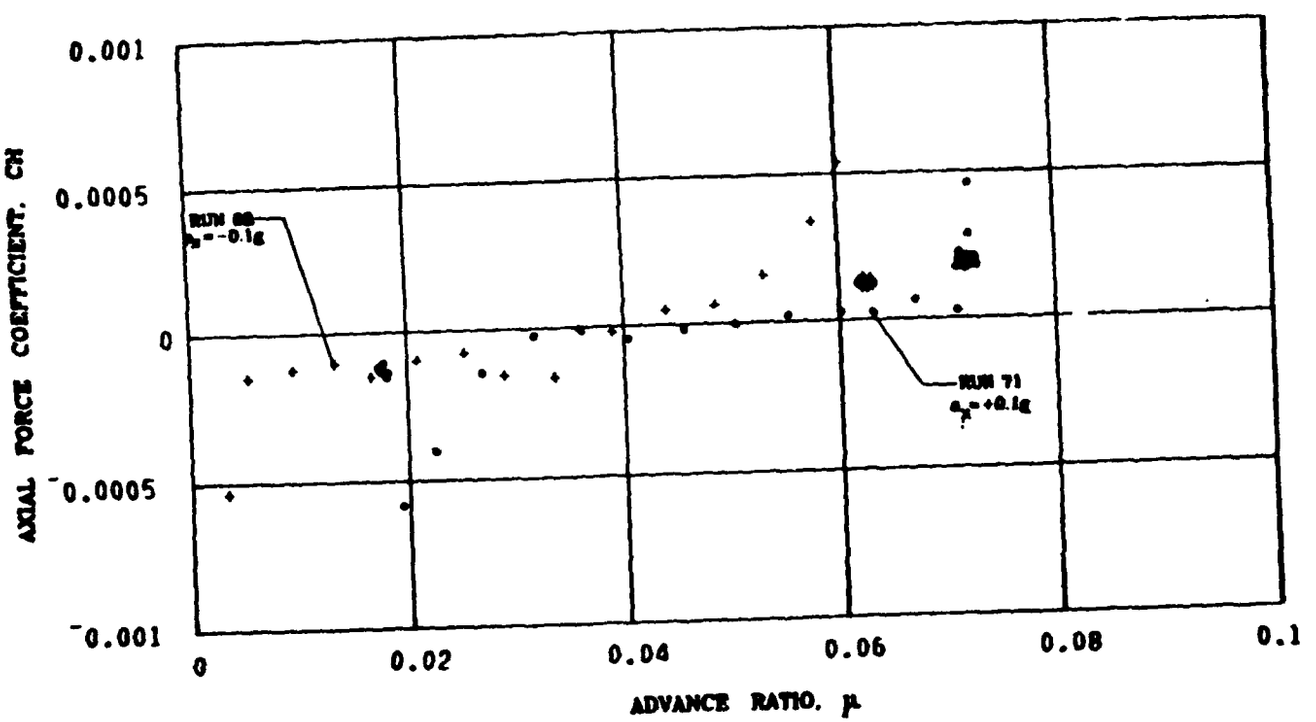

Figure 10. Continued.

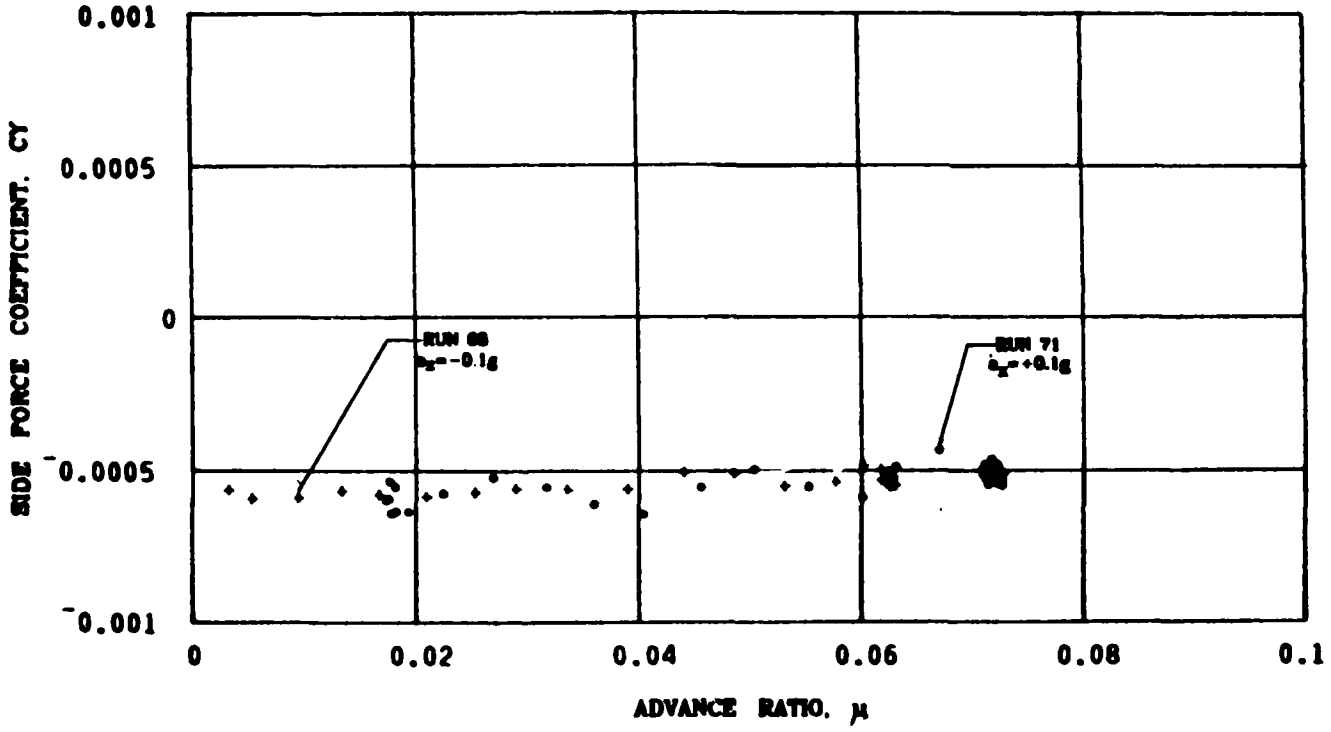

Figure 10. Continued.

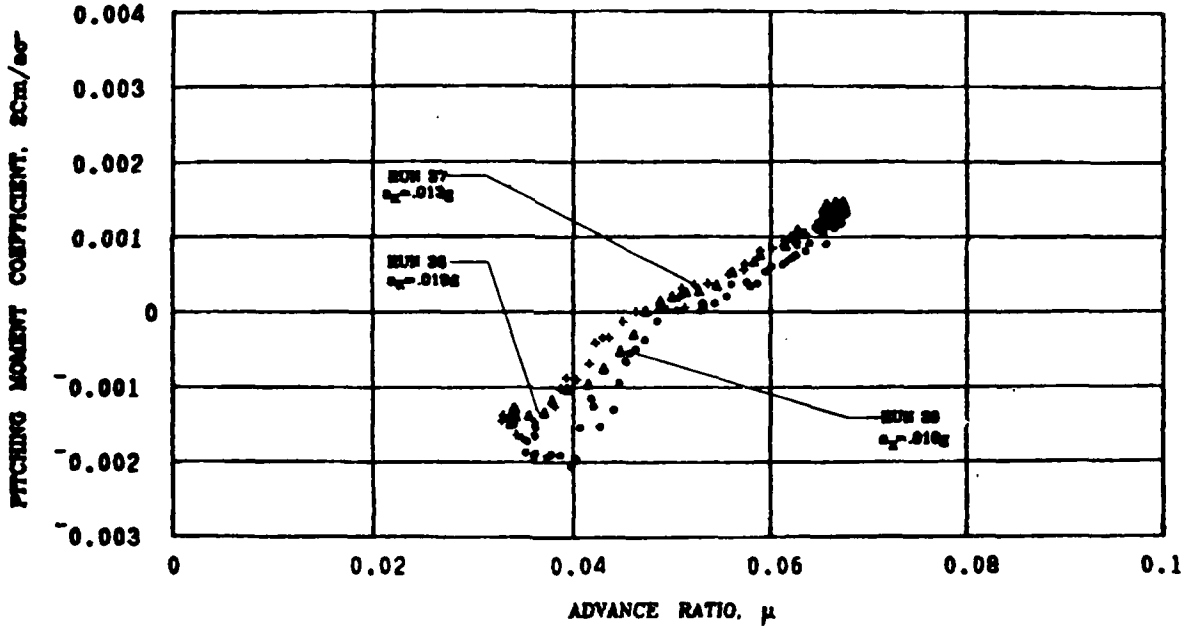

Figure 11. Variation of Rotor Force and Moment Coefficients with Advance Ratio and Acceleration, $\theta_c = 8.4^o$, $\bar{h} = 0.23$, a_x Varying.

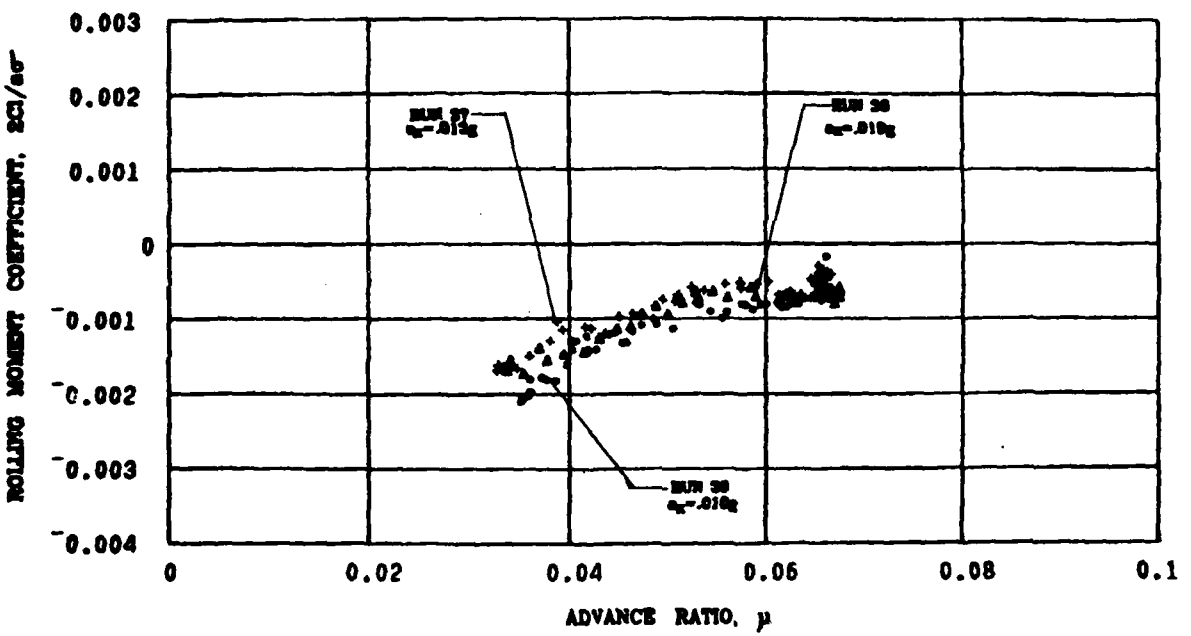

Figure 11. Continued.

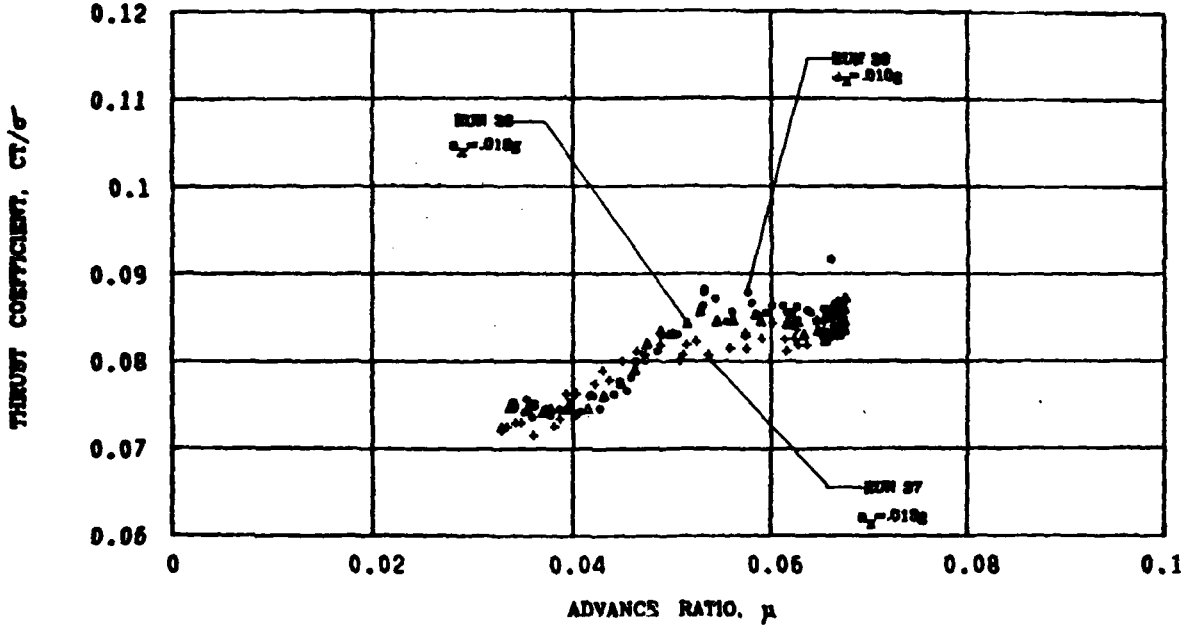

Figure 11. Continued.

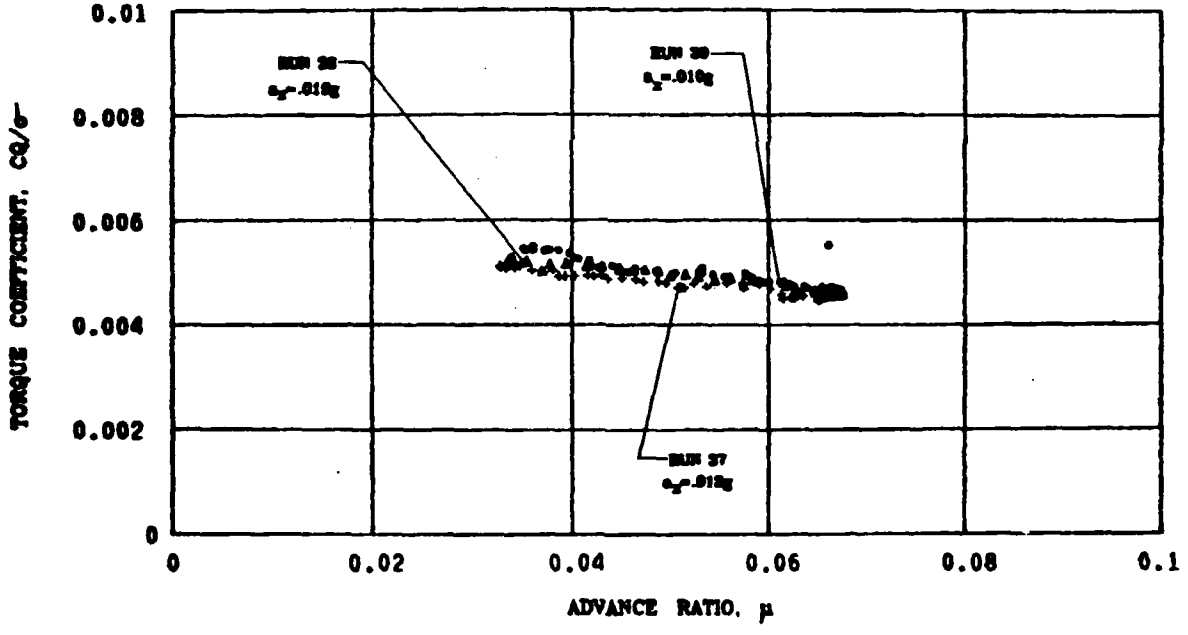

Figure 11. Continued.

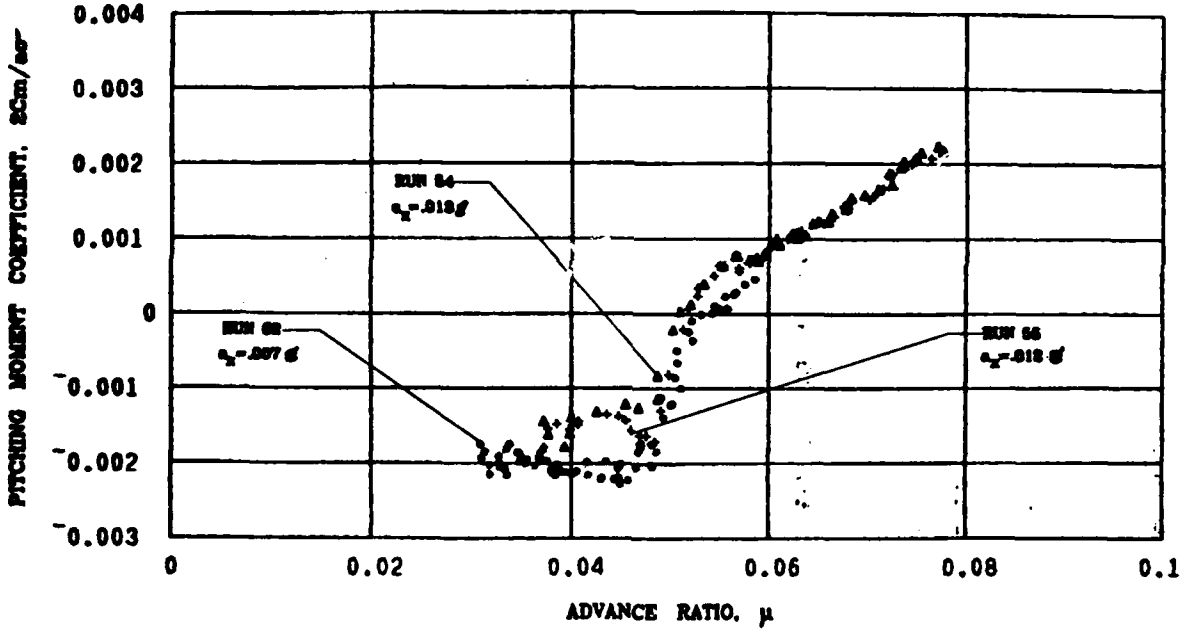

Figure 12. Variation of Rotor Force and Moment Coefficients with Advance Ratio and Translational Acceleration, $\theta_c = 9.8^o$, $\bar{h} = 0.23$, a_x Varying.

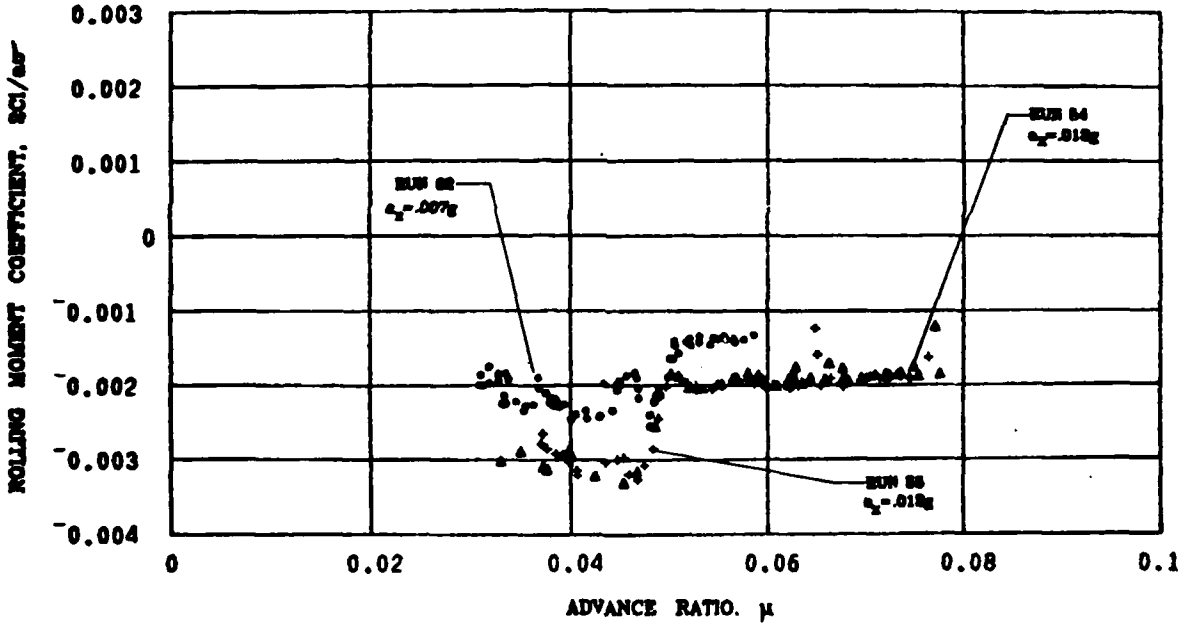

Figure 12. Continued.

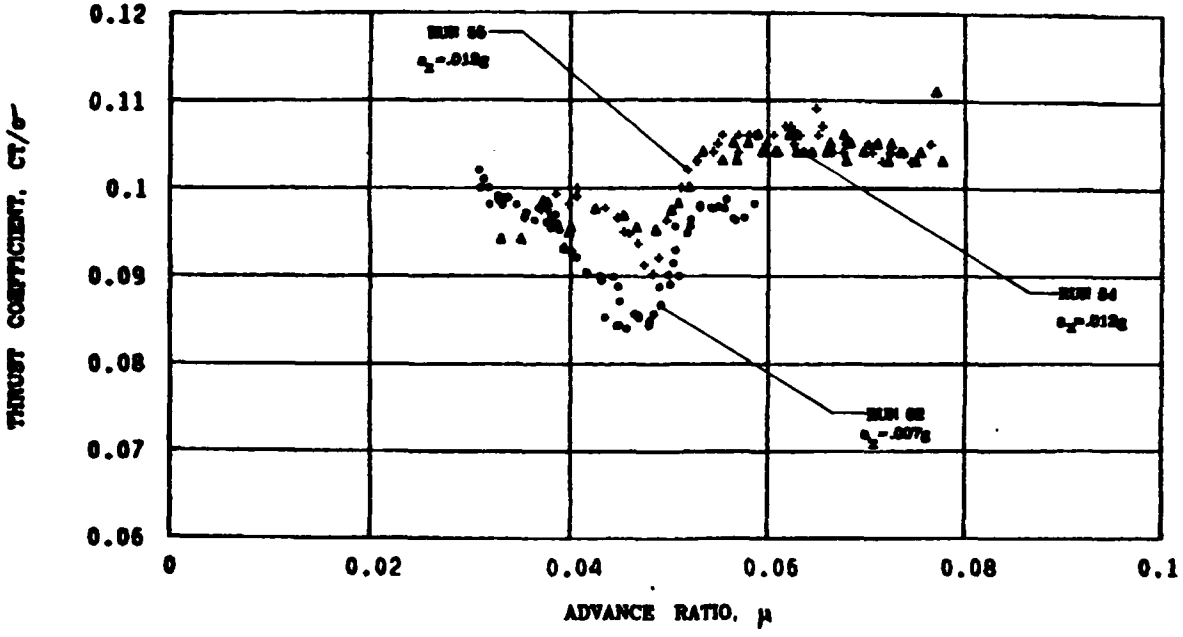

Figure 12. Continued.

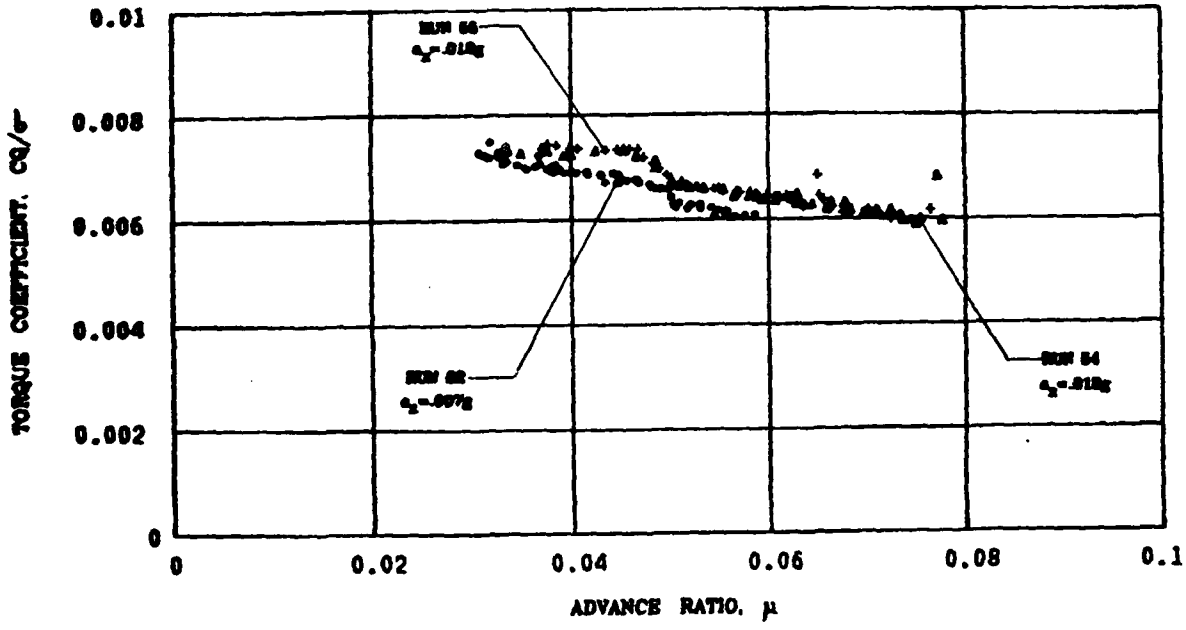

Figure 12. Continued.

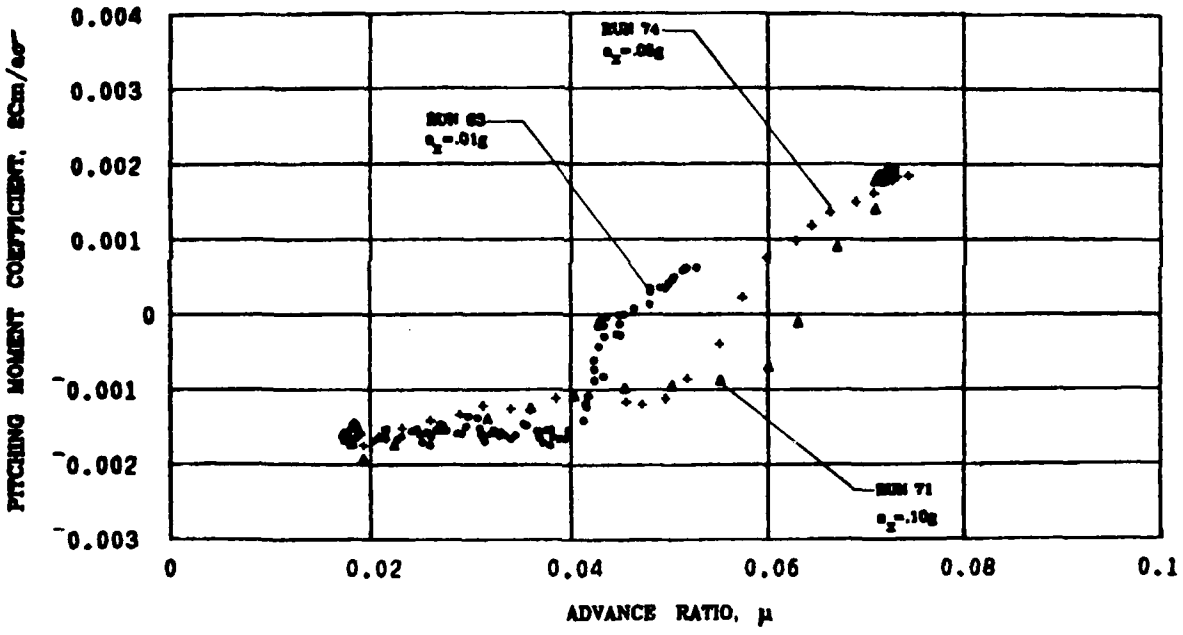

Figure 13. Variation of Rotor Force and Moment Coefficients with Advance Ratio and Translational Acceleration, $\theta_c = 9.8^o$, $\bar{h} = 0.34$, a_x Varying.

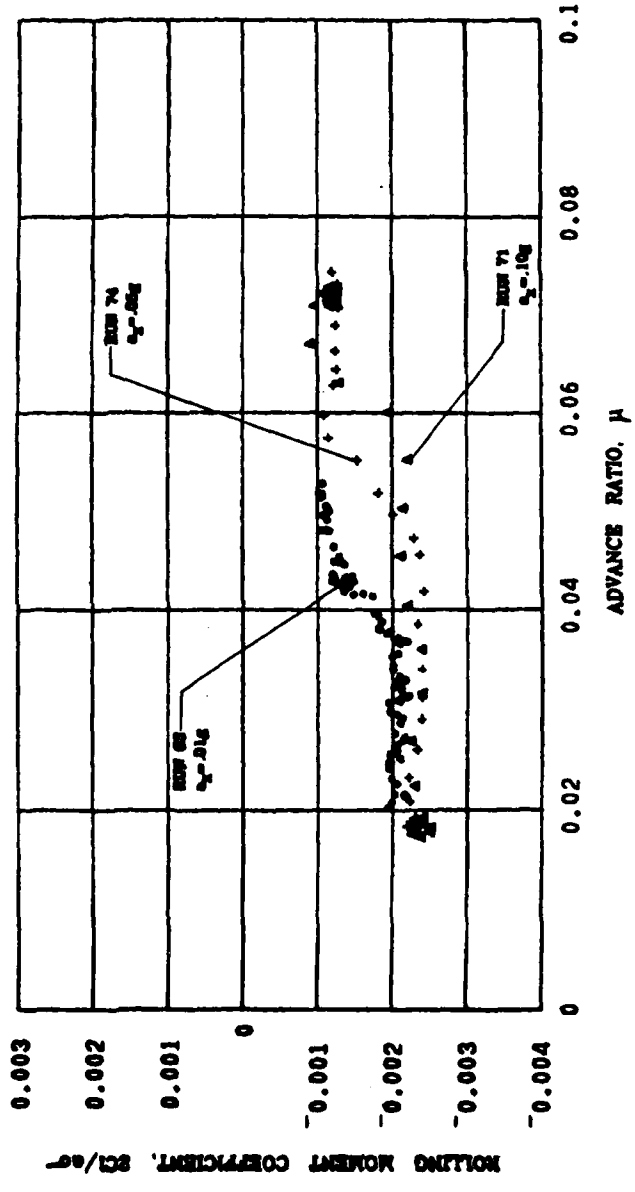

Figure 13. Continued.

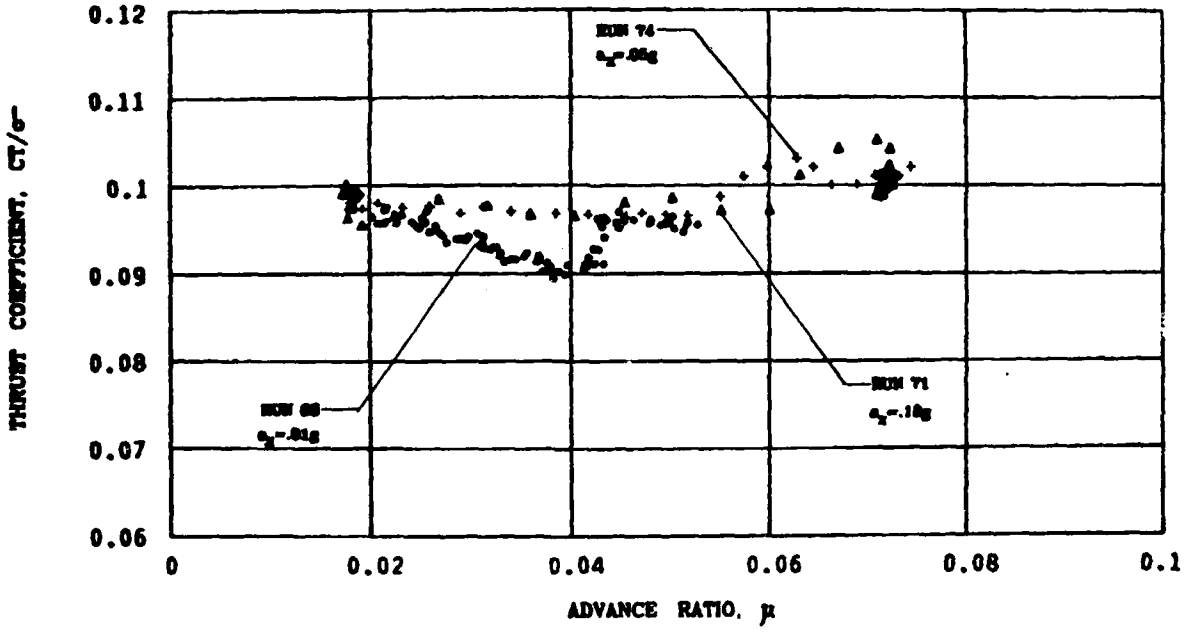

Figure 13. Continued.

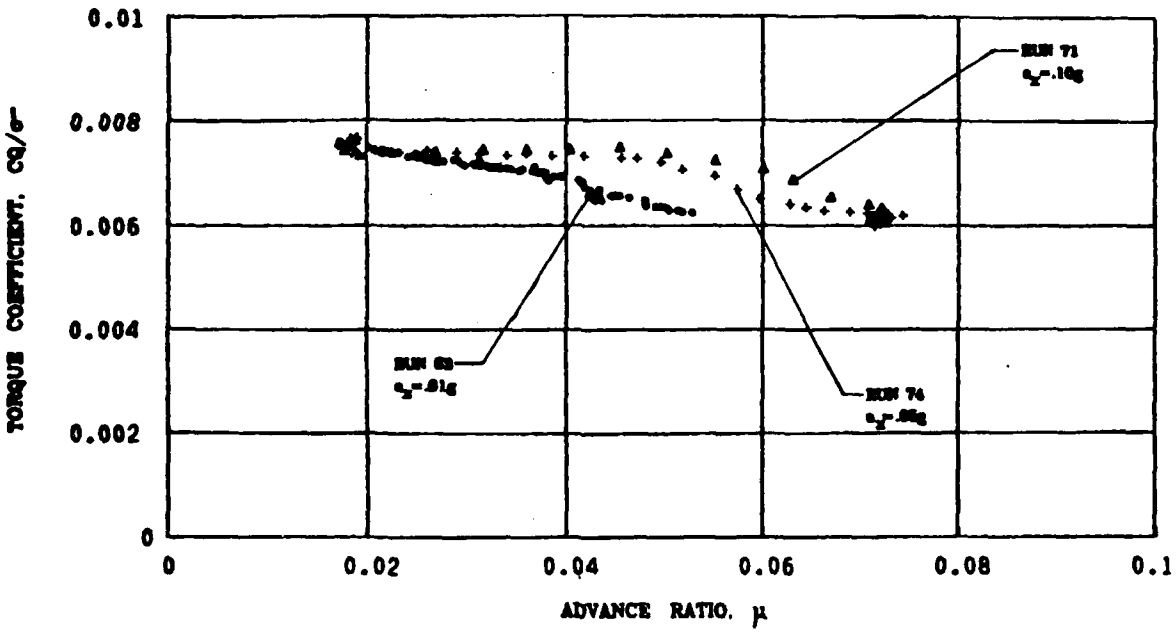

Figure 13. Continued.

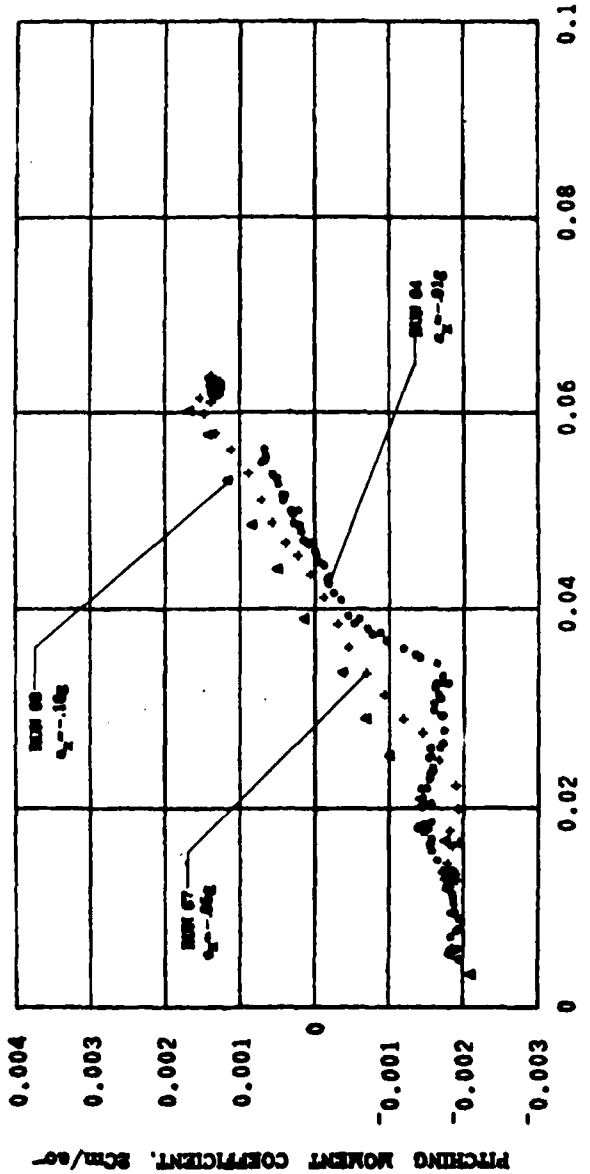

Figure 14. Variation of Rotor Force and Moment Coefficients with Advance Ratio and Translational Deceleration, $\theta_c = 9.8^o$, $i_s = 0.34$, a_x Varying.

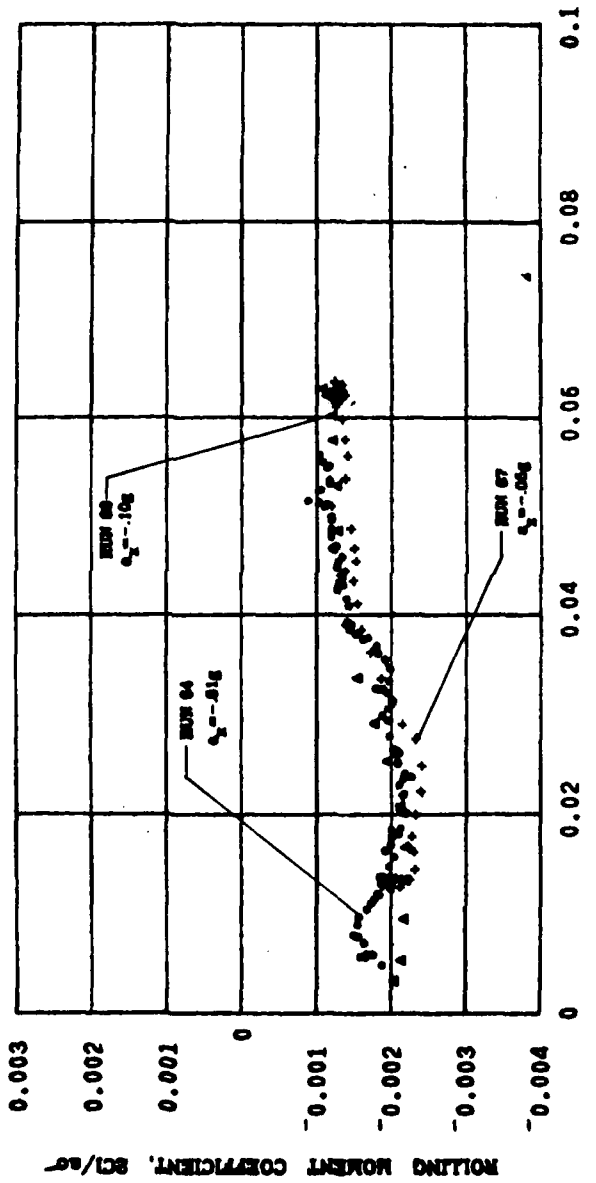

Figure 14. Continued.

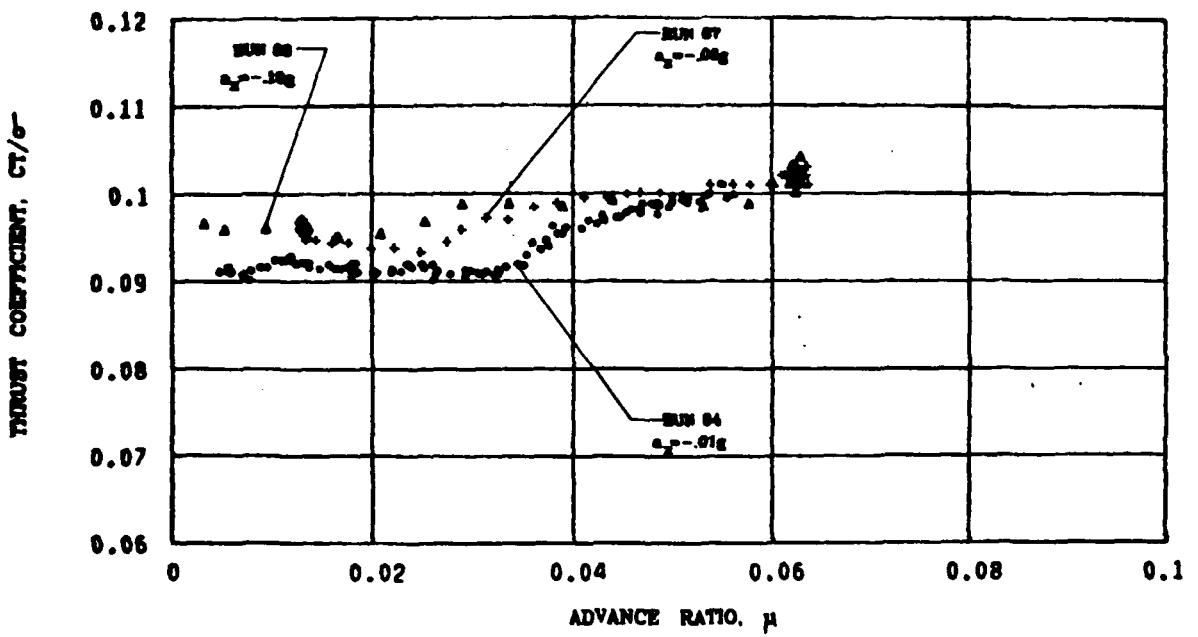

Figure 14. Continued.

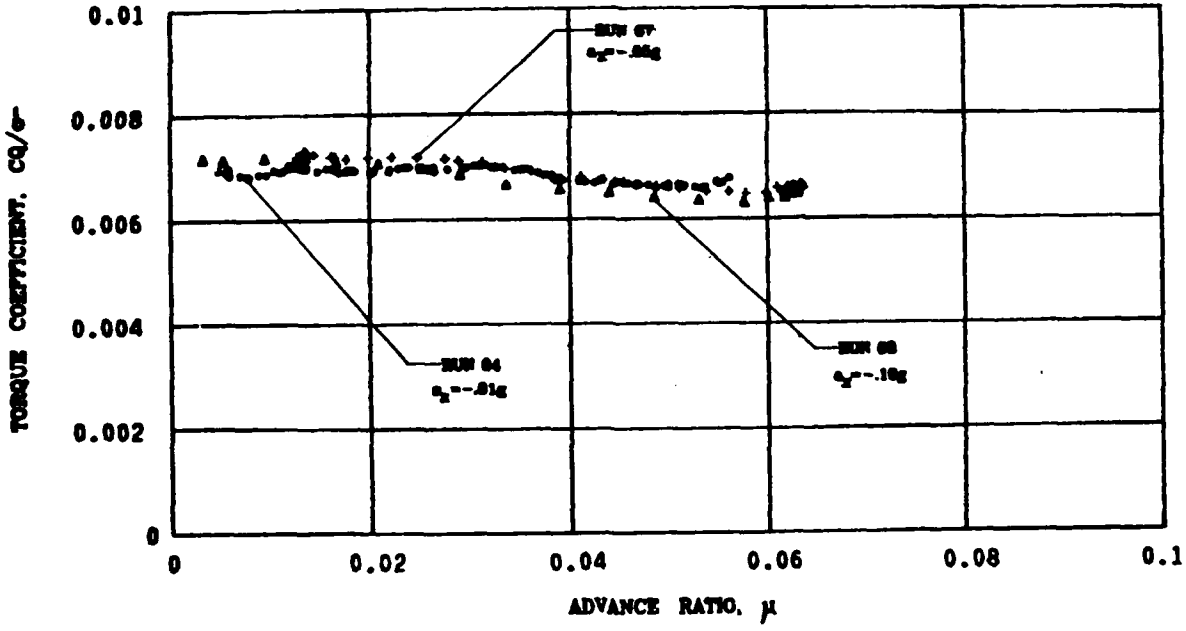

Figure 14. Continued.

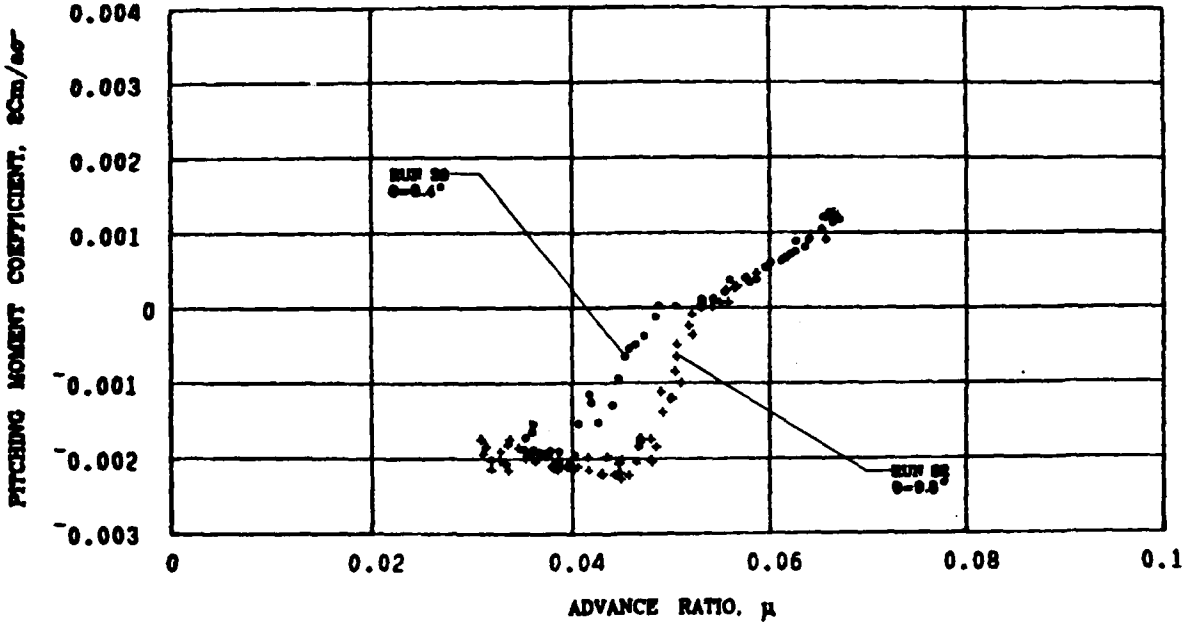

Figure 15. Variation of Rotor Force and Moment Coefficients with Advance Ratio and Collective Pitch, $\bar{h}$ = 0.23, a_x = 0.01g.

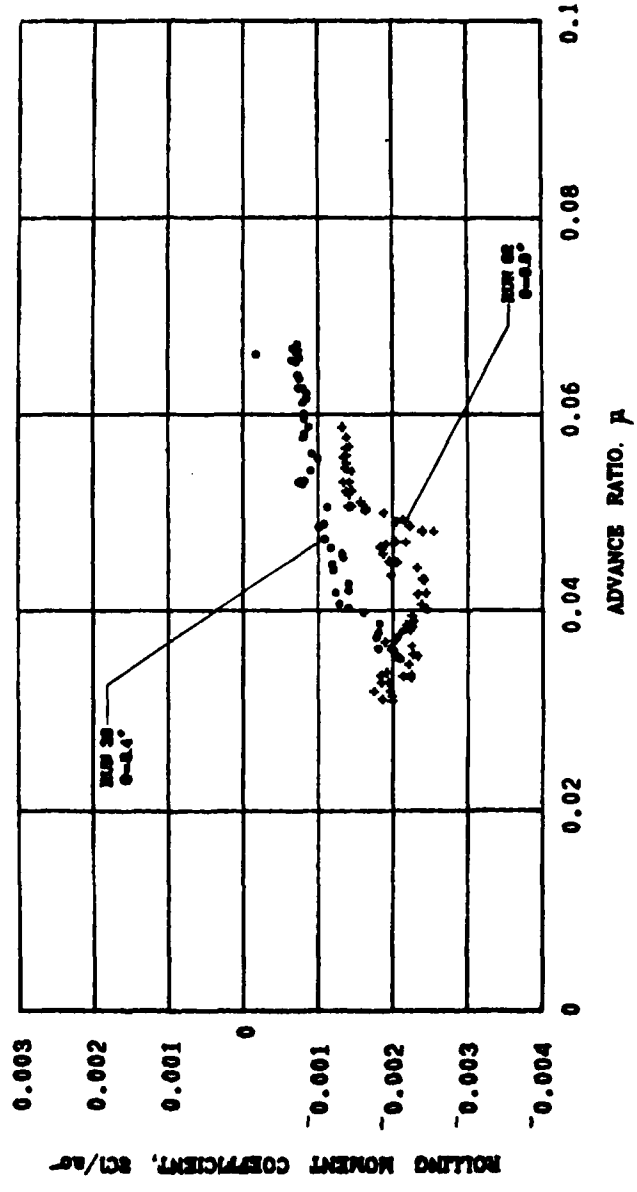

Figure 15. Continued.

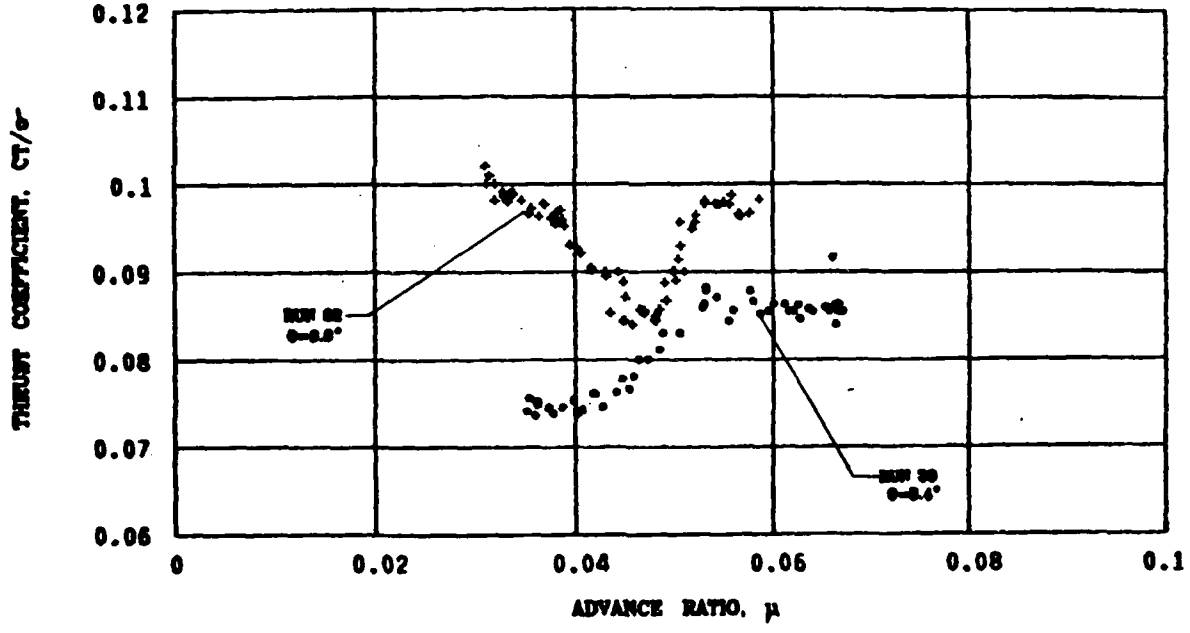

Figure 15. Continued.

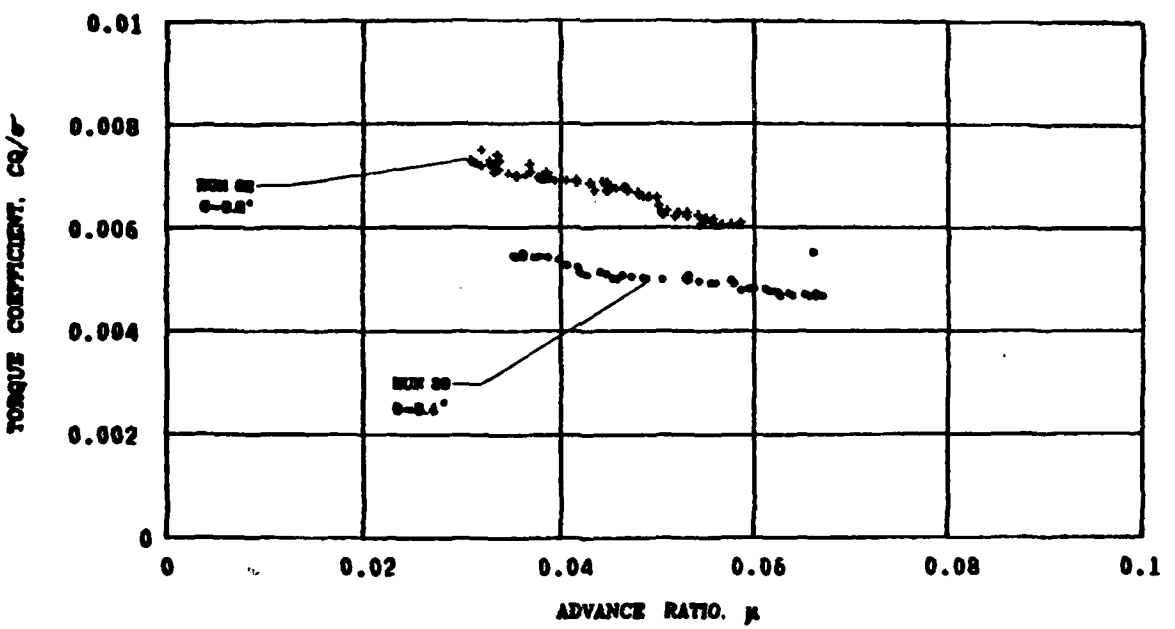

Figure 15. Continued.

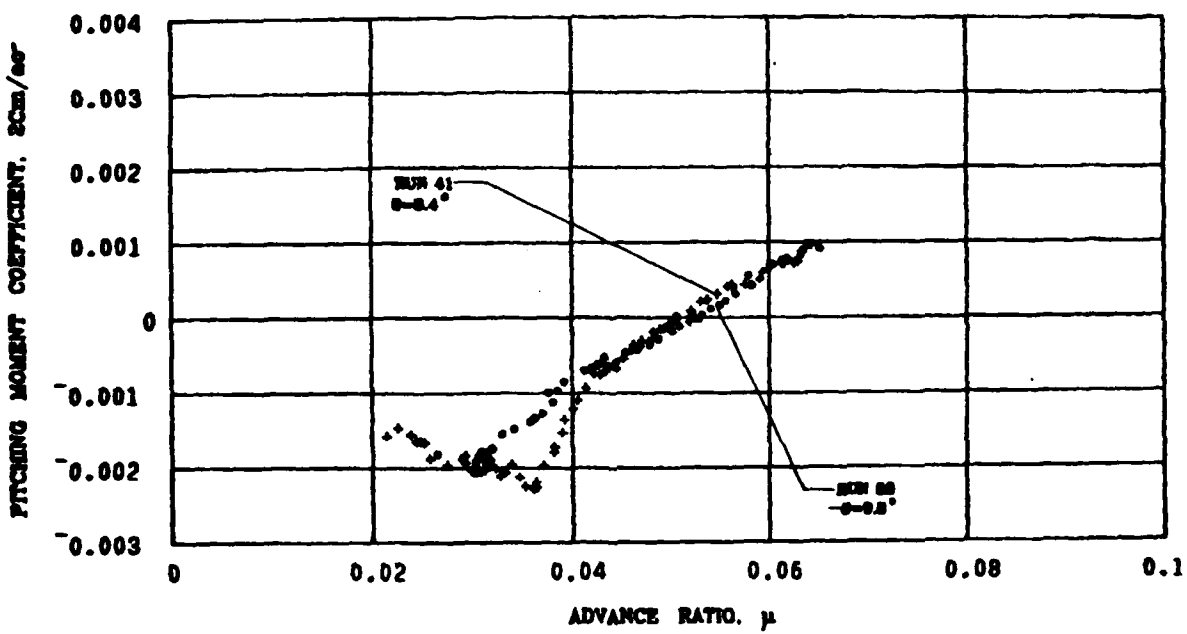

Figure 16. Variation of Rotor Force and Moment Coefficients with Advance Ratio and Collective Pitch, $\bar{h}$ = 0.23, a_x = -0.01g.

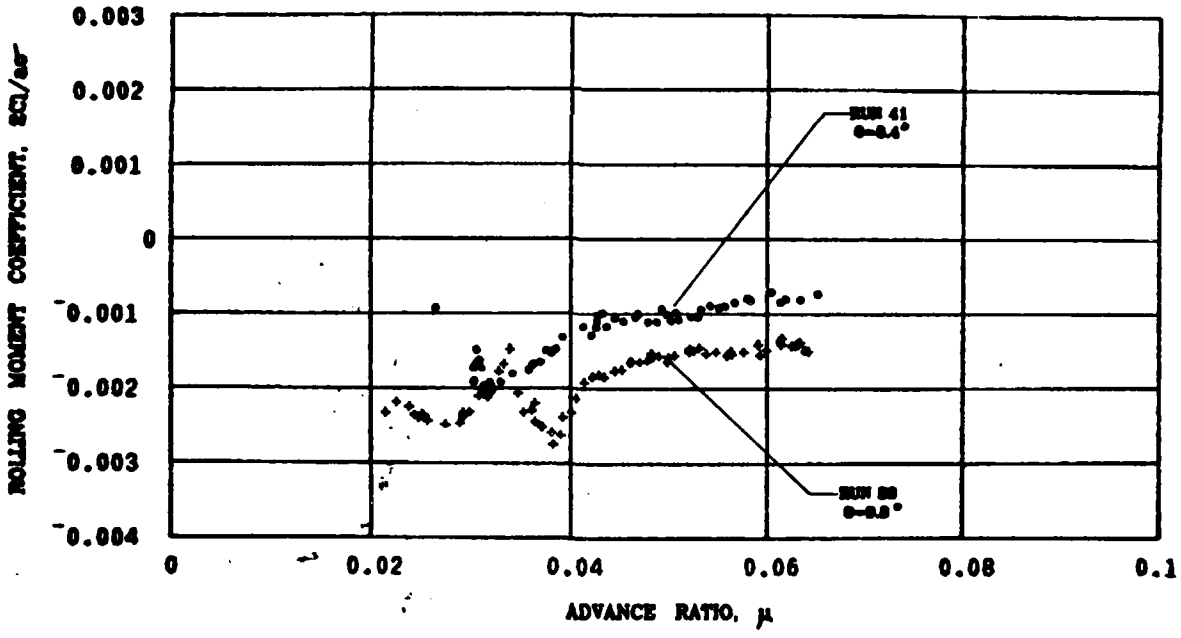

Figure 16. Continued.

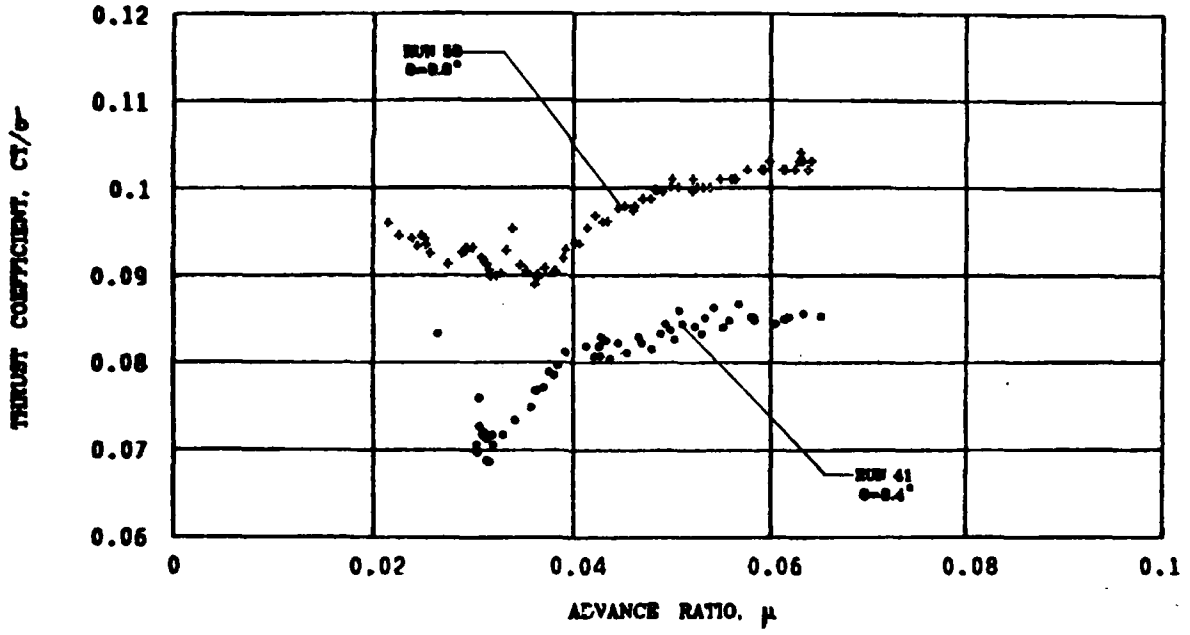

Figure 16. Continued.

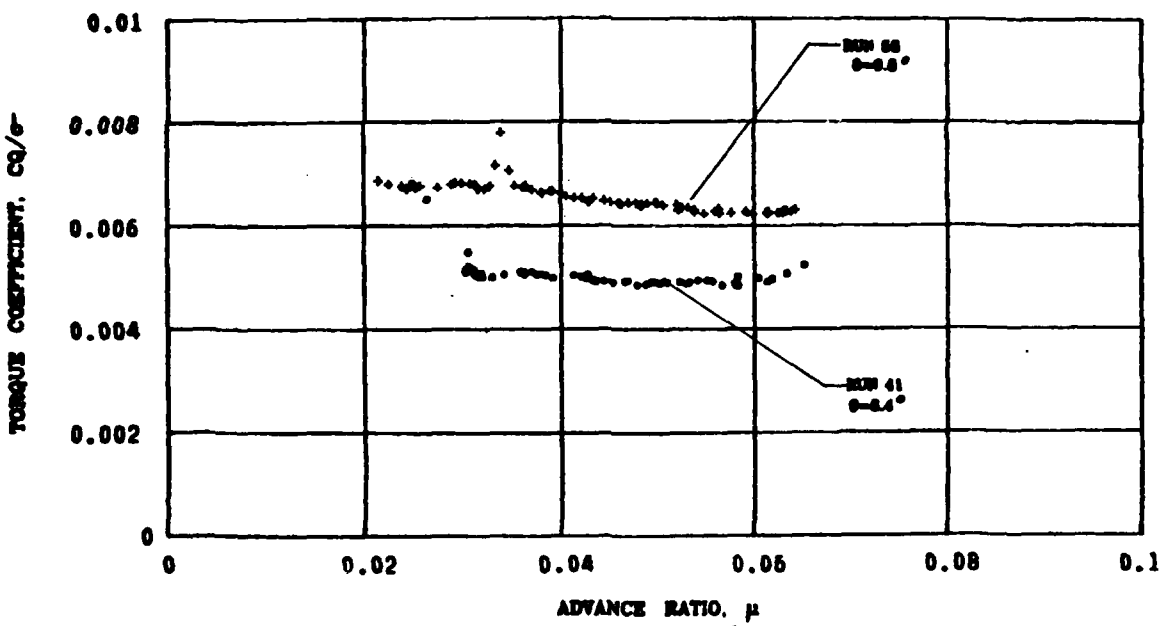

Figure 16. Continued.

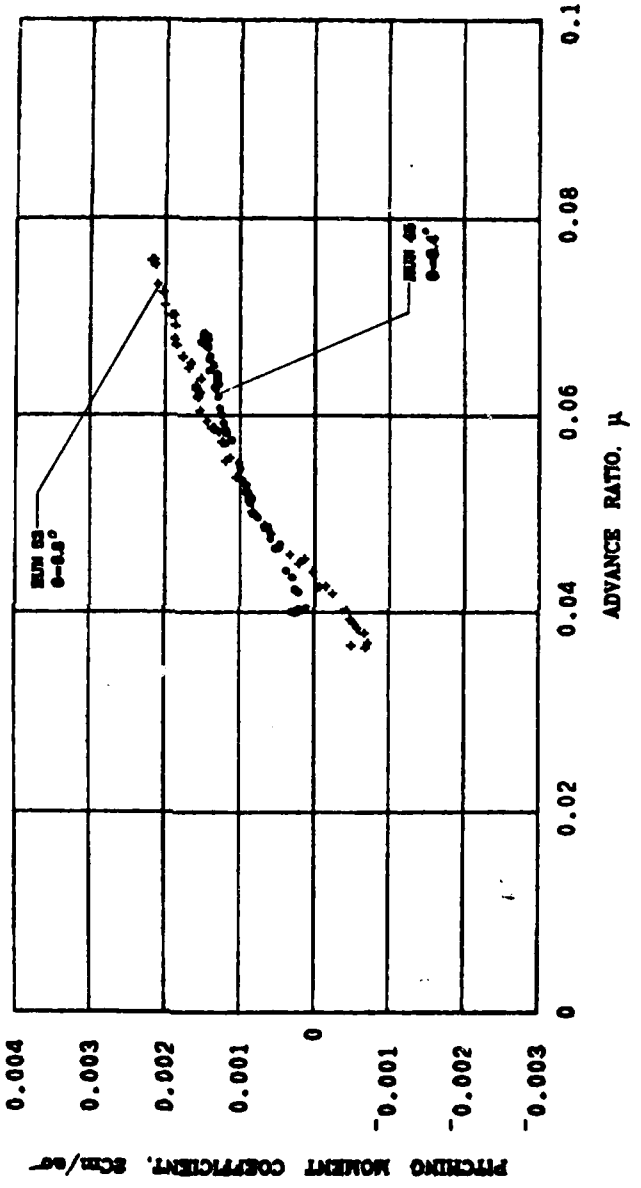

Figure 17. Variation of Rotor Force and Moment Coefficients with Advance Ratio and Collective Pitch, $\bar{h} = 0.45$, $a_x = 0.01g$.

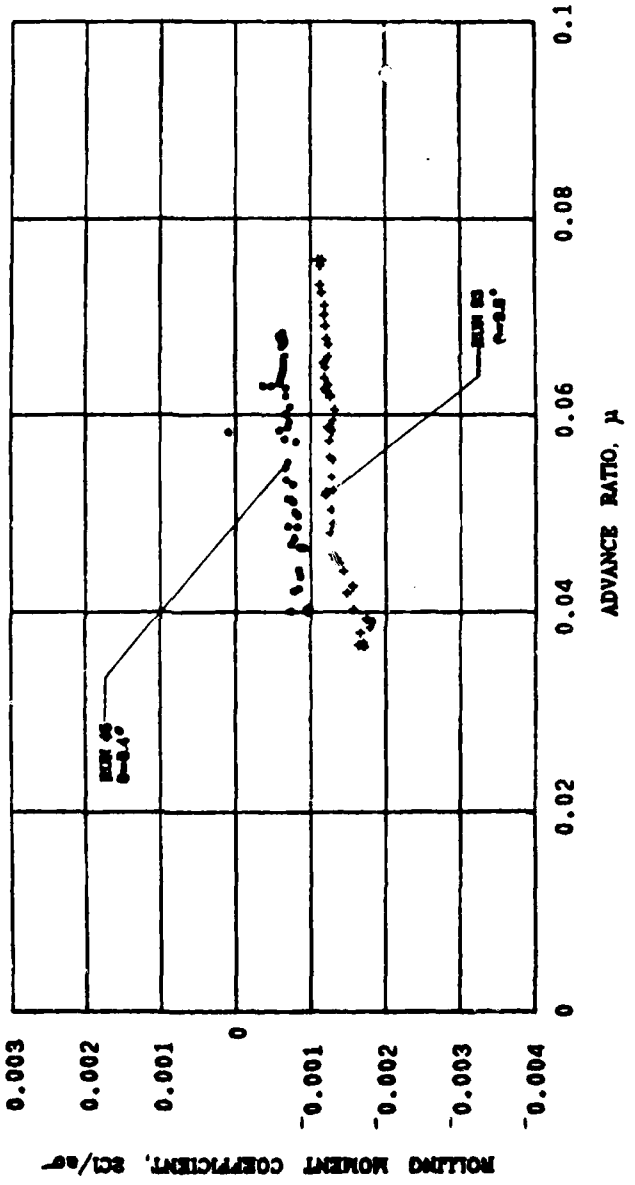

Figure 17. Continued.

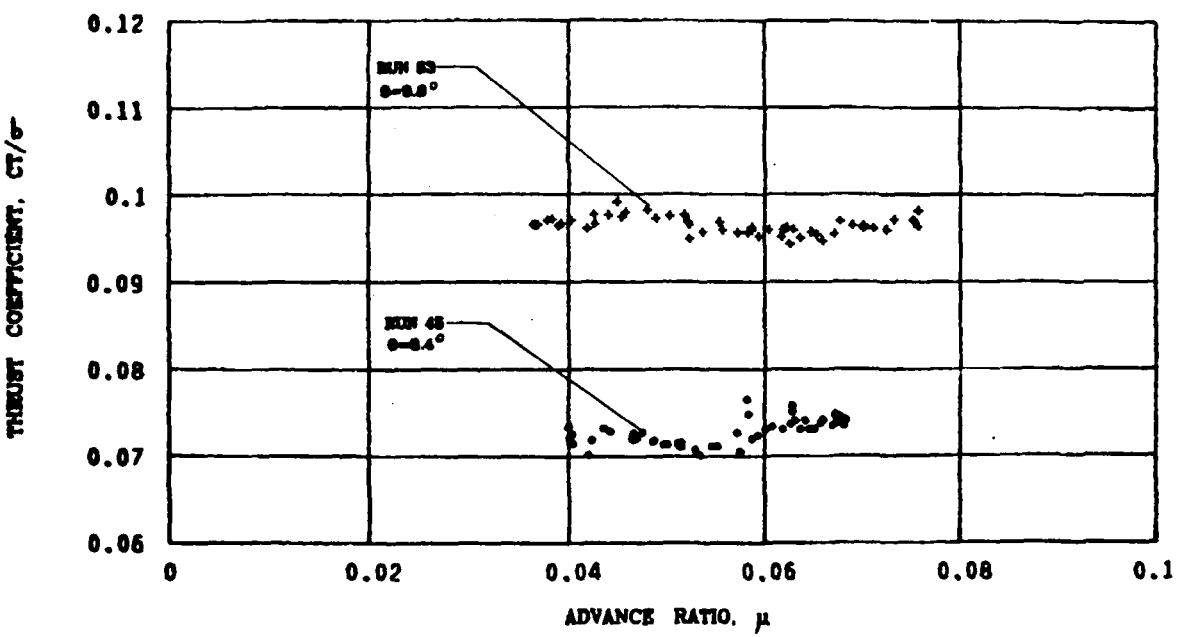

Figure 17. Continued.

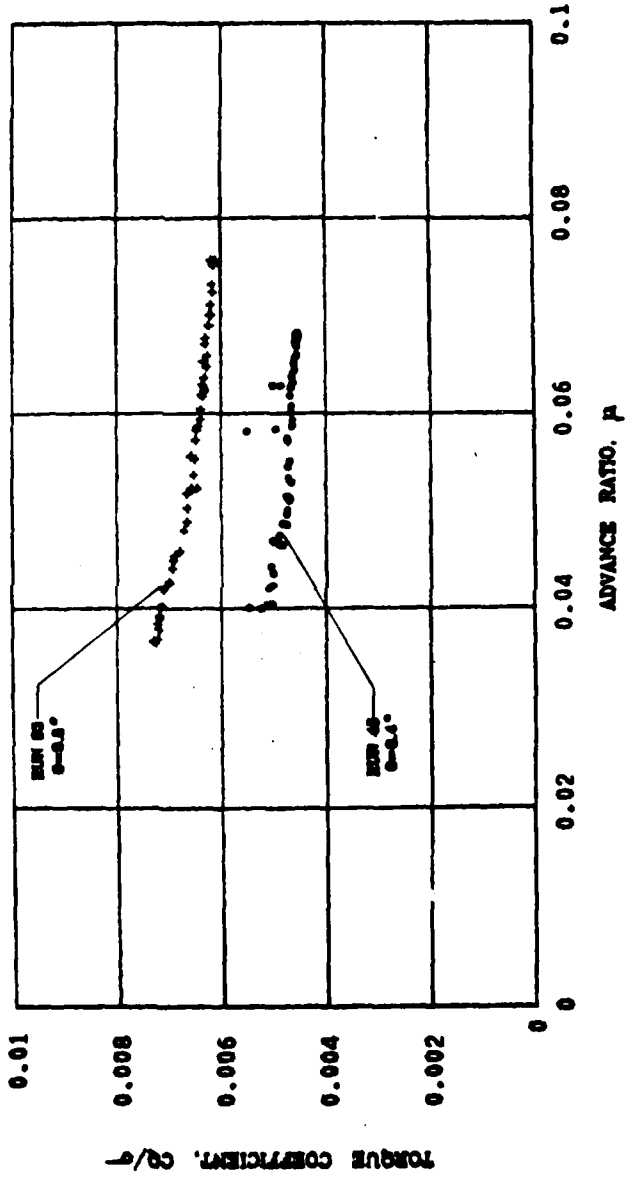

Figure 17. Continued.

REFERENCES

1. Sheridan, P. F. and Wiesner, W., "Aerodynamics of Helicopter Flight Near the Ground", Paper No. 77.33-04, presented at the 33rd Annual National Forum of the American Helicopter Society, Washington, DC May 1977.

2. Huston, R. J. and Morris, C. E. K., Jr., "A Wind-Tunnel Investigation of Helicopter Directional Control in Rearward Flight in Ground Effect", NASA Technical Note D-6118, March 1971.

3. Curtiss, H. C., Jr., Sun, M., Putman, W. F., and Hanker, E. J., Jr., "Rotor Aerodynamics in Ground Effect at Low Advance Ratios", AHS Preprint No. 81-5, presented at the 37th Annual Forum of the American Helicopter Society, New Orleans, LA, May 1981.

PUBLICATION

A paper on this research entitled "Rotor Aerodynamics in Ground Effect at Low Advance Ratios" was presented at the 37th Annual Forum of the American Helicopter Society, May 1981 (AHS Preprint 81-5). This paper has been submitted for publication to the Journal of the American Helicopter Society.

PERSONNEL

In addition to Professor H. C. Curtiss, Jr., the Principal Investigator and Mr. W. F. Putman, a Senior Technical Staff Member, the following graduate students were supported by this research program during the period September 10, 1979 to February 29, 1982. This work has been funded by the Army Research Office under two Grant Numbers. For the period September 10, 1978 through September 9, 1980 the Grant Number was DAAG-29-78-G-0194 and for the period September 10, 1980 through February 29, 1982, DAAG-29-80-K-0098.

1978-79 S. Parvez. Mr. Parvez worked on this project for a brief period of time and then decided to work on another topic.

1979-80 E. Hanker. Mr. Hanker completed course work and research for the MSE degree and is presently working at Boeing-Vertol. I expect that he will complete his M.S.E. thesis during August 1982 and receive his MSE degree in October 1982. Mr. Hanker won the Mideast Region Lichten Award (March 1981) for a paper based on his research.

1980-82 F. Ebert. Mr. Ebert contributed to this research program during the 1980-81 academic year. He decided to take a leave of absence from graduate school and has been working at Sikorsky Aircraft since June 1981. He plans to return to Princeton to continue graduate study in September 1982.

M. Sun. Mr. Sun is currently continuing research for his Ph.D. dissertation on rotor aerodynamics in ground effect. He completed the required course work for the Ph.D. degree and passed the General Examination in May 1981. He received the M.A. degree in June 1981. I expect that he will complete his dissertation in June 1983 on the topic of rotor aerodynamics in ground effect.

APPENDIX A

EXPERIMENTAL DATA

Figures A-1 through A-14 present additional experimental data taken in the course of this research program that is not presented or discussed in the main body of the report.

Figure A-1 shows experimental results for the force and moment coefficients at a collective pitch of 8.4^{o} and a height-to-diameter ratio of 0.23 at various advance ratios for steady conditions with no translational acceleration. Figures A-2 and A-3 show the effect of acceleration and deceleration for the same collective pitch and height-to-diameter ratio as Figure A-1. Figure A-4 presents a direct comparison of the data presented in Figures A-1 through A-3. Figure A-5 shows the effects of acceleration and deceleration at $\theta_c = 8.4^{o}$, $\bar{h} = 0.45$.

Figures A-6 and A-7 show comparisons in two cases (acceleration and deceleration) where multiple runs were made at the same collective pitch and height-to-diameter ratio indicating the repeatibility of the experimental data particularly with respect to the effect of acceleration and deceleration.

Figures A-8 through A-10 show additional results on the effect of acceleration and deceleration.

Figures A-11 through A-14 show directly the effect of height-to-diameter ratio at various values of collective pitch and horizontal acceleration.

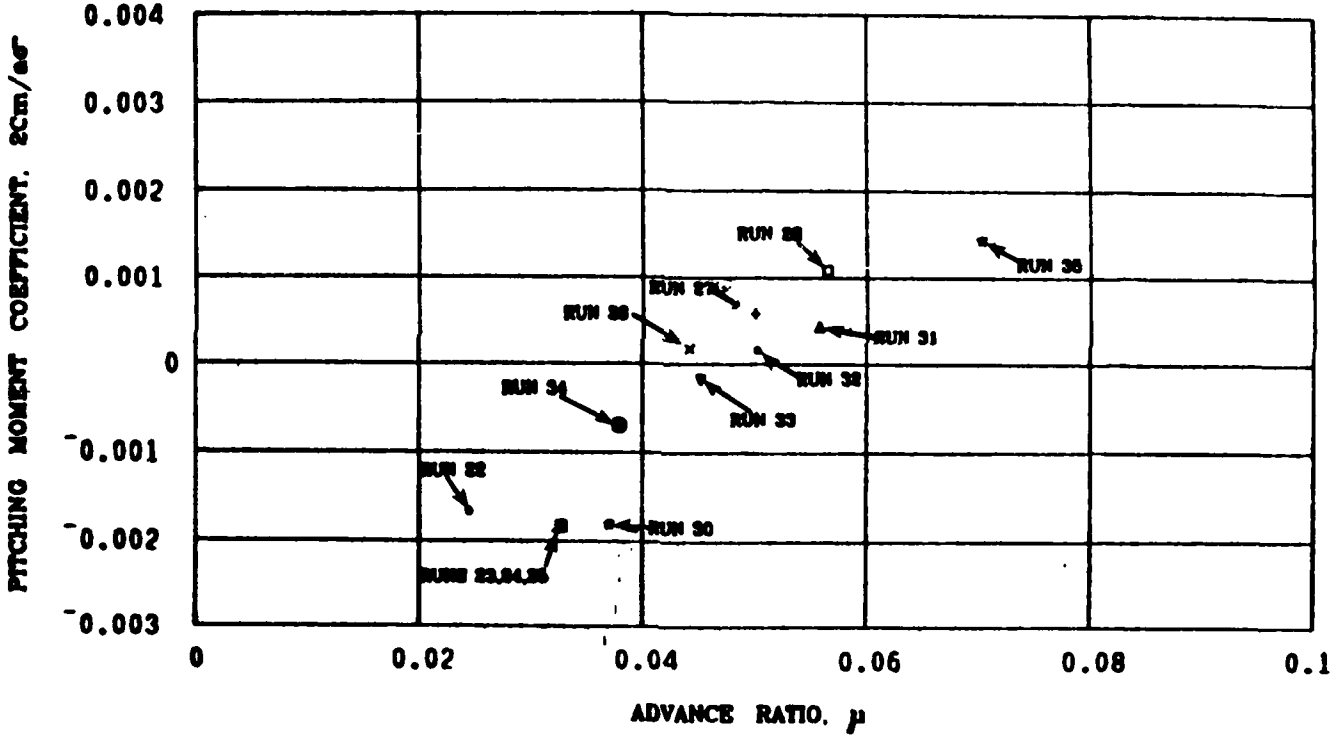

Figure A-1. Variation of Rotor Force and Moment Coefficients with Advance Ratio, $\theta_c = 8.4^o$, $\bar{h} = 0.23$. Measurements at Constant Velocity.

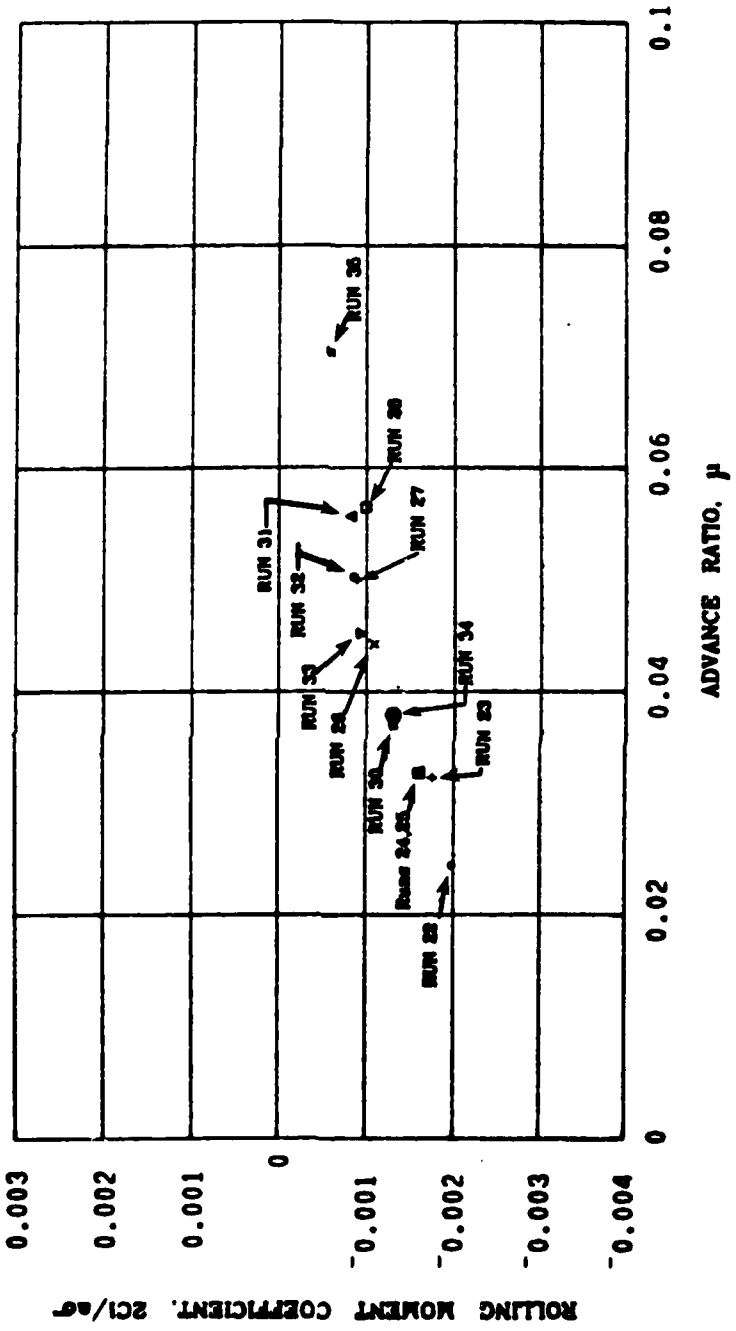

Figure A-1. Continued.

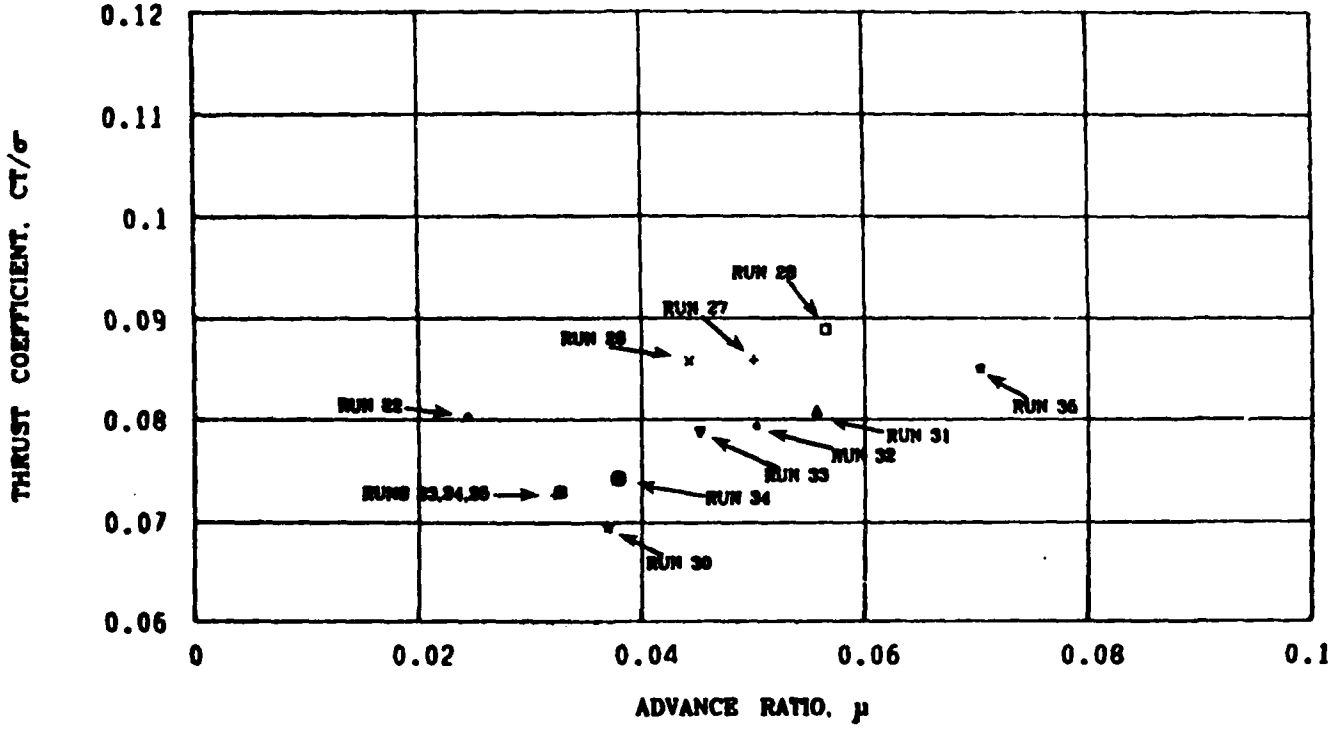

Figure A-1. Continued.

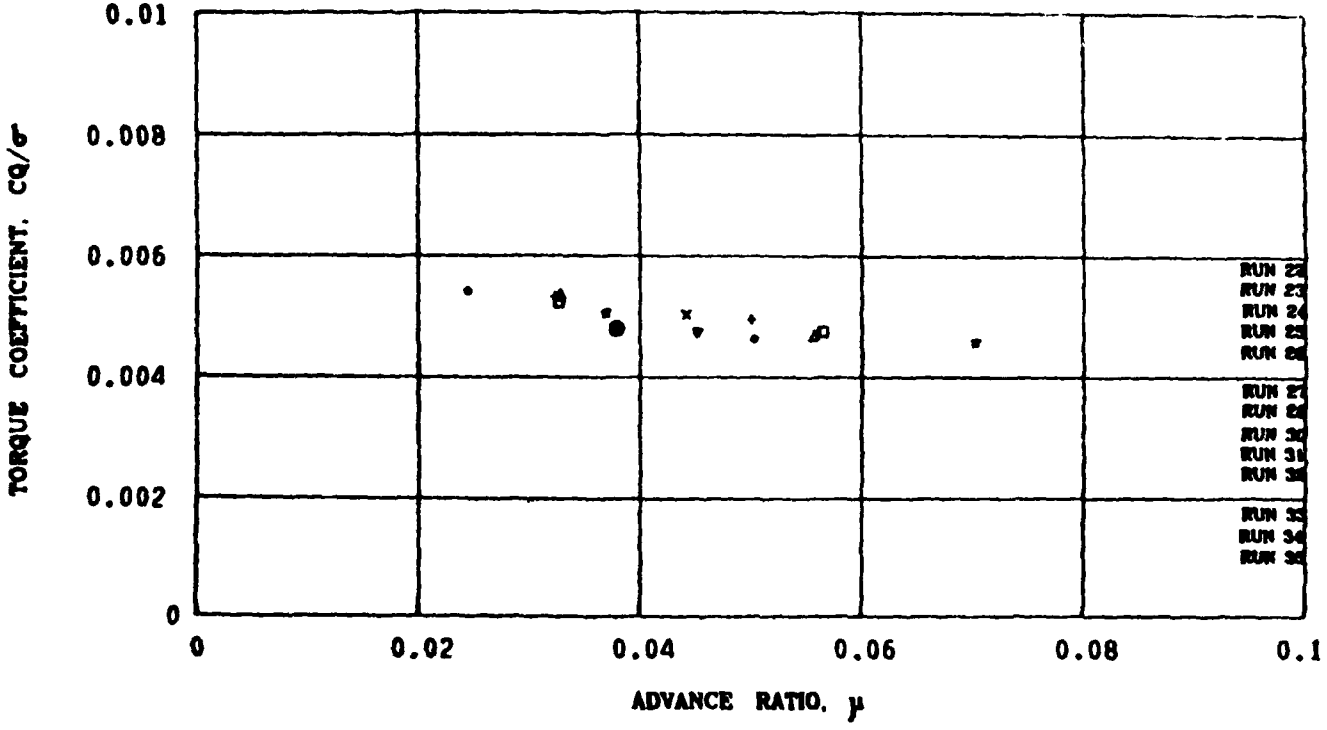

Figure A-1. Continued.

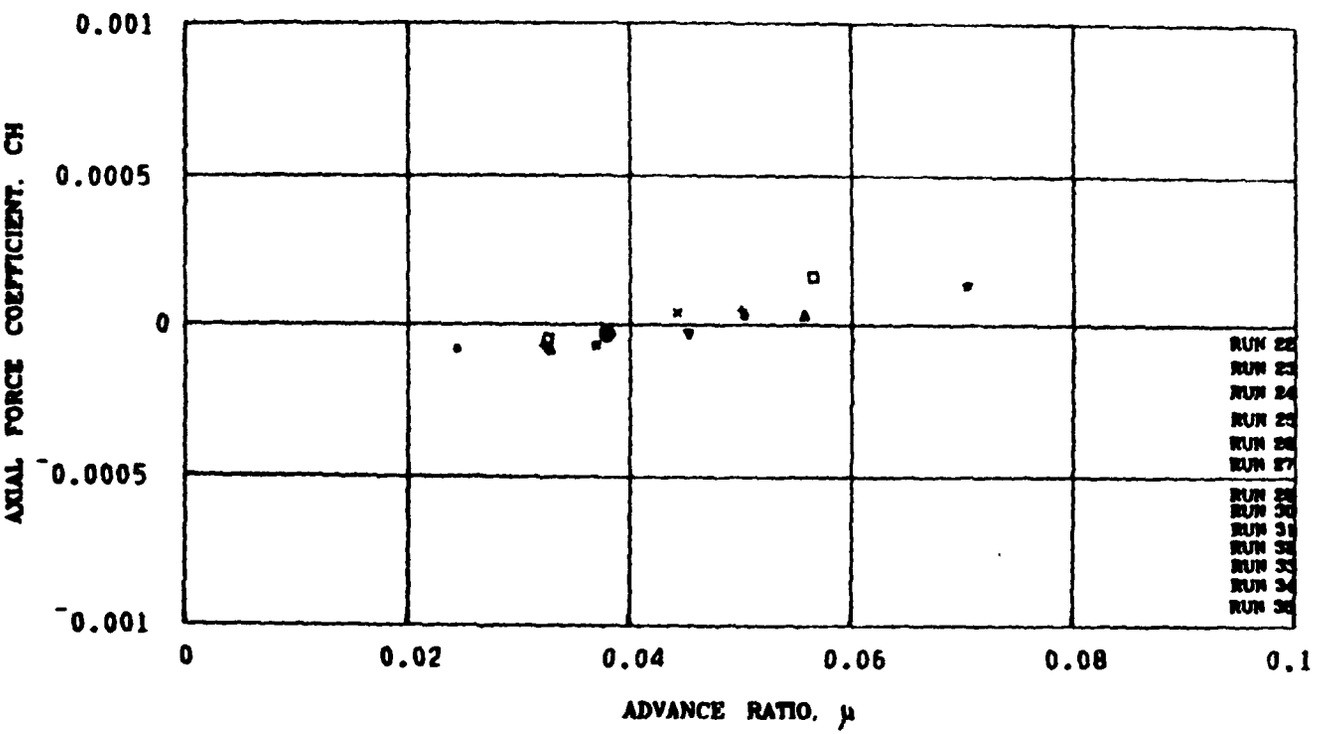

Figure A-1. Continued.

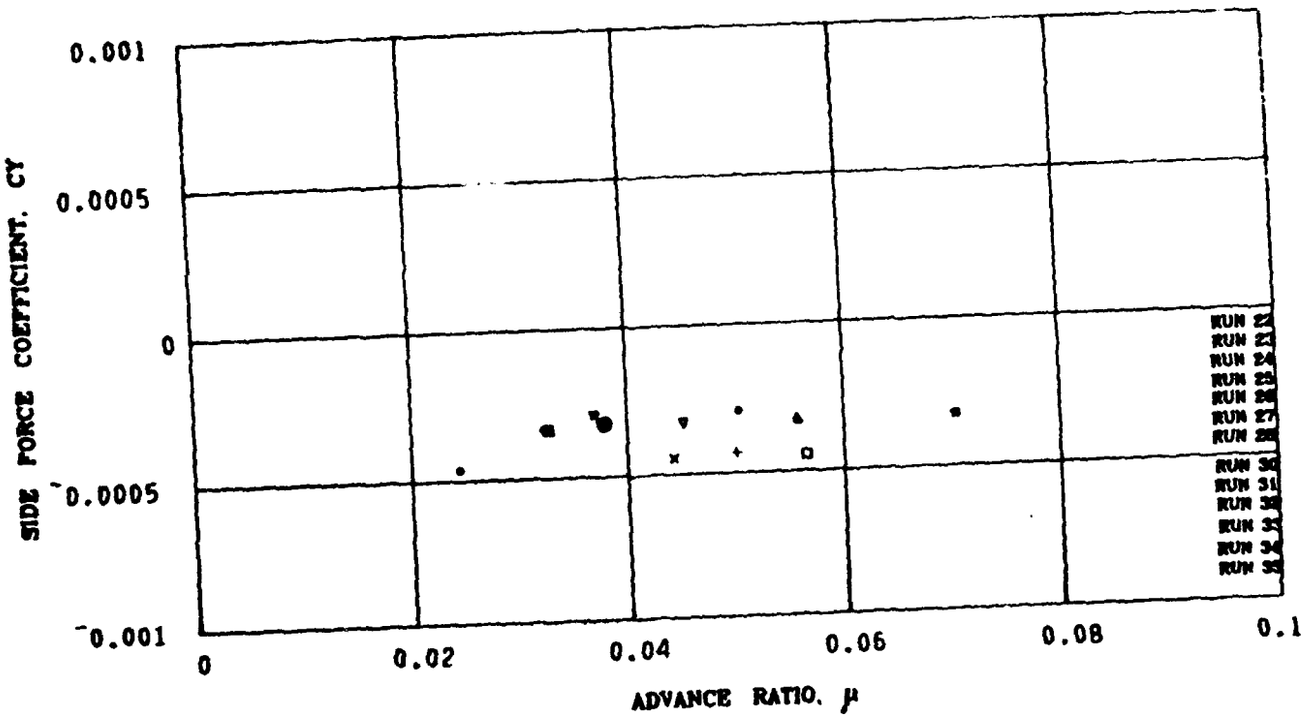

Figure A-1. Continued.

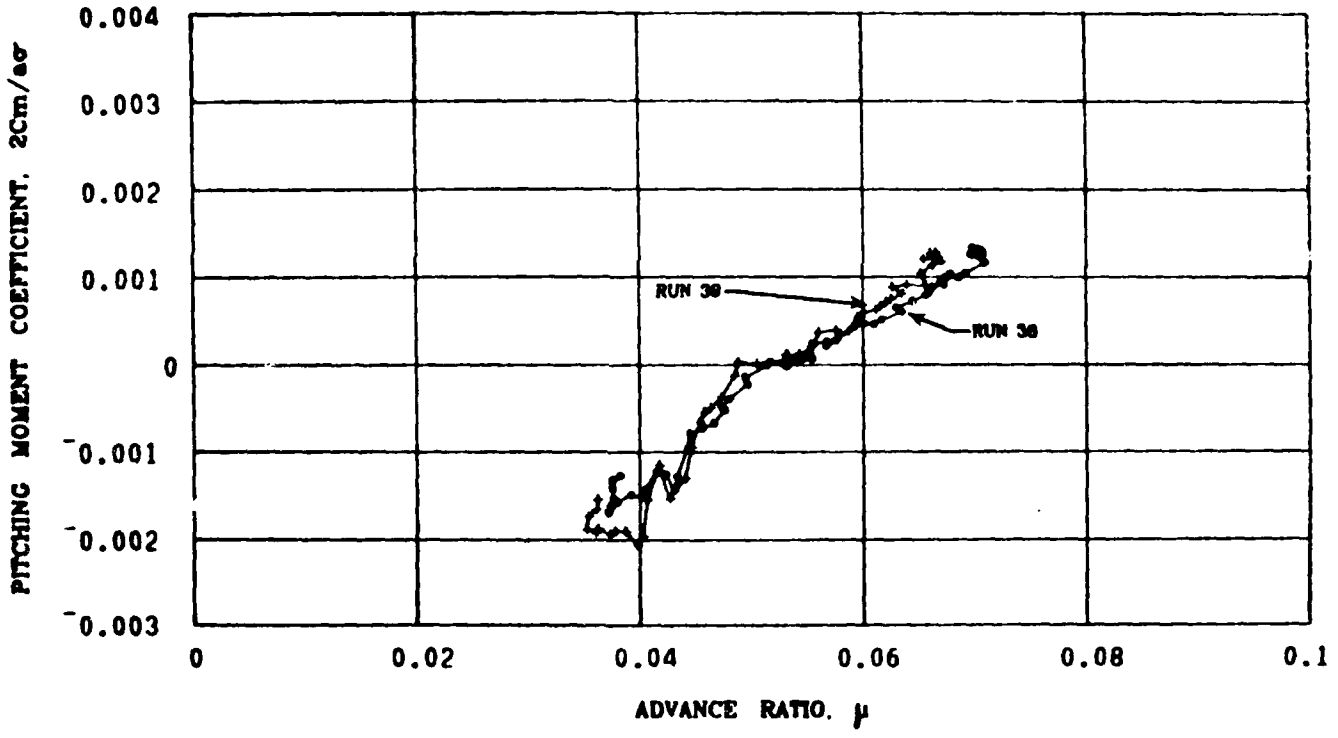

Figure A-2. Variation of Rotor Force and Moment Coefficients with Advance Ratio, $\theta_c = 8.4^{o}$, $\bar{h} = 0.23$, $a_x = 0.01g$.

AD-A118 609 PRINCETON UNIV NJ DEPT OF MECHANICAL AND AEROSPACE --ETC F/G 20/4
ROTOR AERODYNAMICS IN GROUND EFFECT AT LOW ADVANCE RATIOS.(U)
JUL 82 H C CURTISS, W F PUTMAN, E J HANKER DAAG29-80-K-0098
UNCLASSIFIED MAE-1571 ARO-16061.2-EG NL

2 OF 2
AD
A118 609

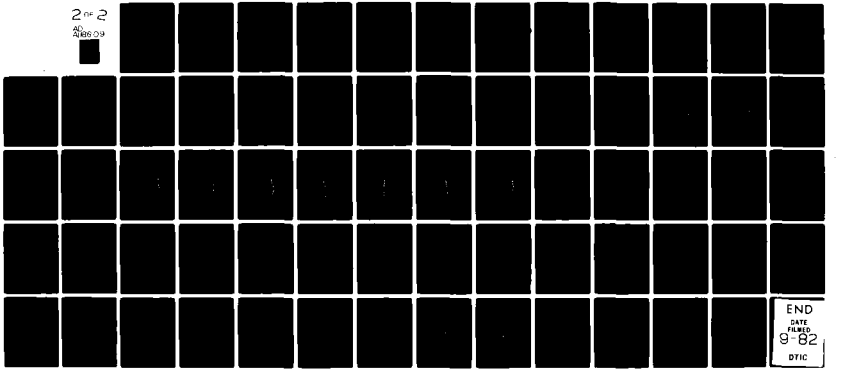

END
DATE FILMED
9-82
DTIC

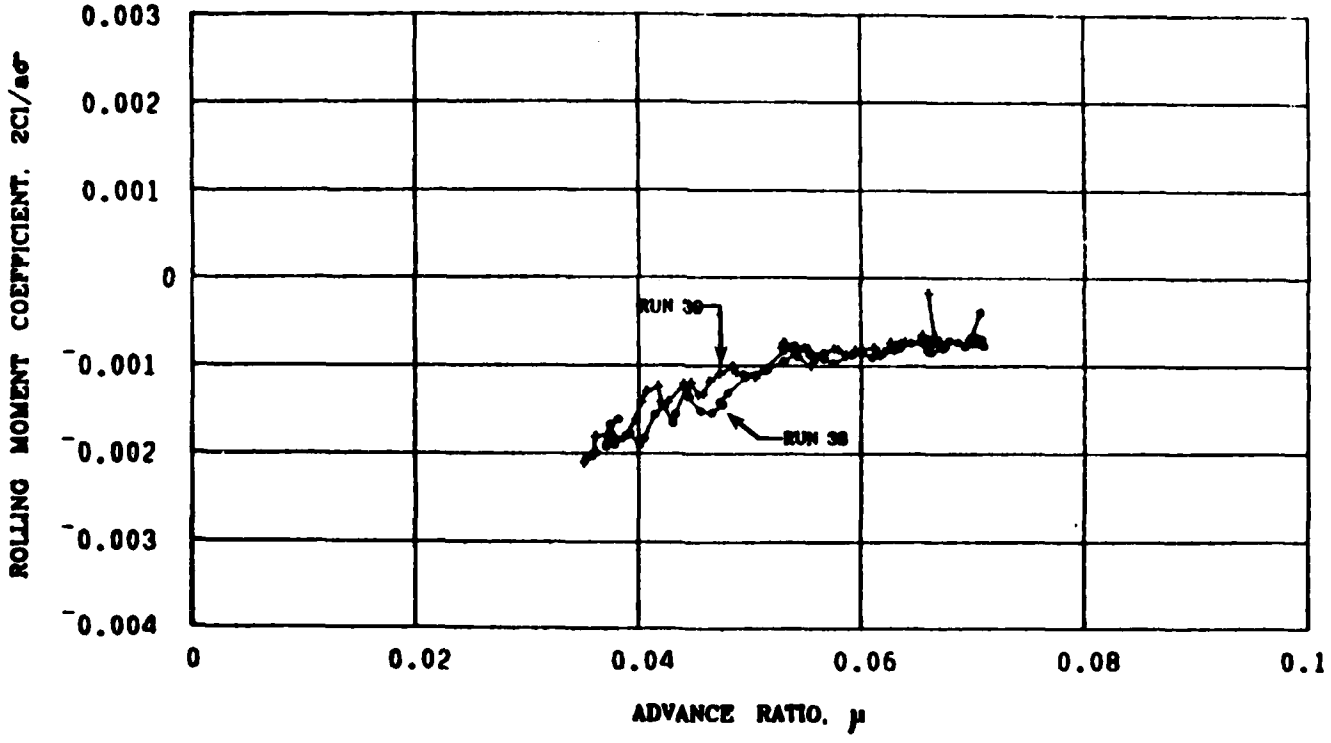

Figure A-2. Continued.

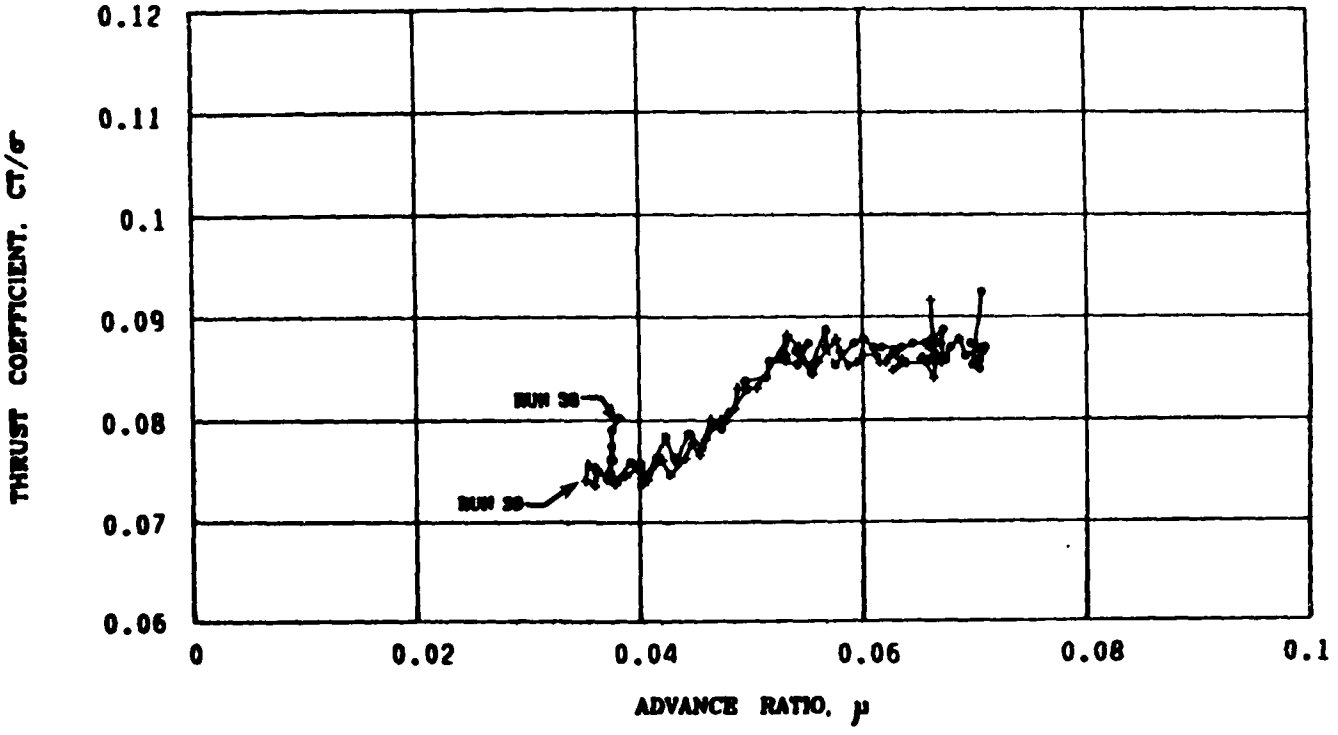

Figure A-2. Continued.

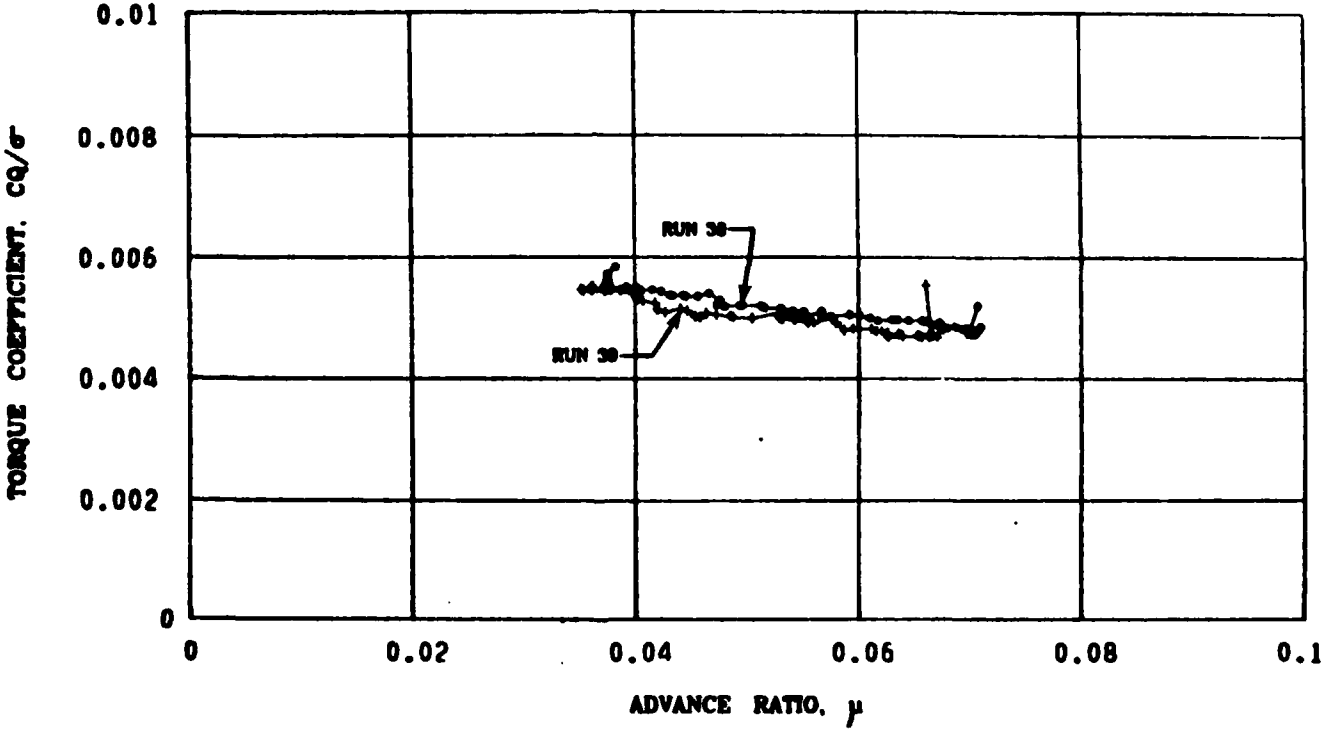

Figure A-2. Continued.

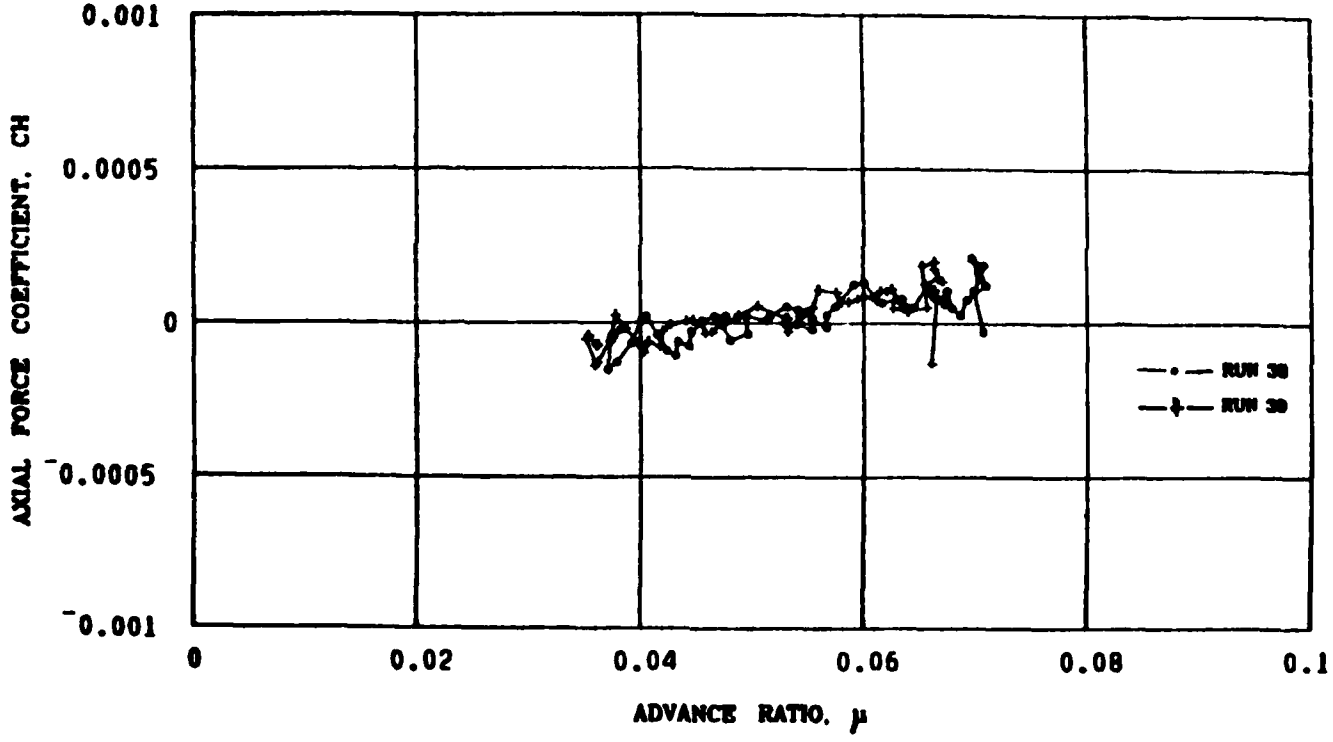

Figure A-2. Continued.

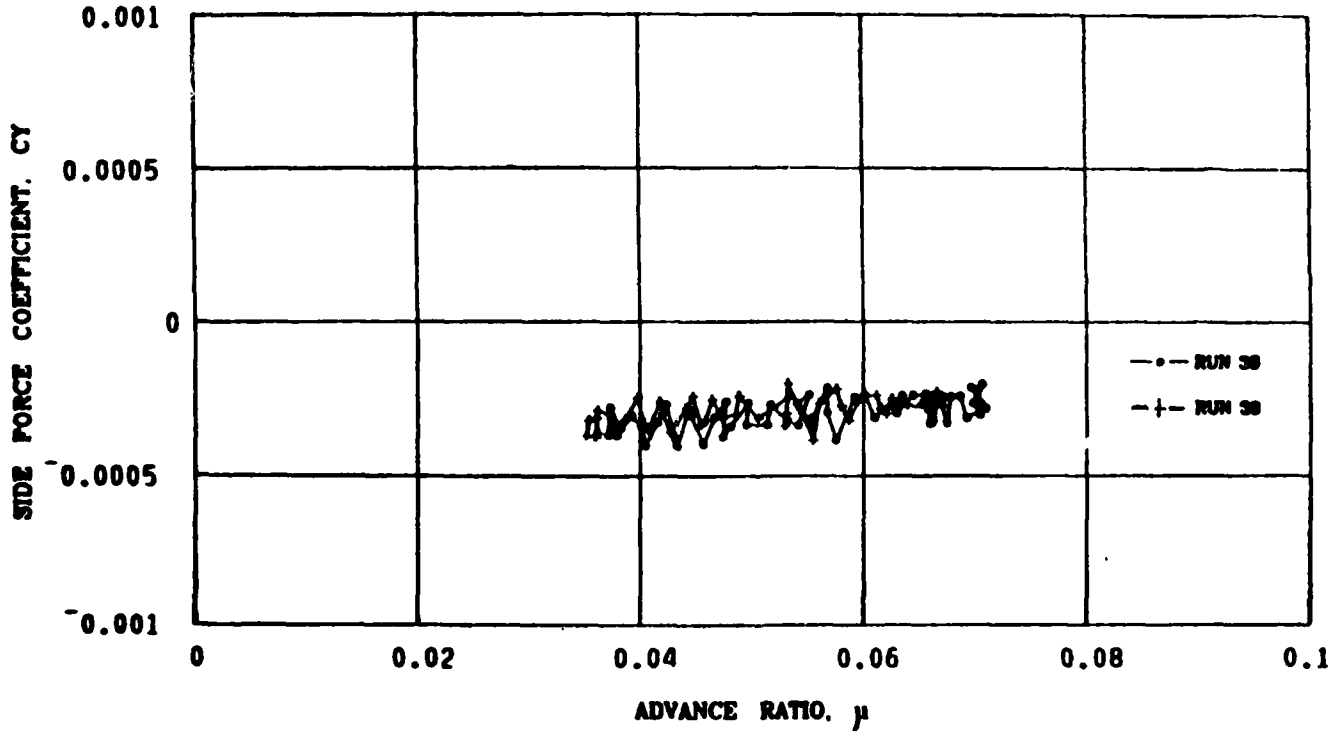

Figure A-2. Continued.

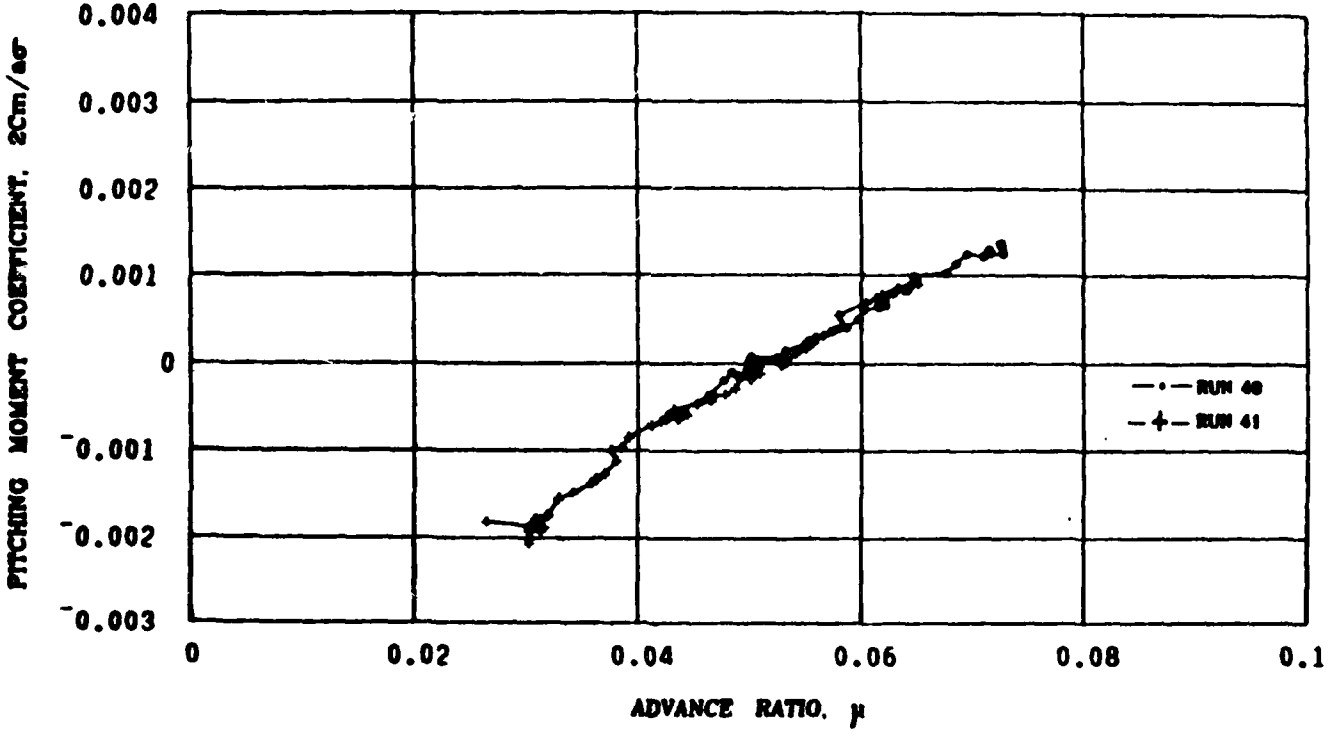

Figure A-3. Variation of Rotor Force and Moment Coefficients with Advance Ratio, $\theta_c = 8.4^o$, $\bar{h} = 0.23$, $a_x = -0.01g$.

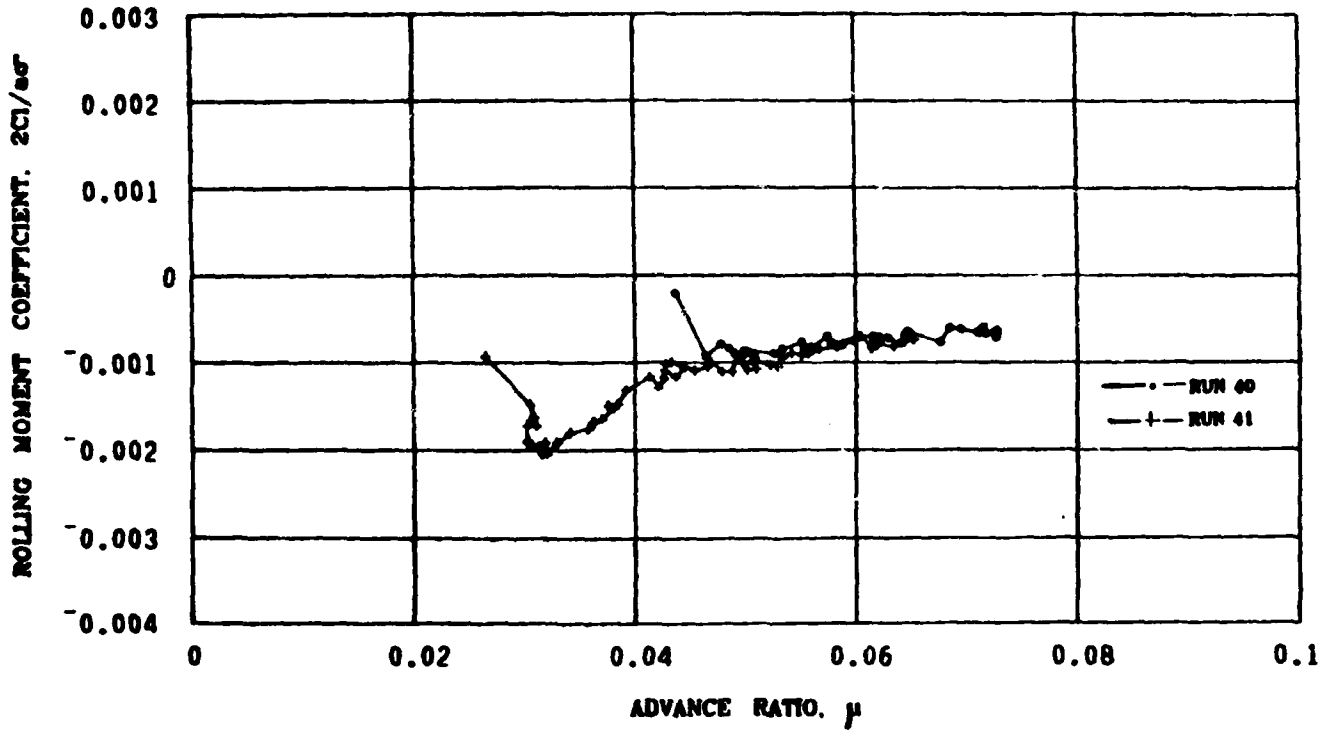

Figure A-3. Continued.

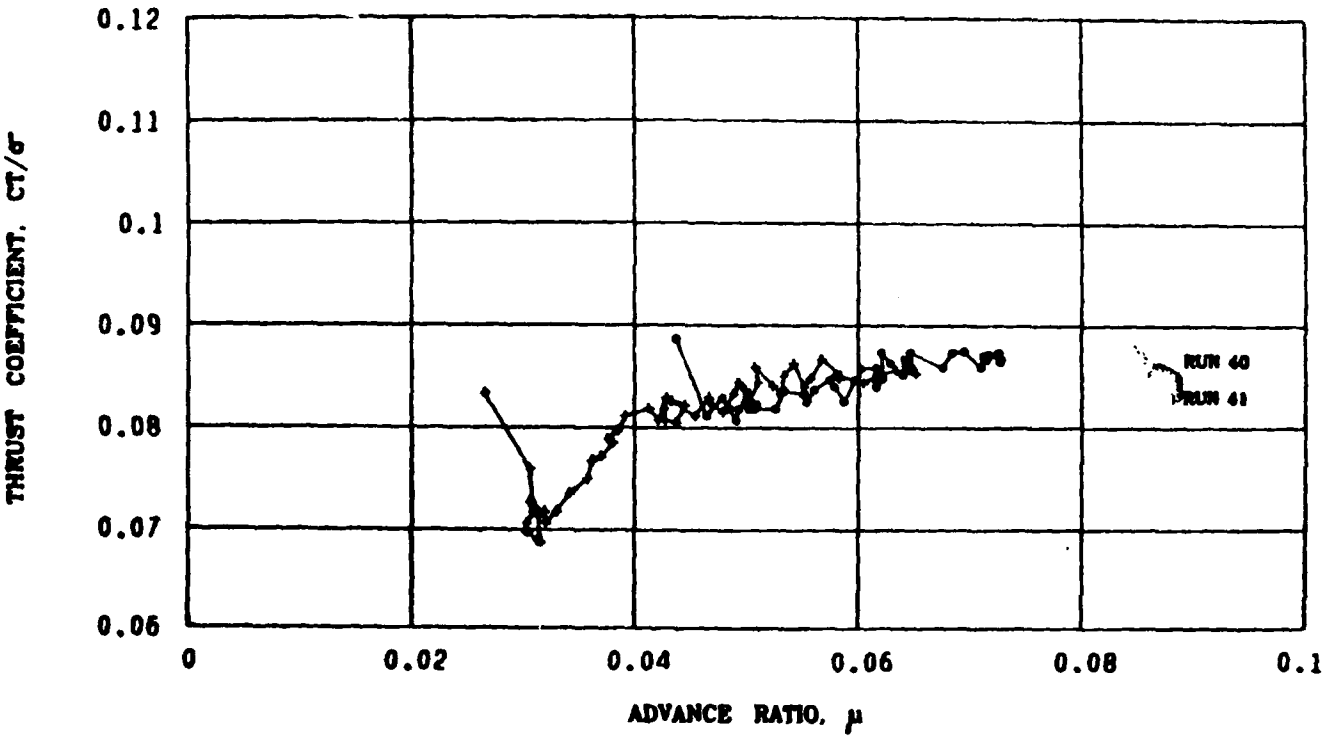

Figure A-3. Continued.

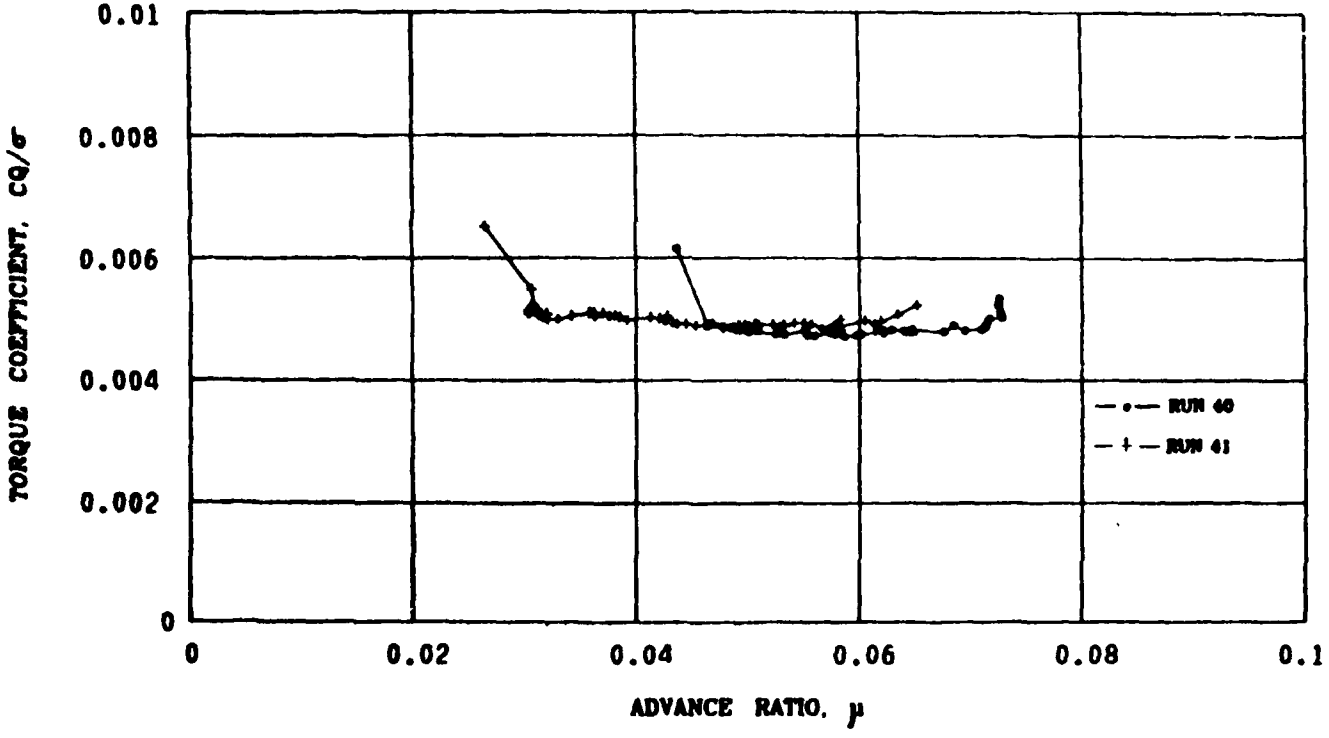

Figure A-3. Continued.

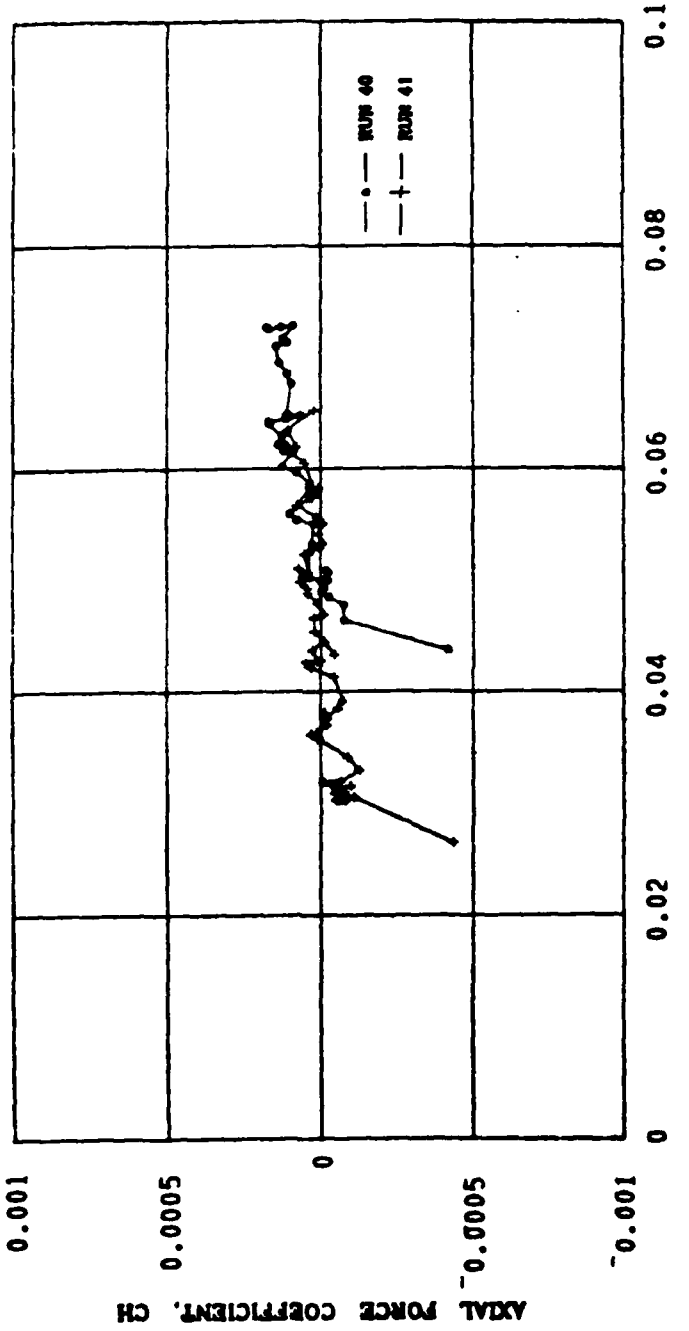

Figure A-3. Continued.

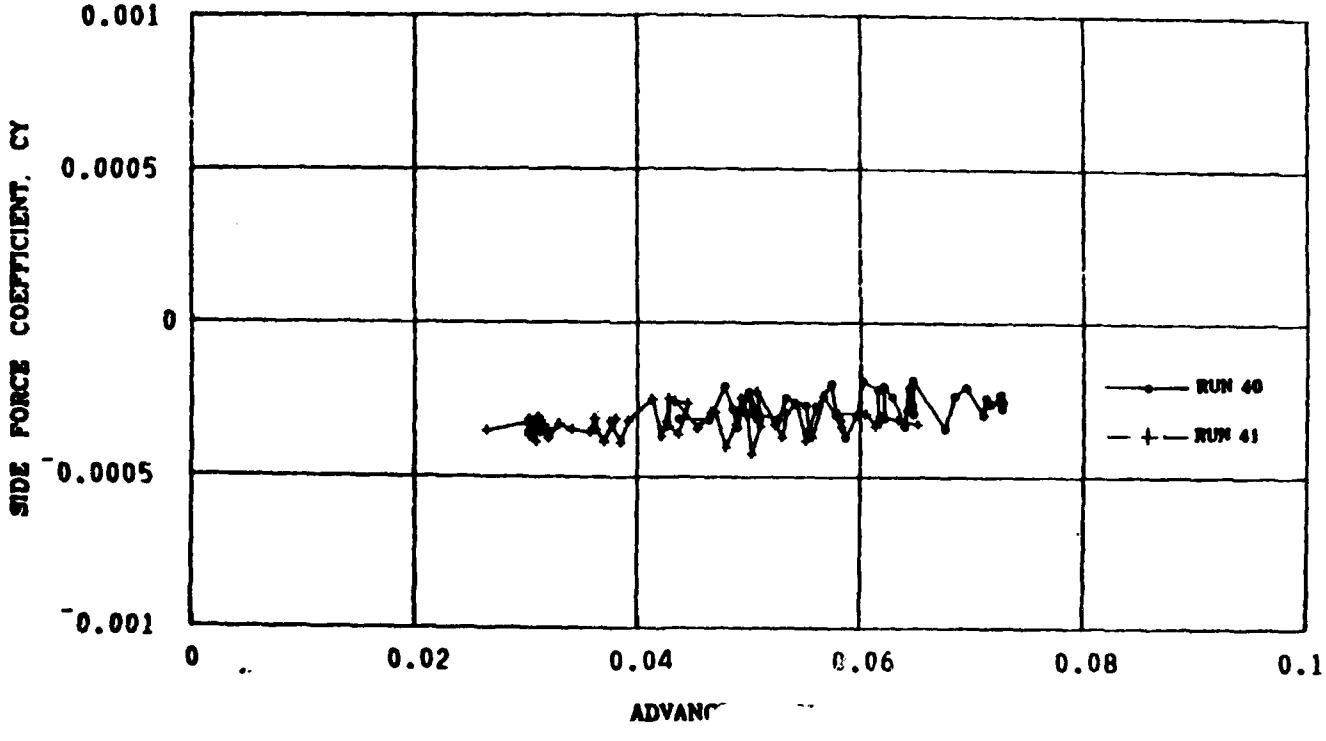

Figure A-3. Continued.

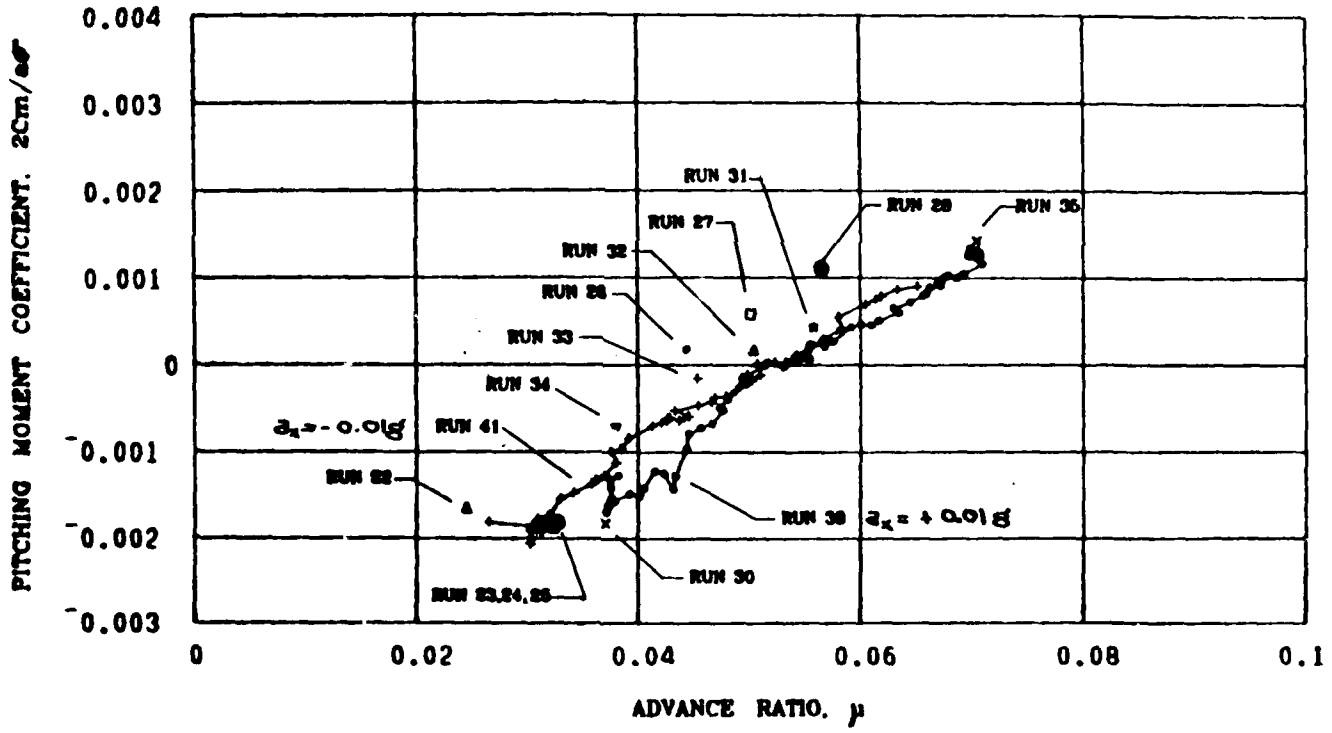

Figure A-4. Comparison of Rotor Force and Moment Coefficient Variations with Advance Ratio and Translational Acceleration (from Figures A-1 through A-3) $\theta_c = 8.4^o$, $\bar{h} = 0.23$, $a_x = 0, \pm 0.01g$.

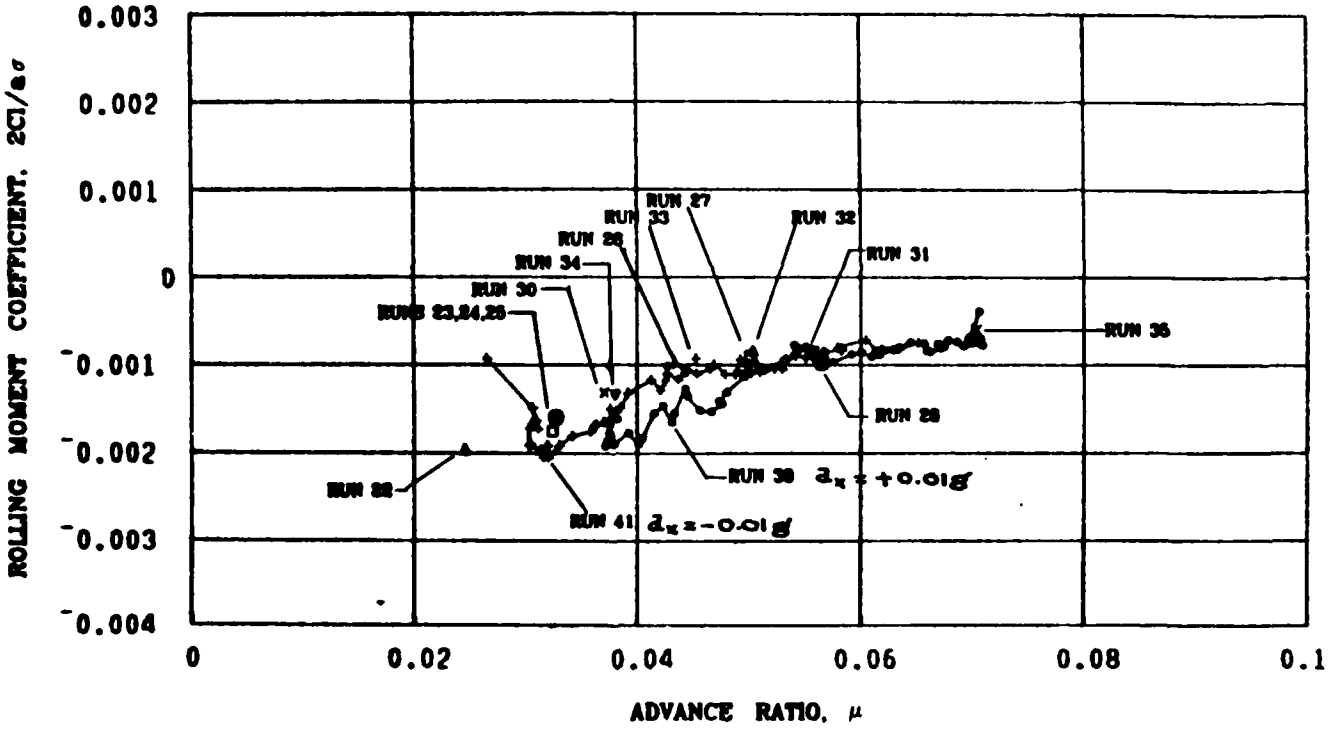

Figure A-4. Continued.

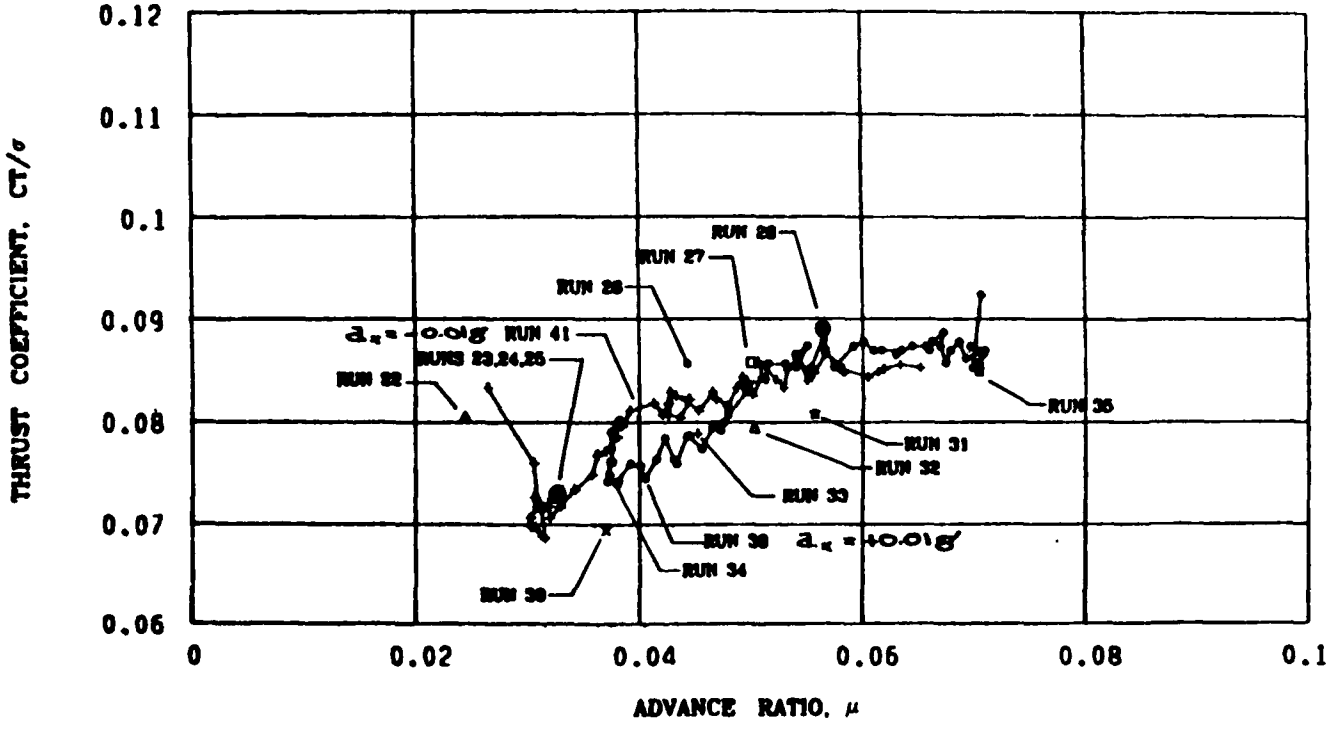

Figure A-4. Continued.

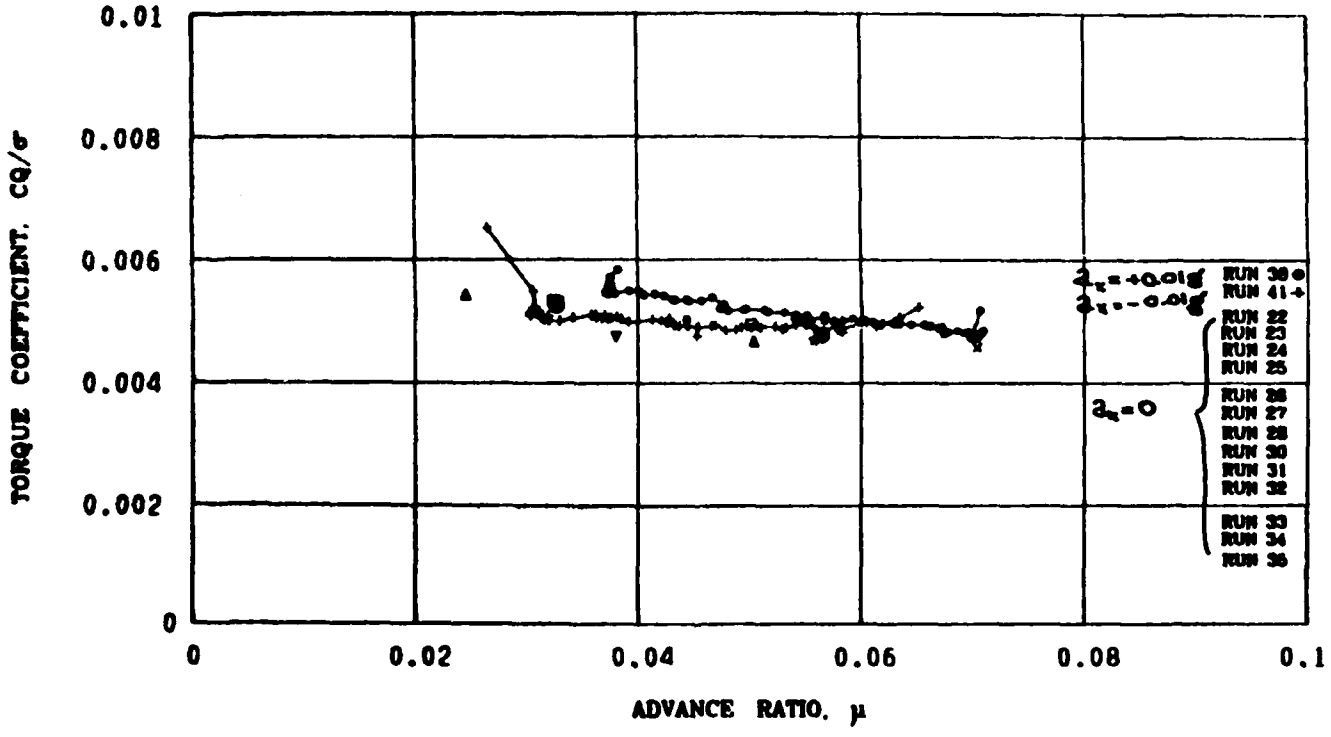

Figure A-4. Continued.

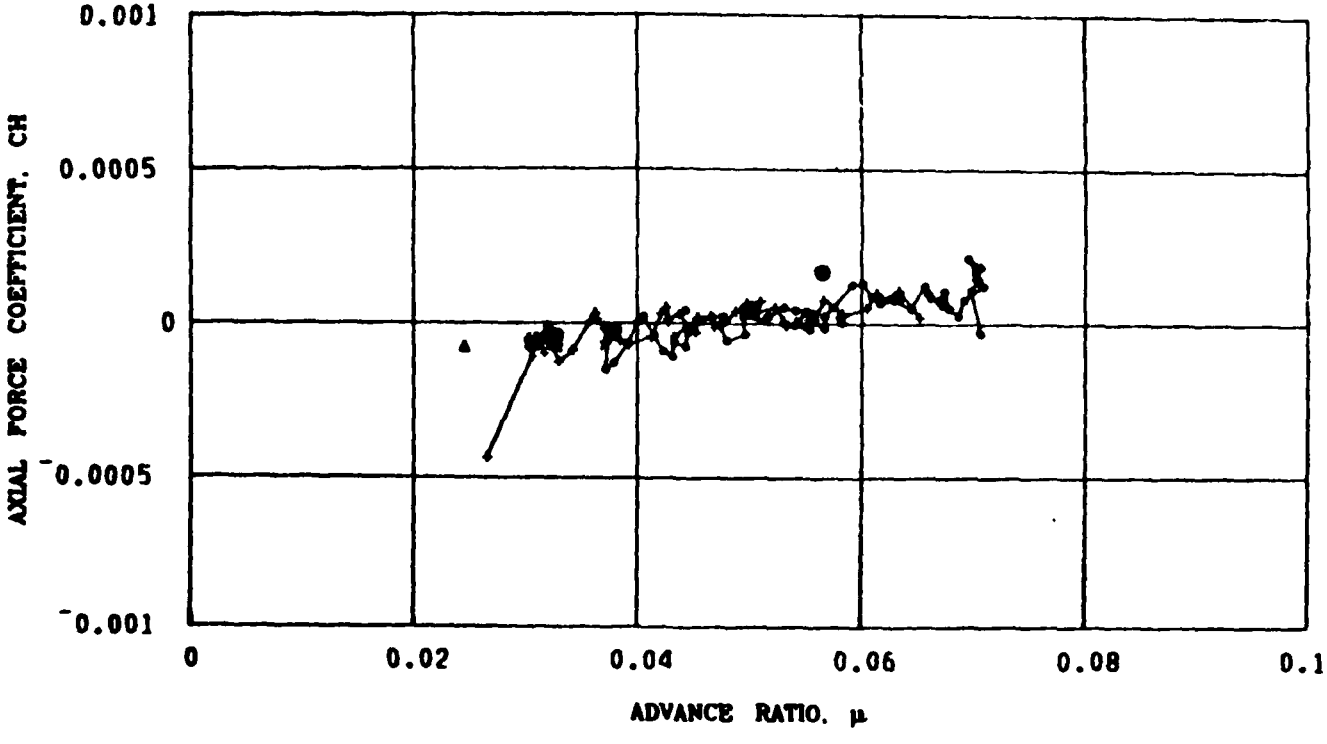

Figure A-4. Continued.

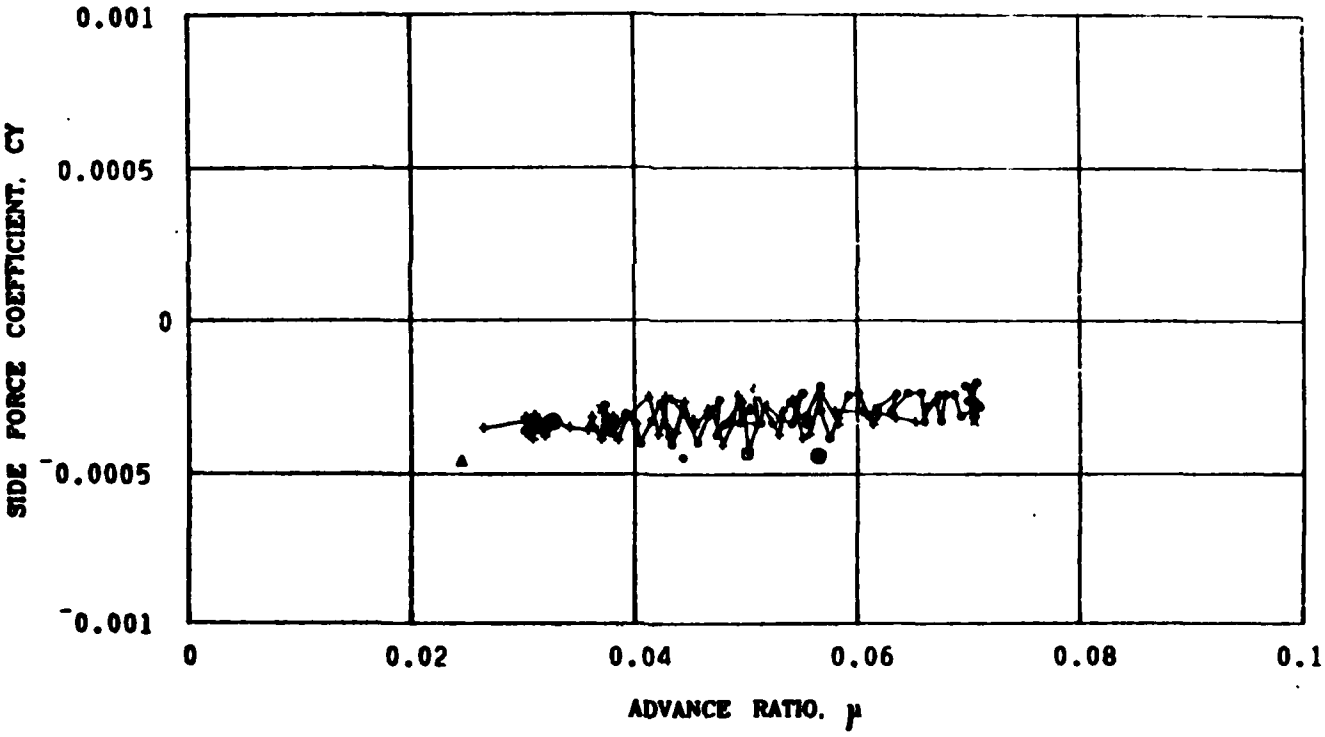

Figure A-4. Continued.

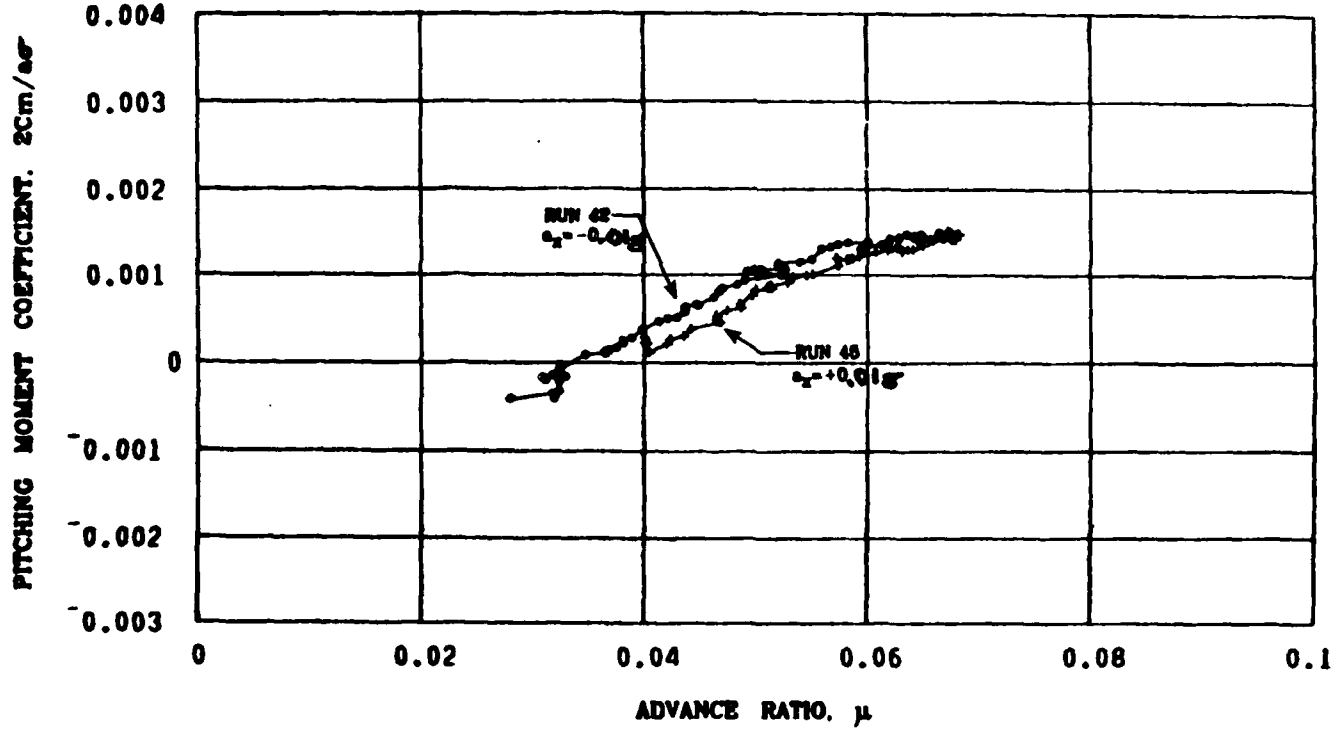

Figure A-5. Variation of Rotor Force and Moment Coefficients with Advance Ratio and Translational Acceleration, $\theta_c = 8.4^o$, $\bar{h} = 0.45$, $a_x = \pm 0.01g$.

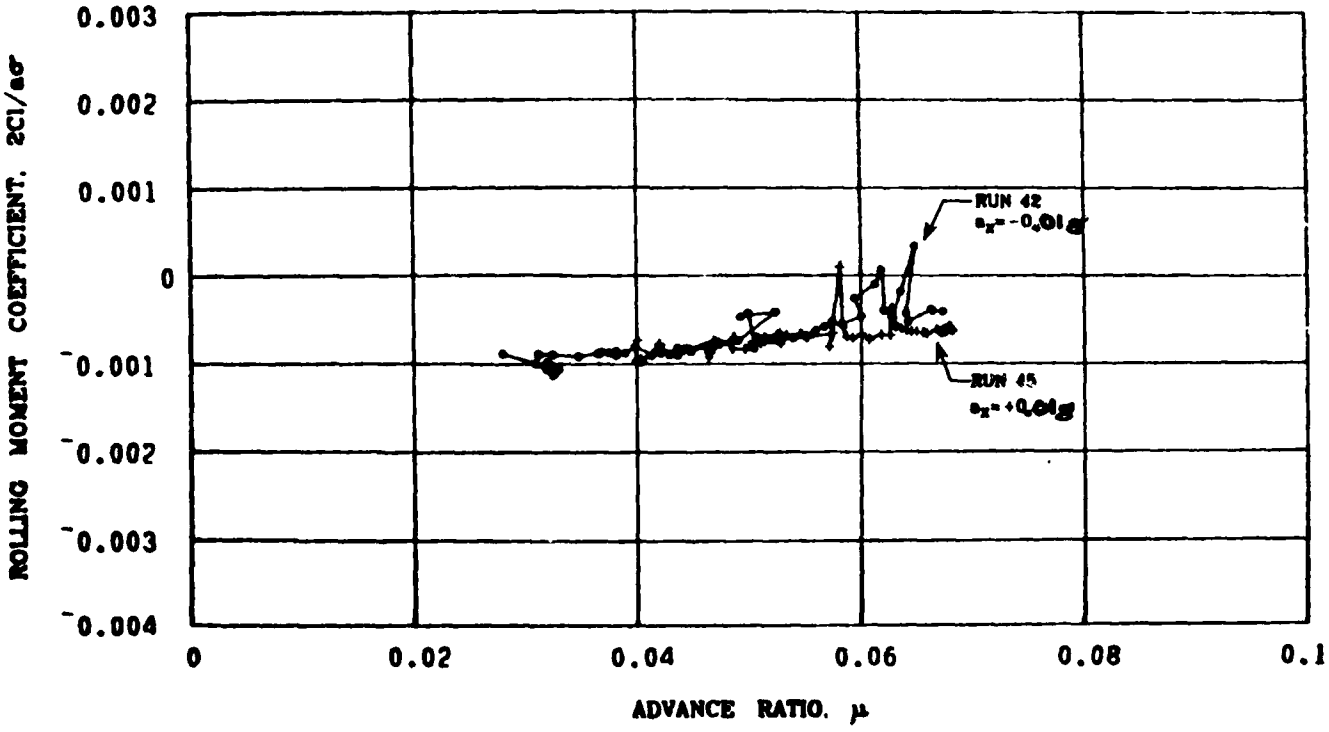

Figure A-5. Continued.

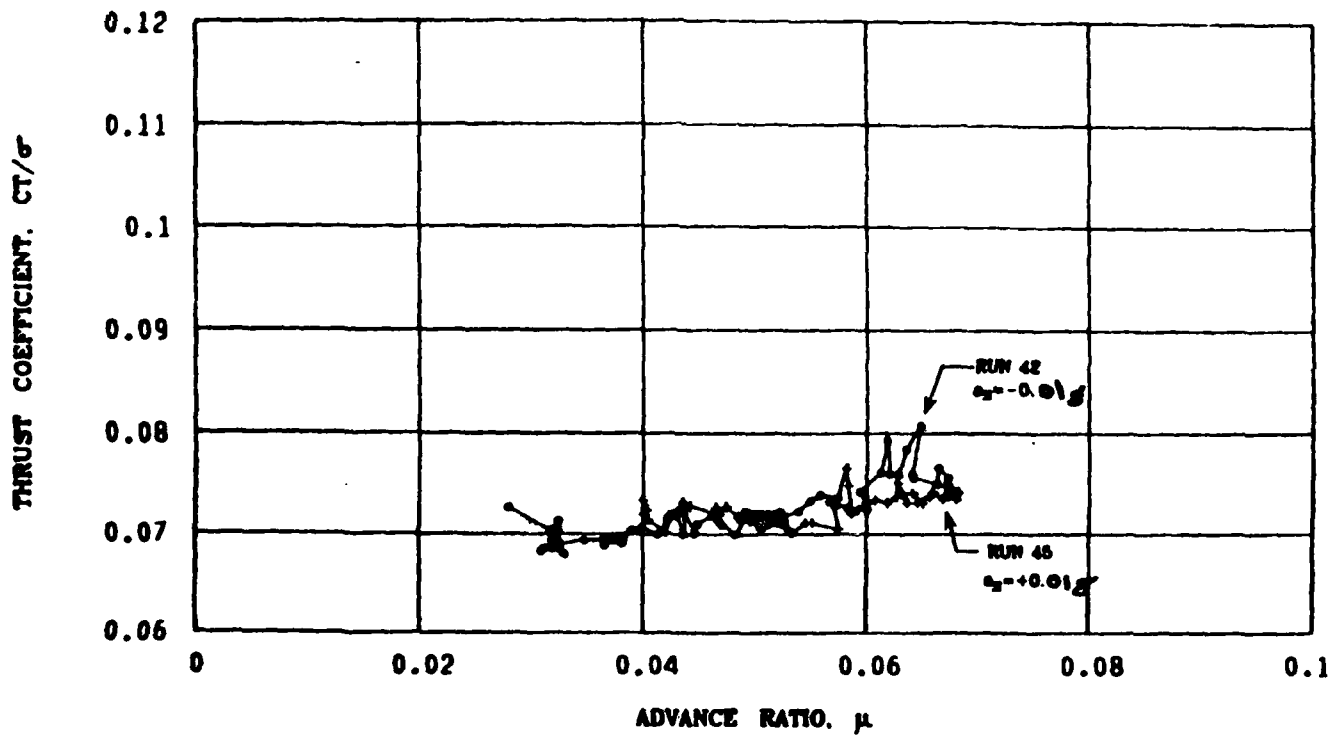

Figure A-5. Continued.

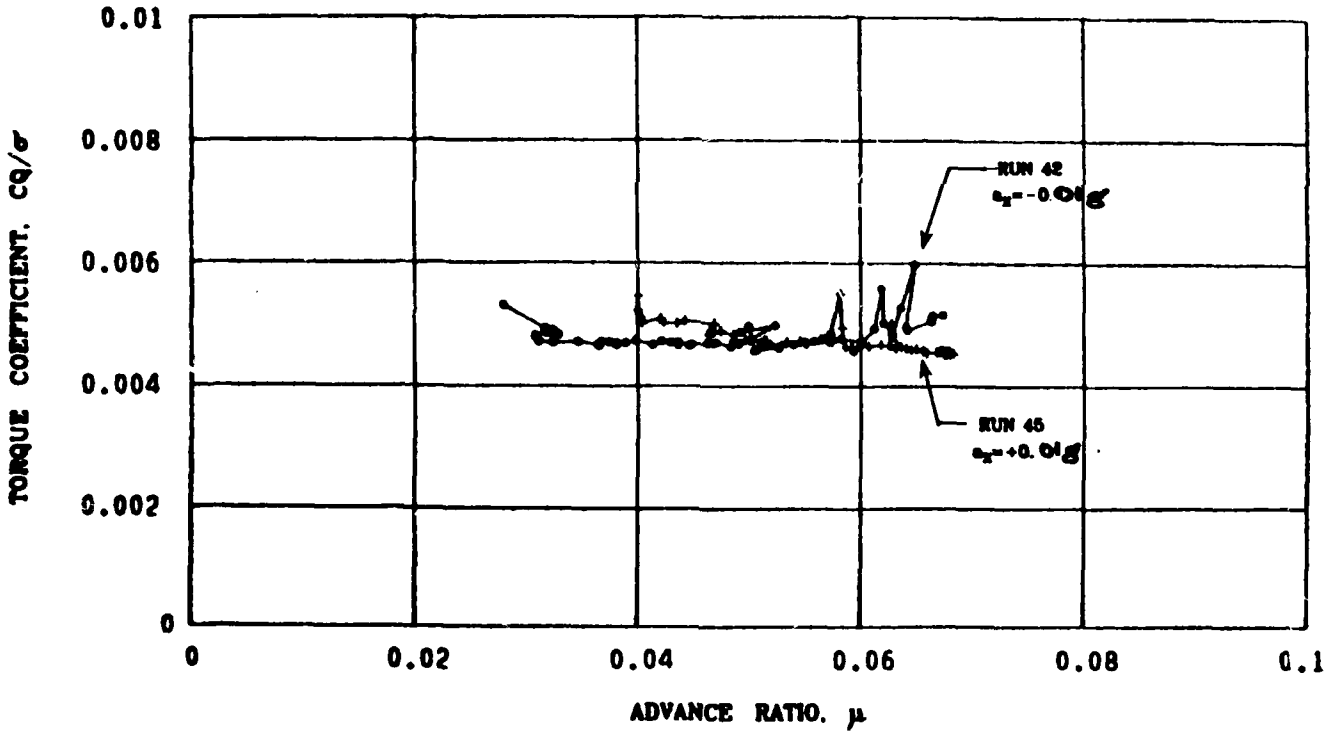

Figure A-5. Continued.

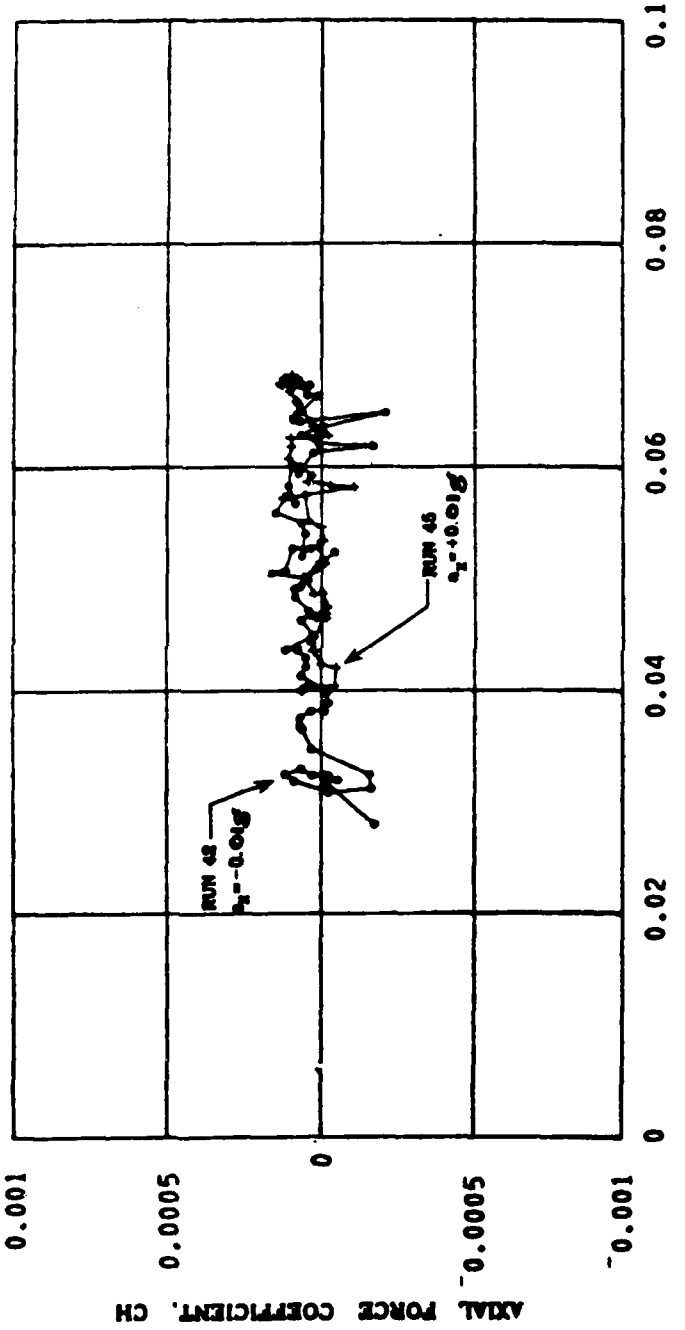

Figure A-5. Continued.

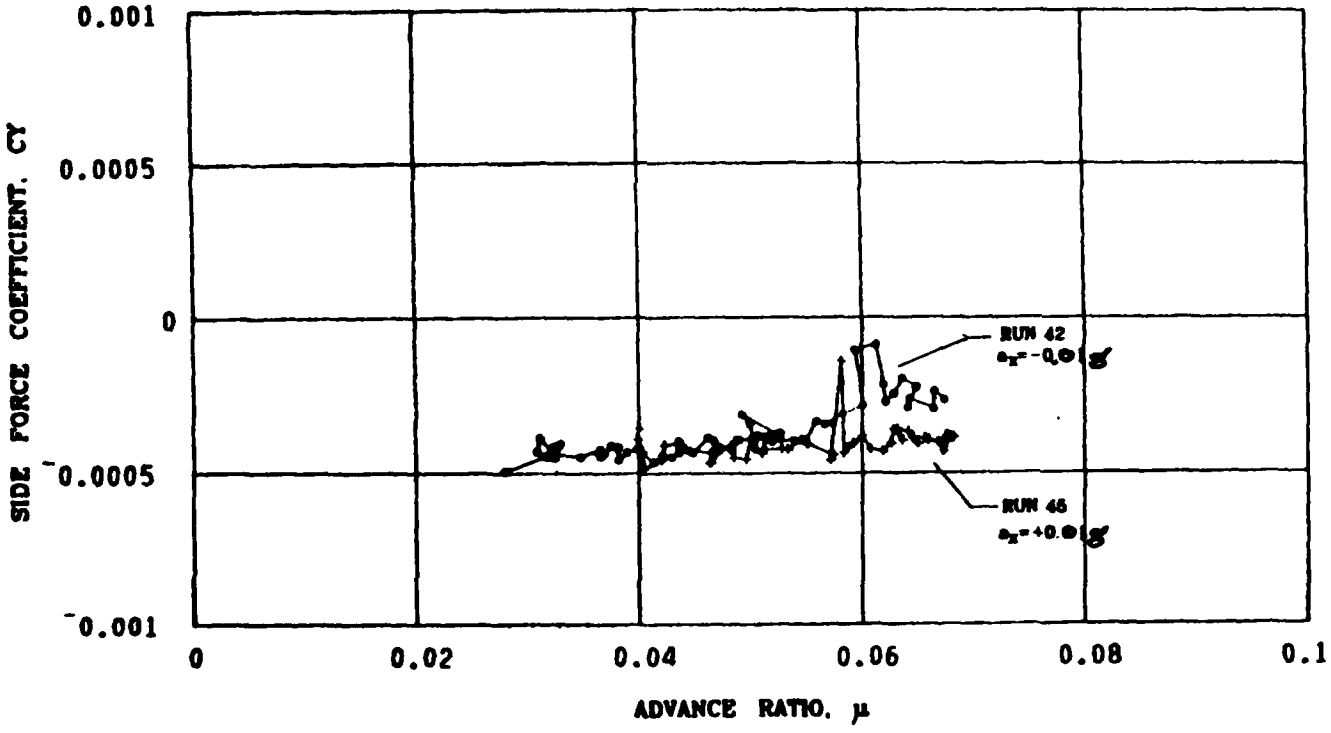

Figure A-5. Continued.

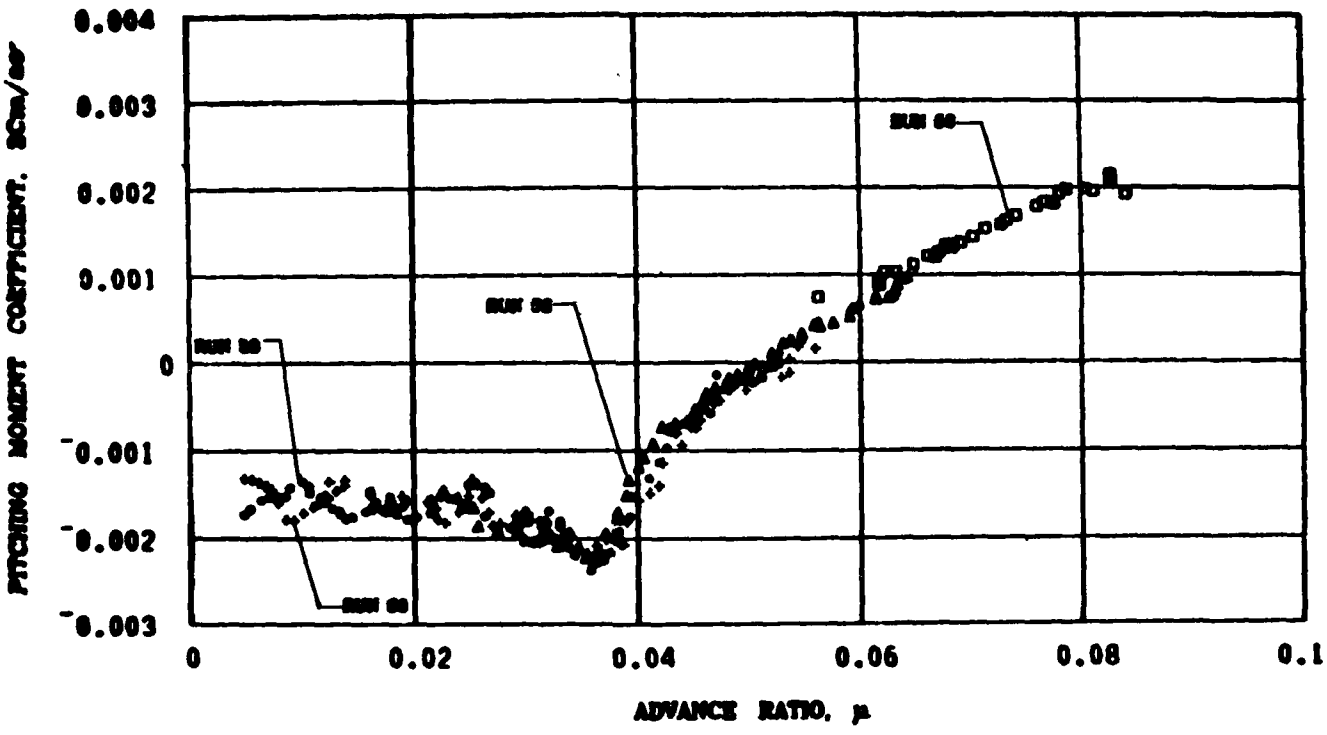

Figure A-6. Comparison of Rotor Force and Moment Coefficient Variations with Advance Ratio and Translational Acceleration (Multiple Data Runs) $\theta_c = 9.8^o$, $\bar{h} = 0.23$, $a_x = 0.01g$.

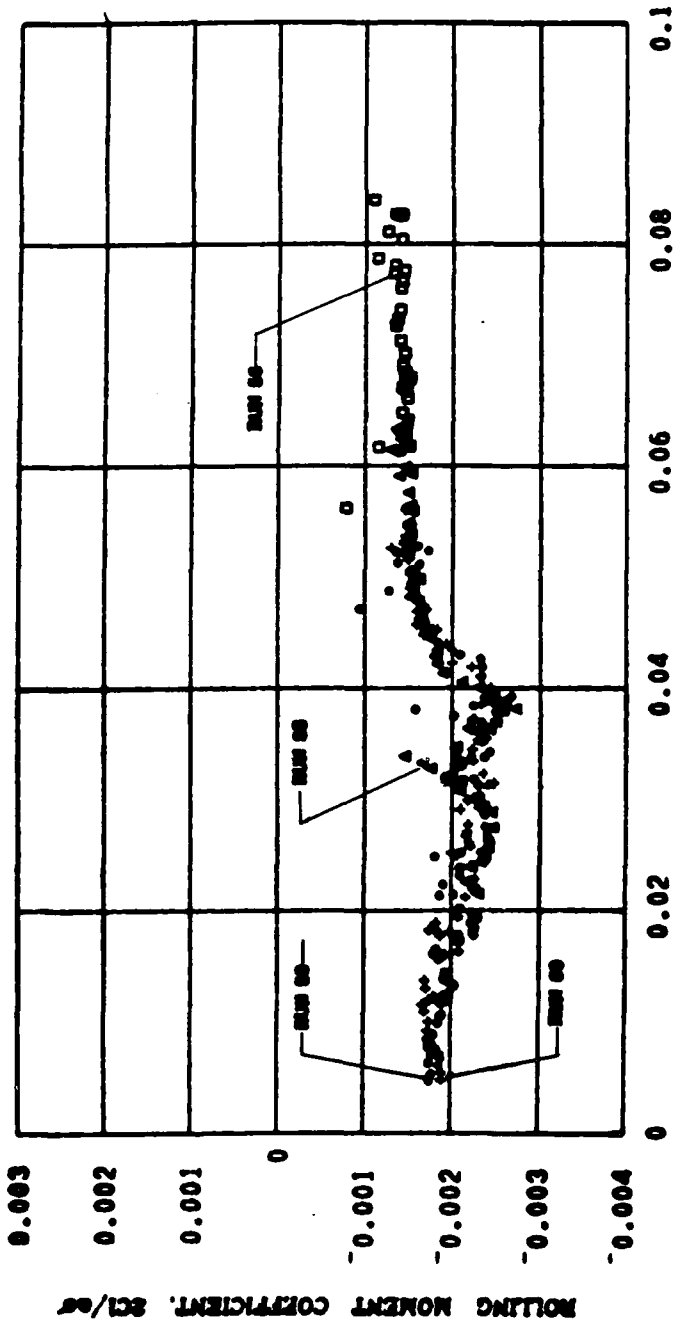

Figure A-6. Continued.

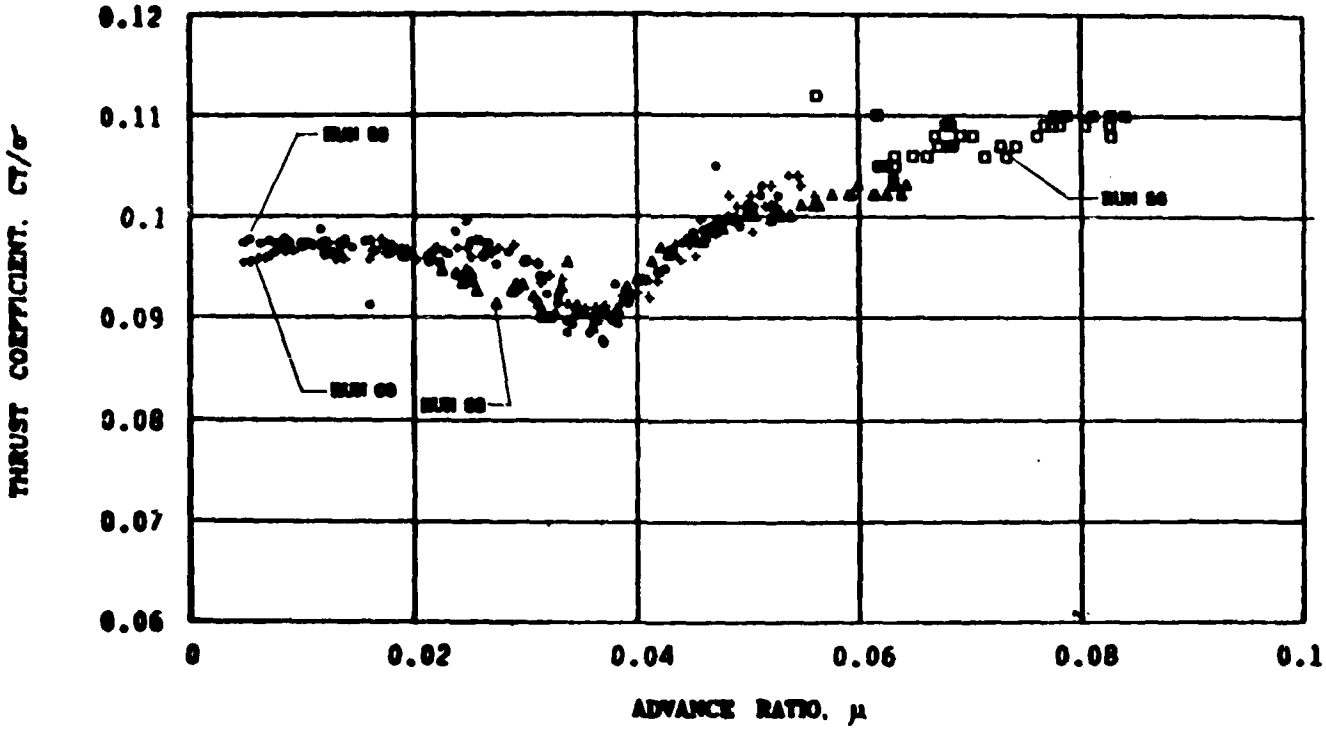

Figure A-6. Continued.

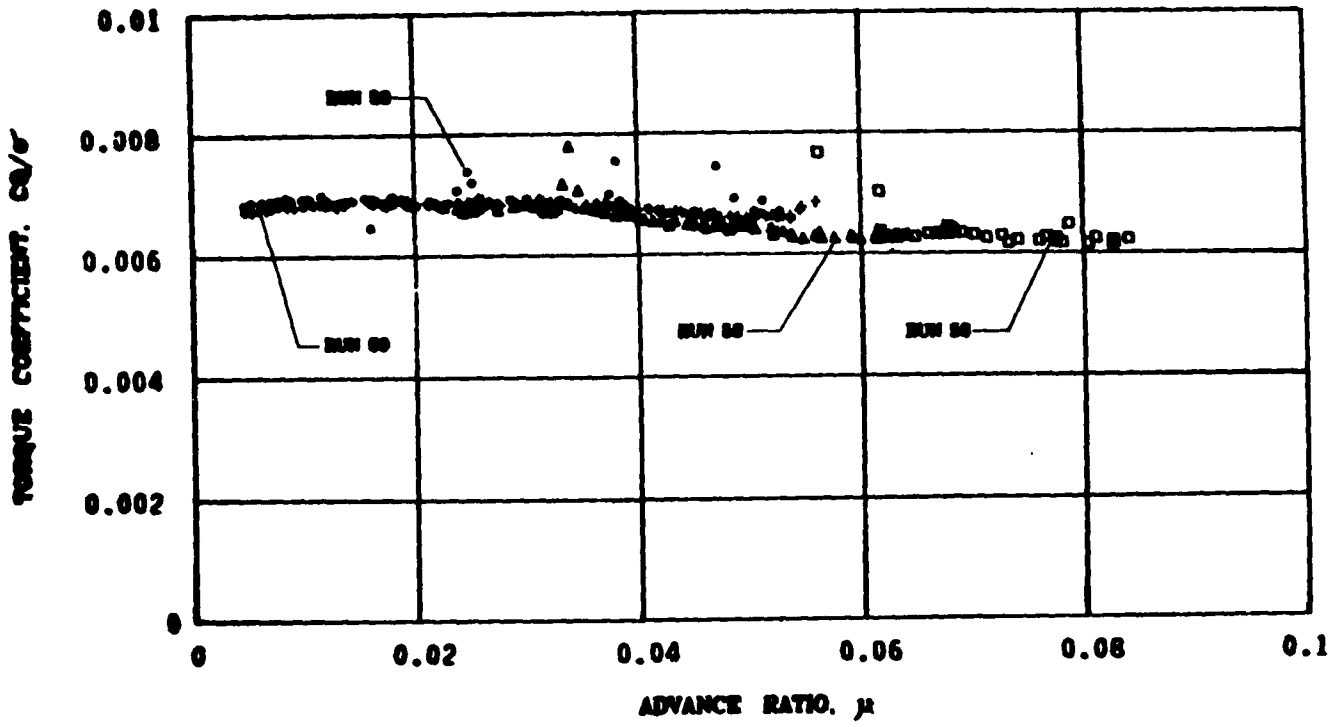

Figure A-6. Continued.

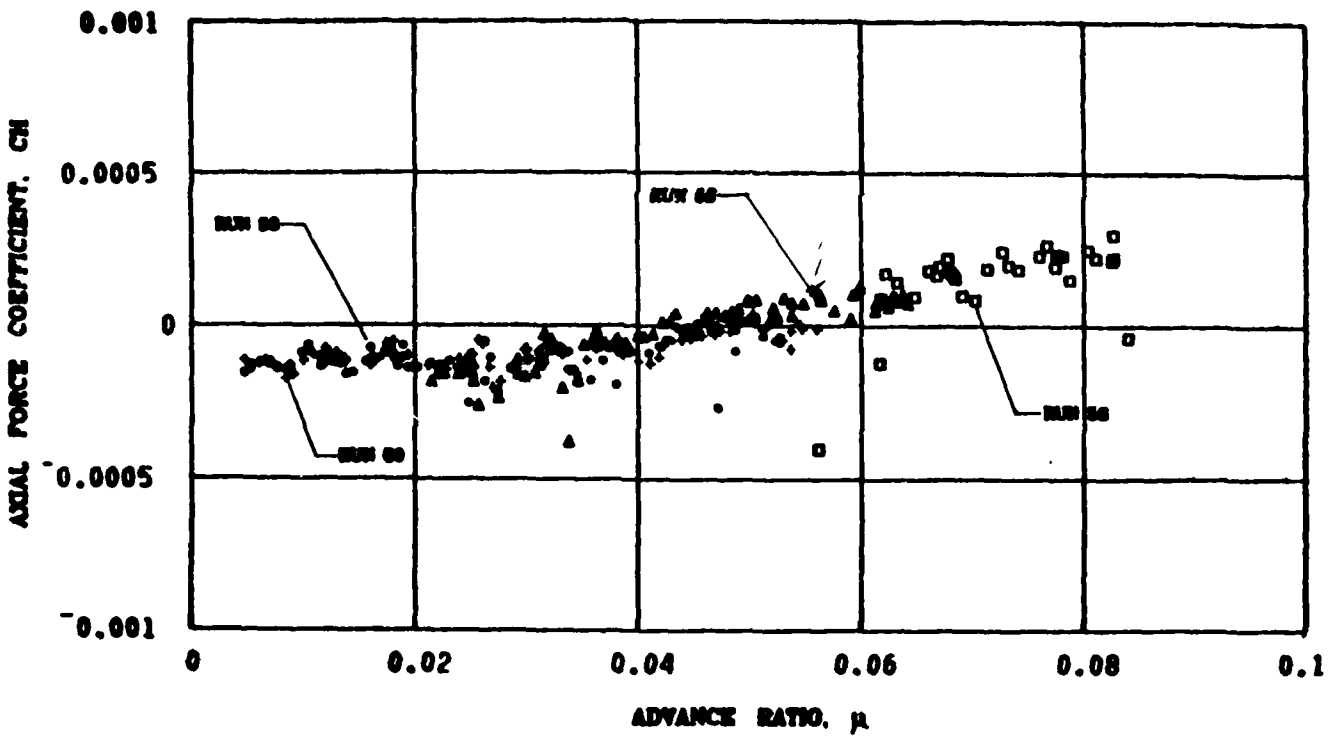

Figure A-6. Continued.

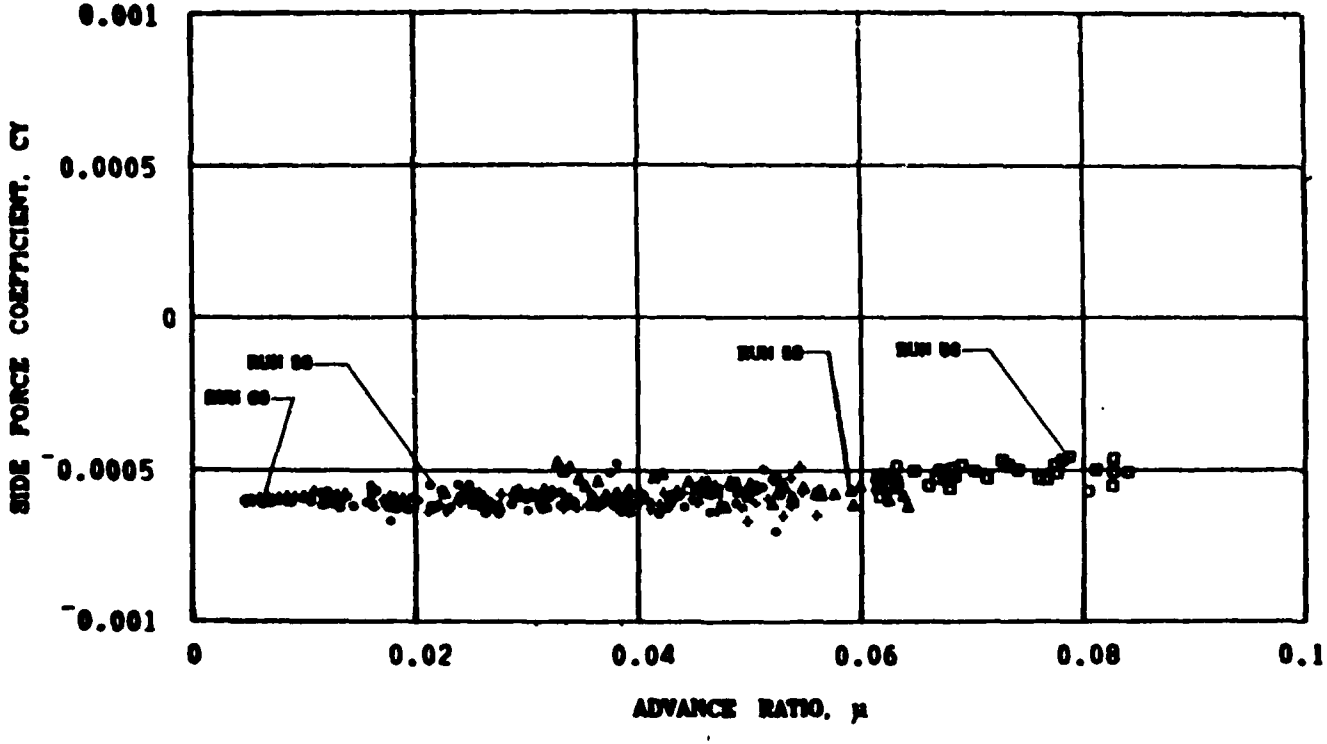

Figure A-6. Continued.

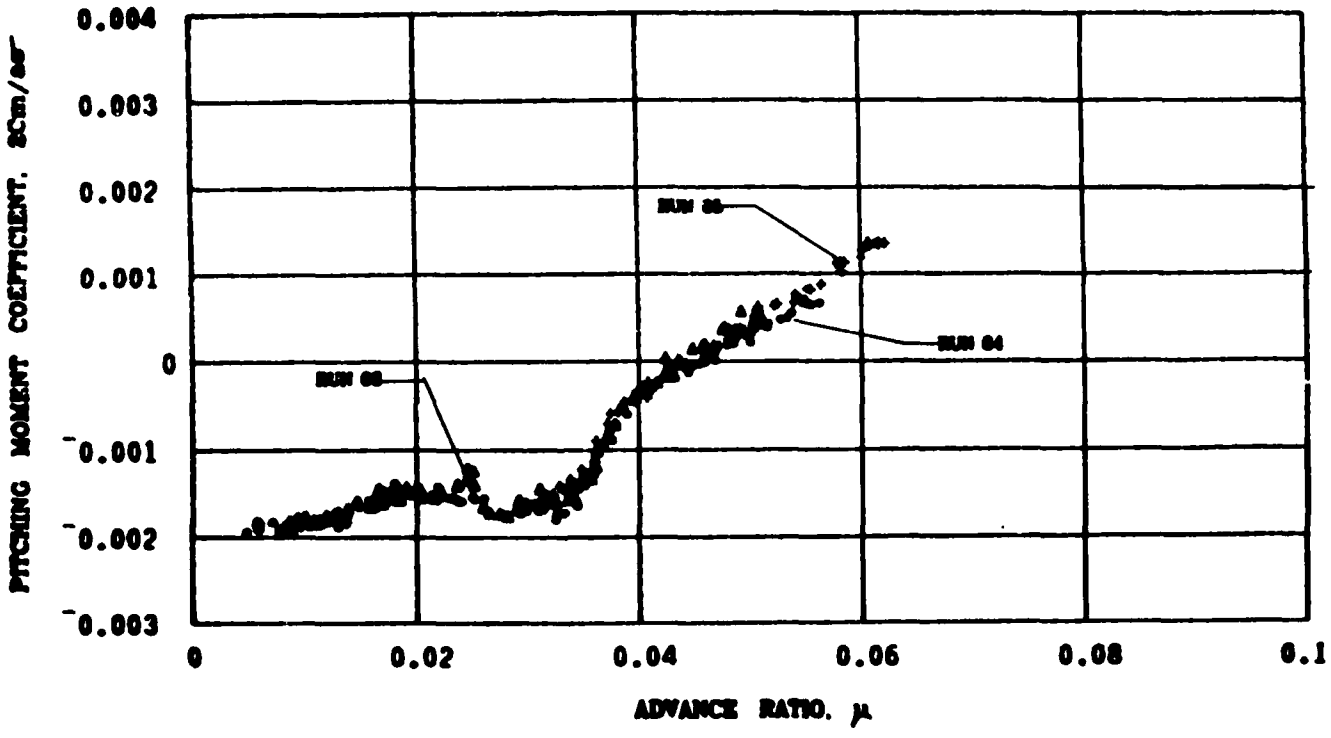

Figure A-7. Comparison of Rotor Force and Moment Coefficient Variations with Advance Ratio and Translational Deceleration (Multiple Data Runs) $\theta_c = 9.8^{\circ}$, $\bar{h} = 0.34$, $a_x = -0.01g$.

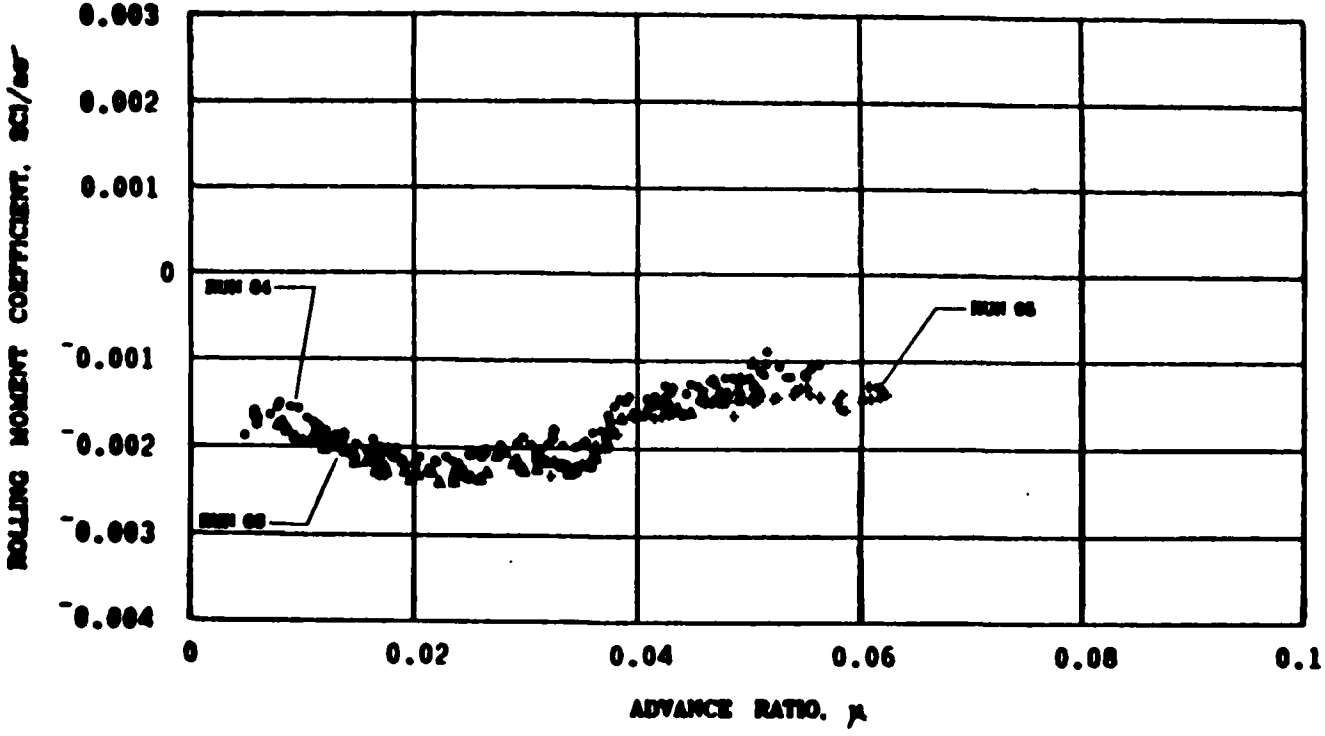

Figure A-7. Continued.

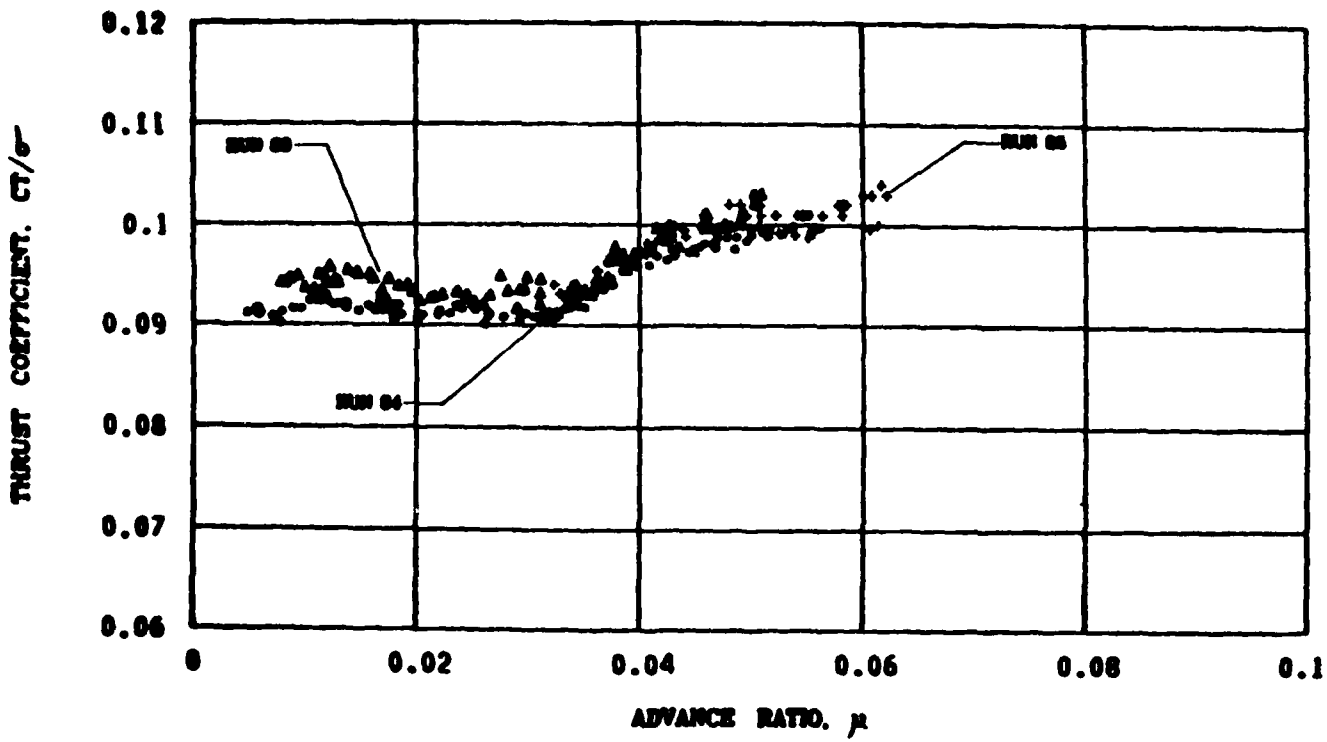

Figure A-7. Continued.

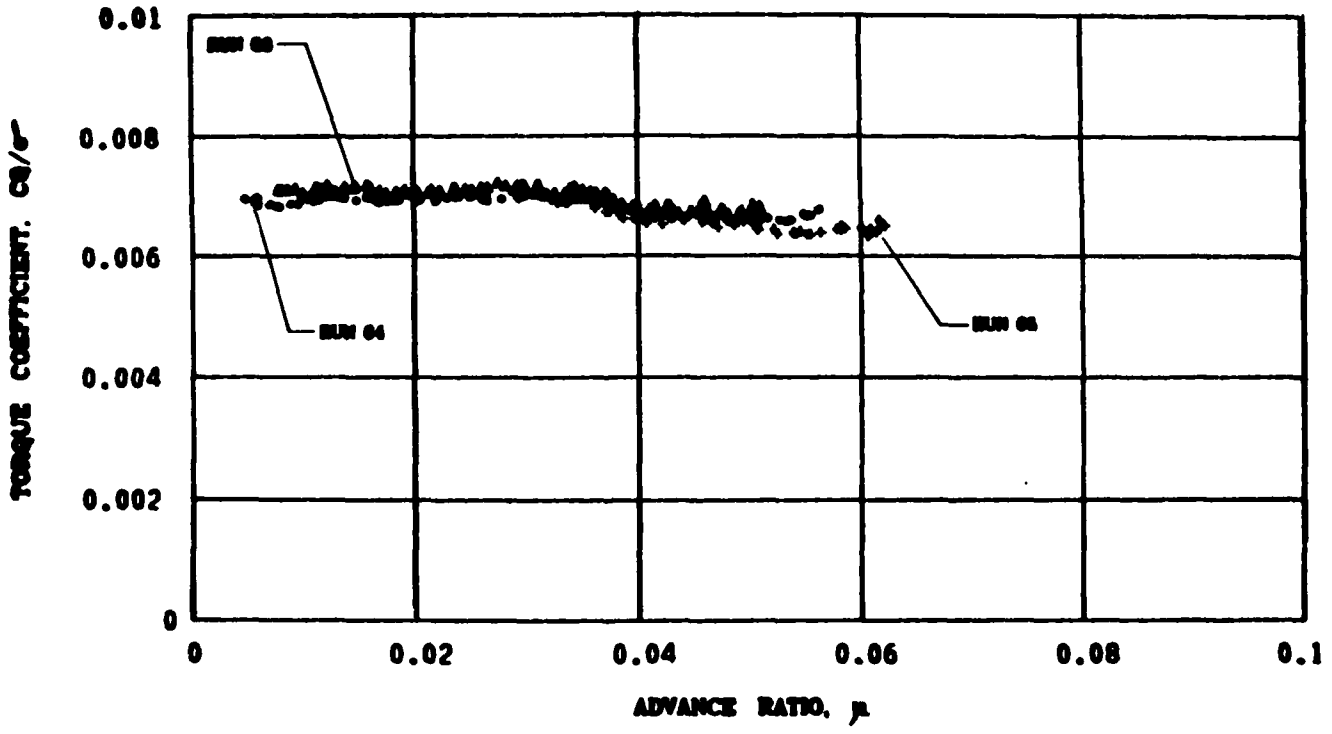

Figure A-7. Continued.

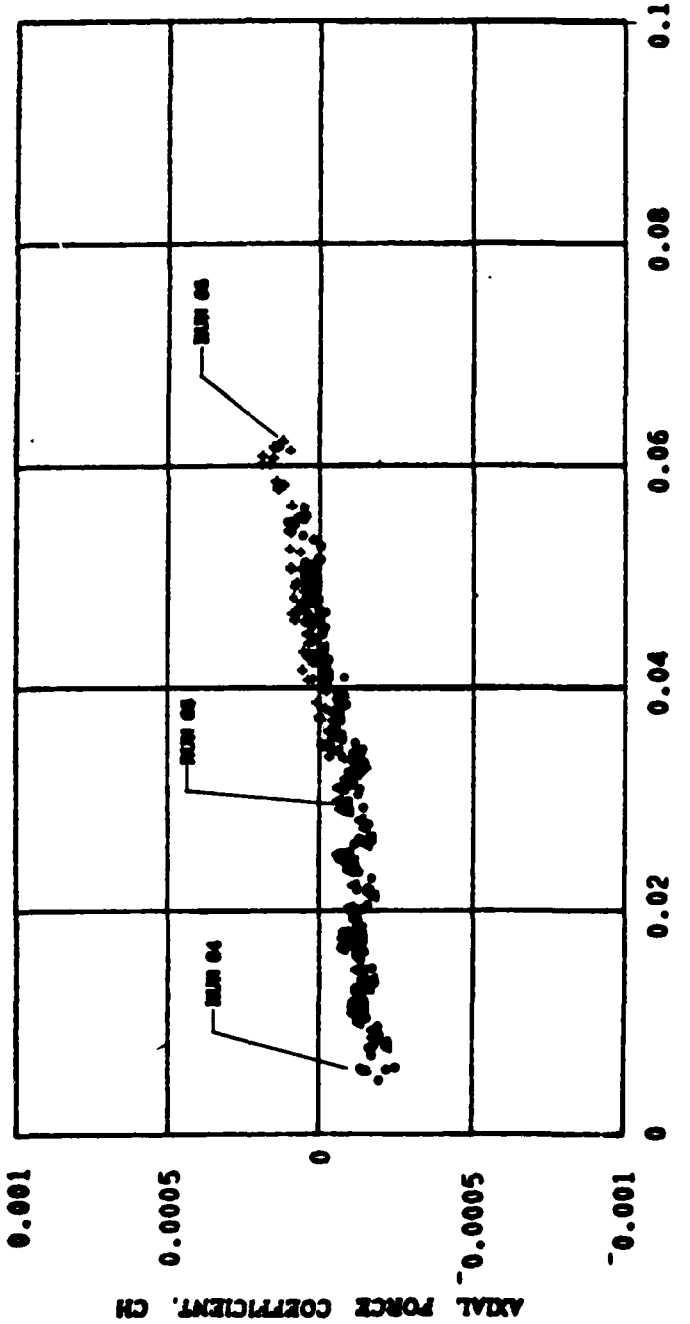

Figure A-7. Continued.

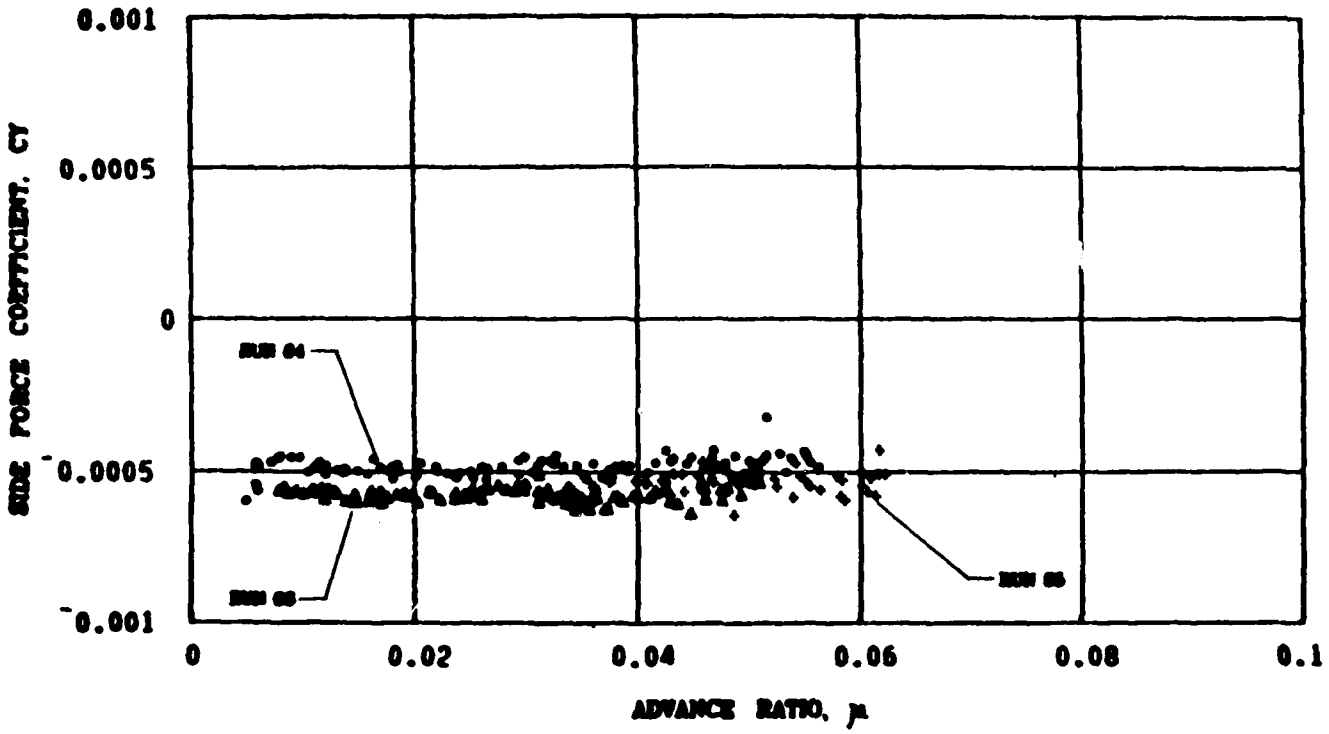

Figure A-7. Continued.

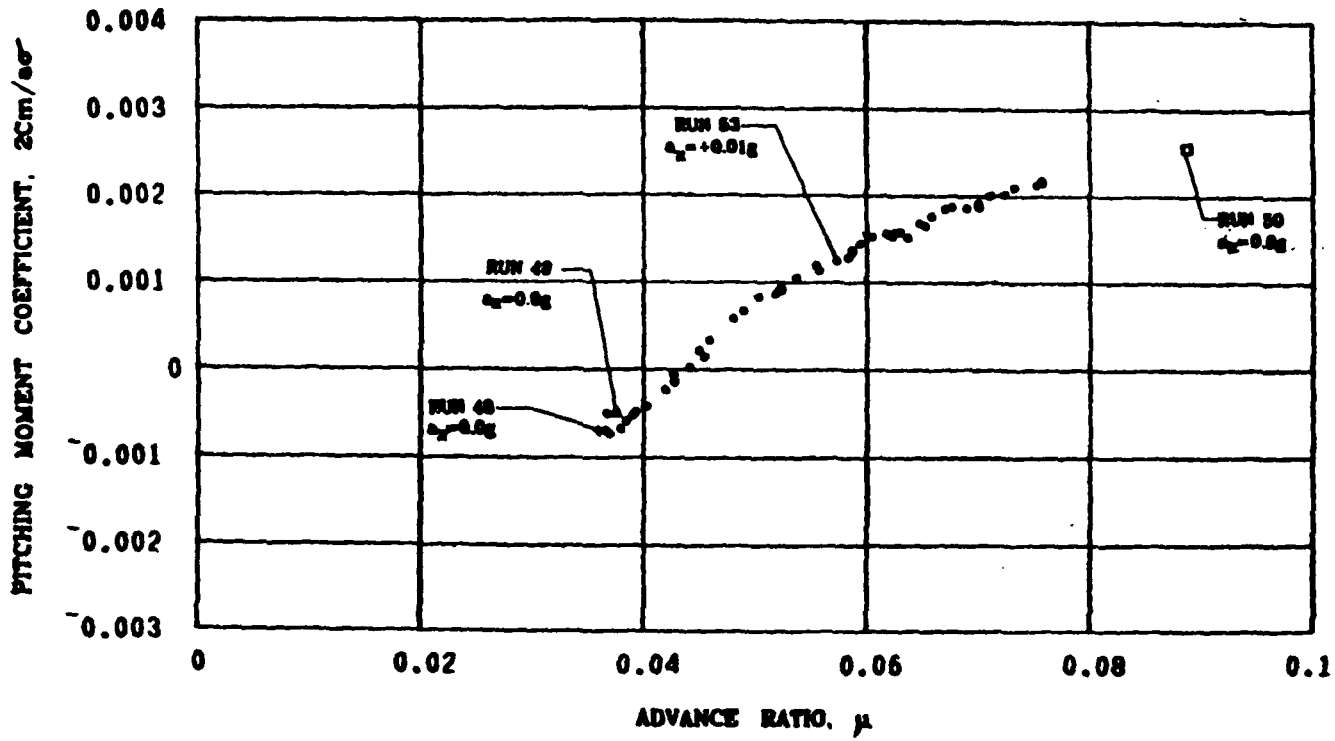

Figure A-8. Comparison of Rotor Force and Moment Coefficient Variations with Advance Ratio and Translational Acceleration, $\theta_c = 9.8^o$, $\bar{h} = 0.45$, $a_x = 0, 0.01g$.

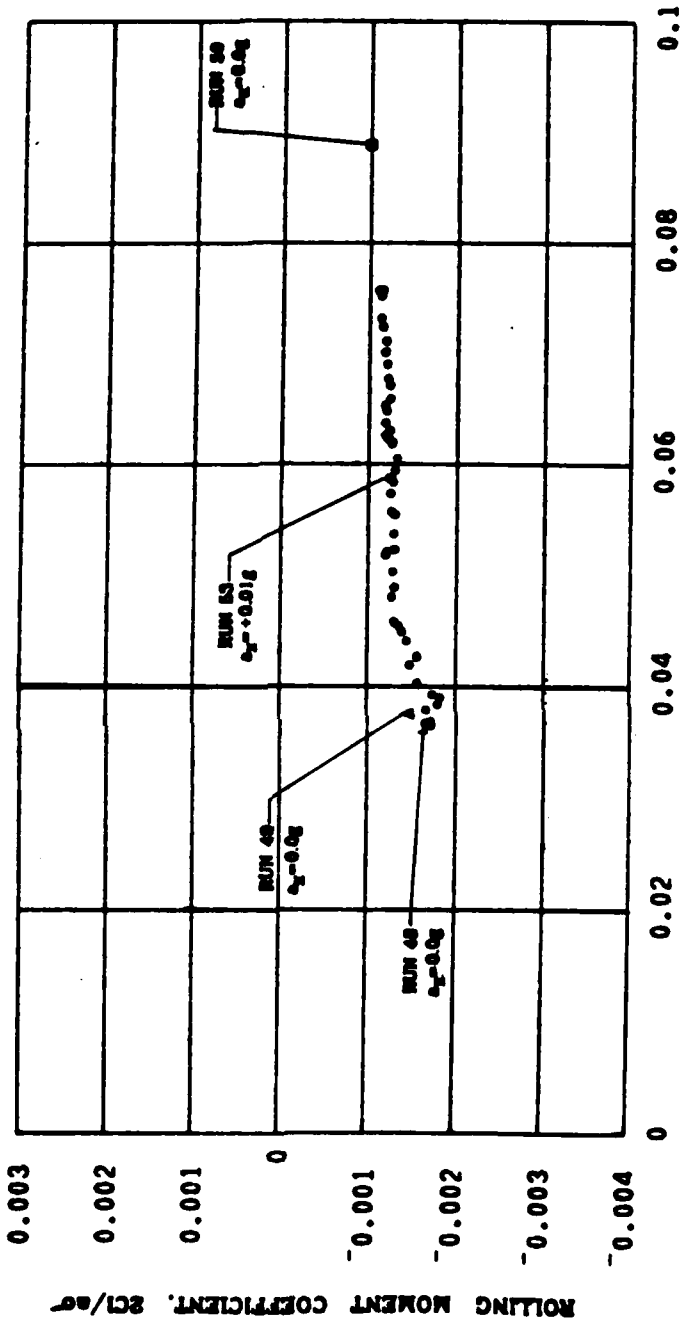

Figure A-8. Continued.

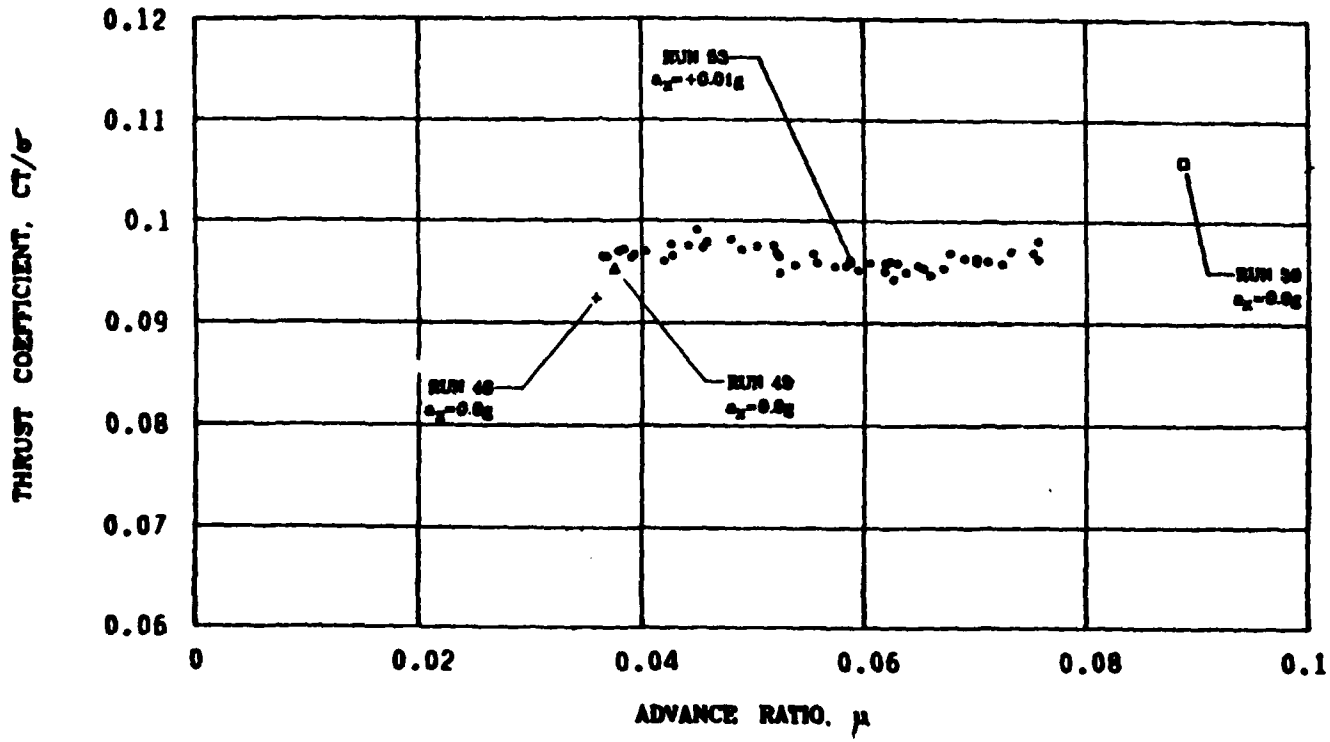

Figure A-8. Continued.

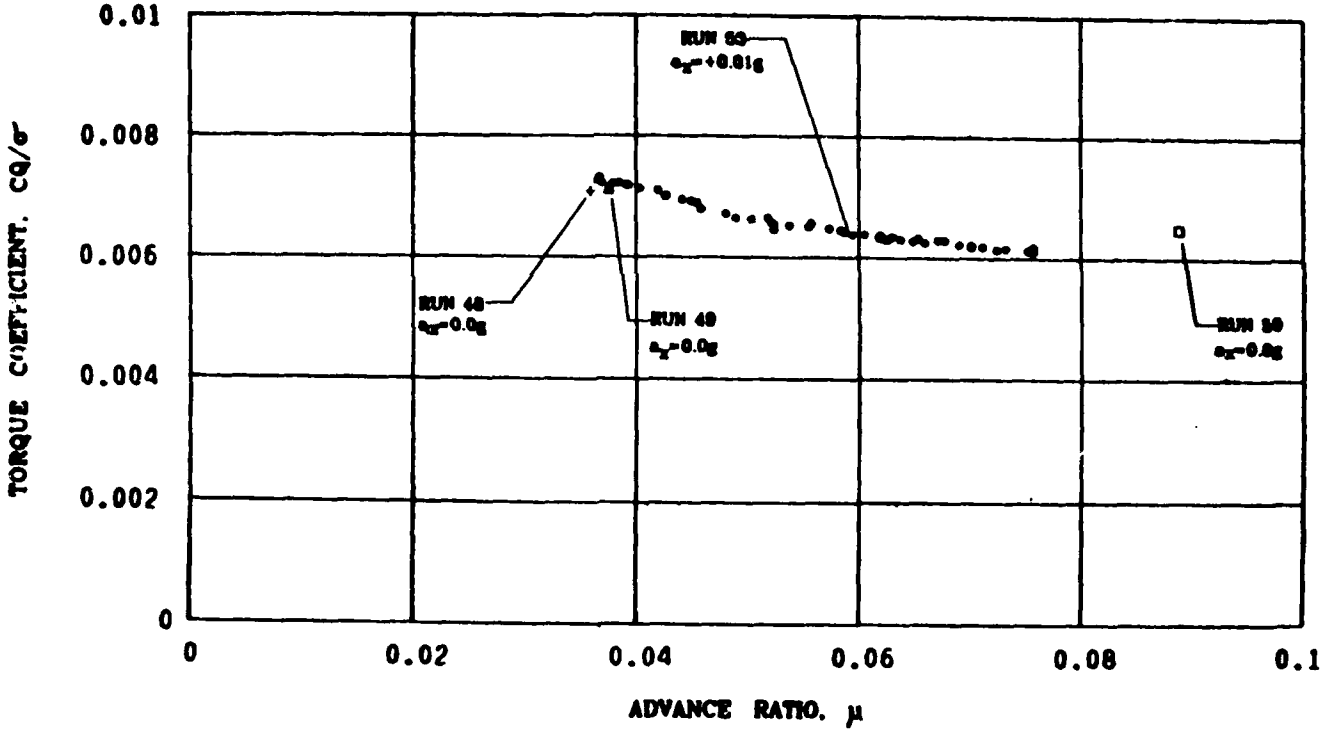

Figure A-8. Continued.

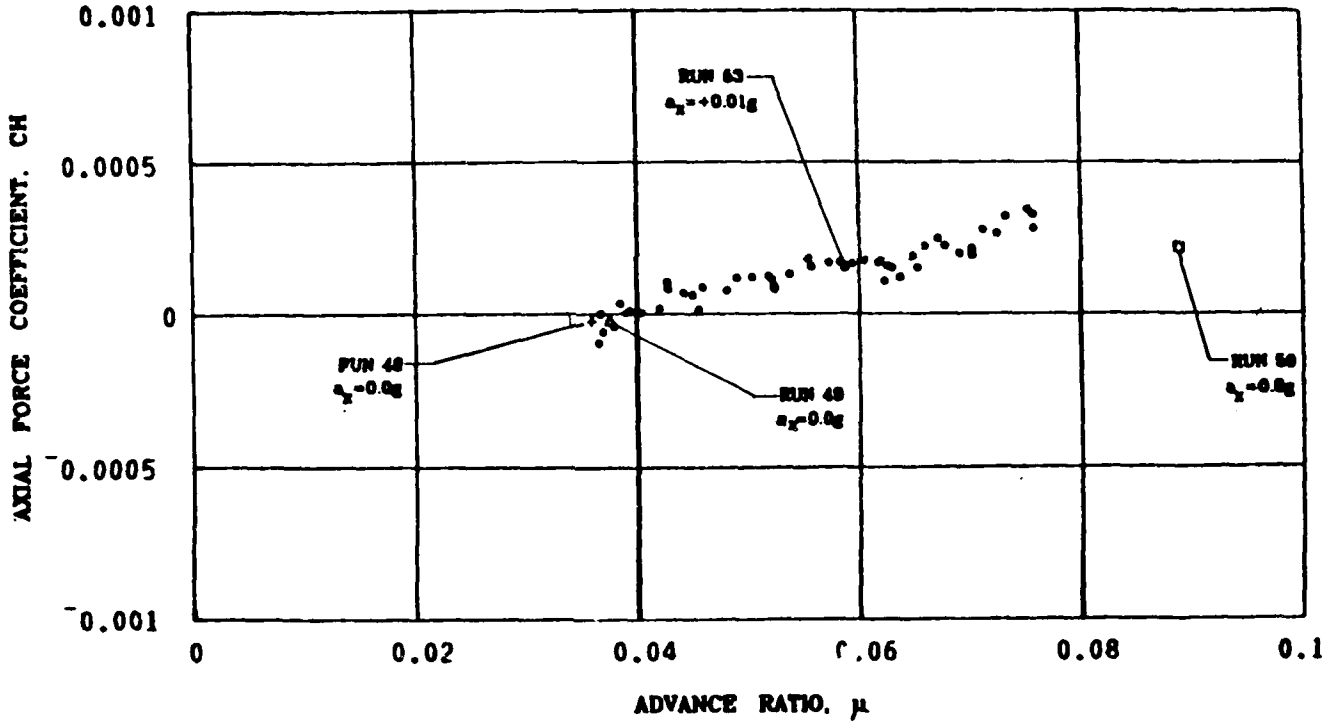

Figure A-8. Continued.

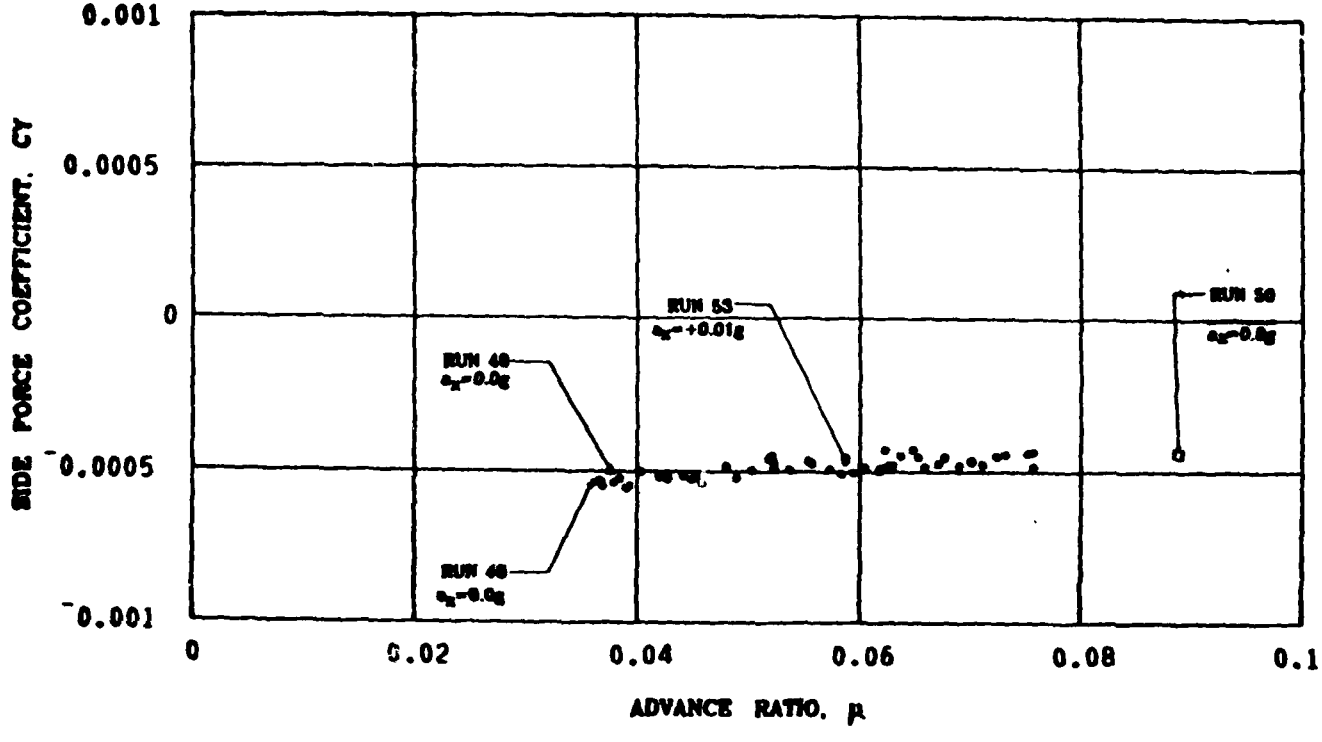

Figure A-8. Continued.

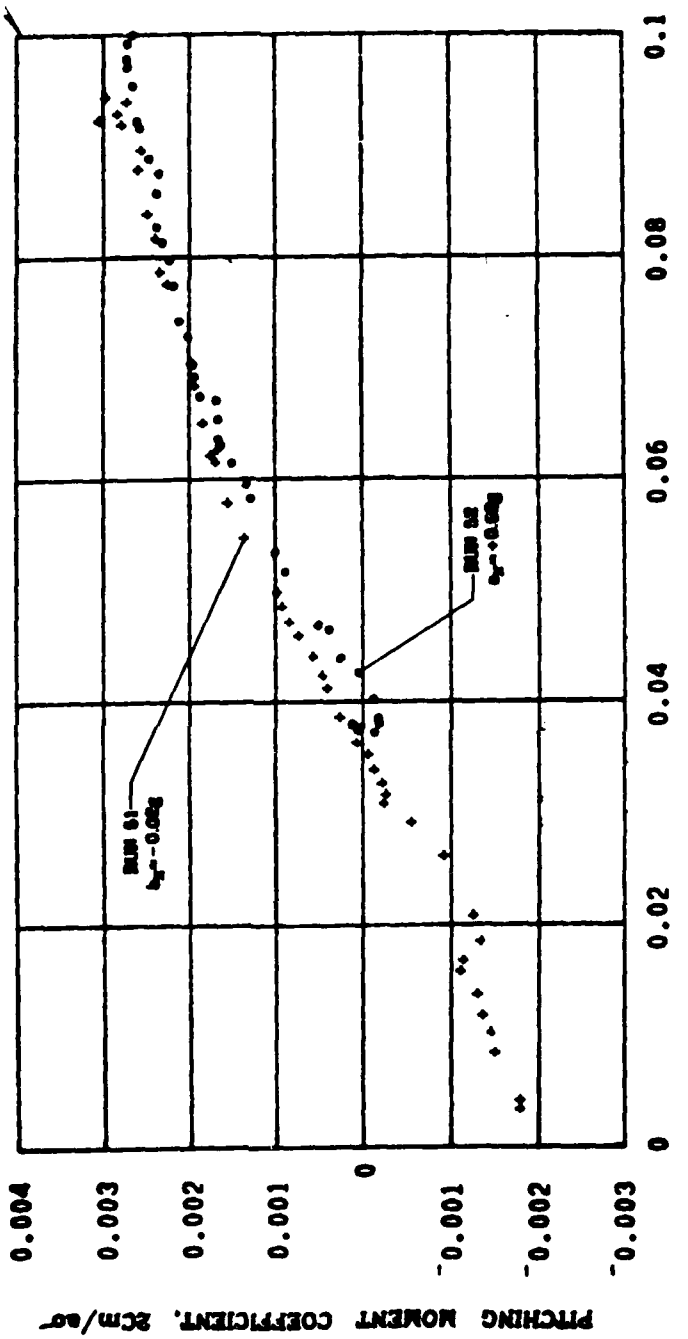

Figure A-9. Comparison of Rotor Force and Moment Coefficient Variations with Advance Ratio and Translational Acceleration and Deceleration, $\theta_c = 9.8^o$, $\bar{h} = 0.45$, $a_x = \pm 0.02g$.

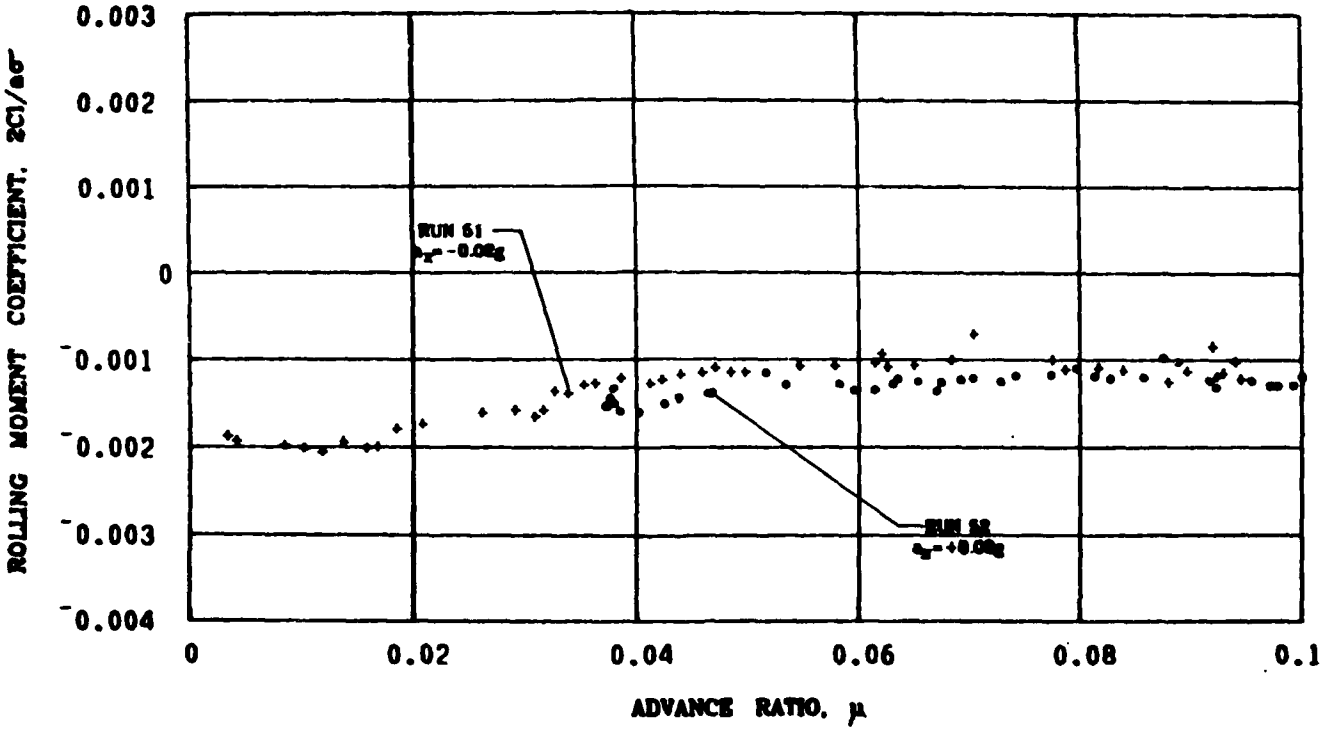

Figure A-9. Continued.

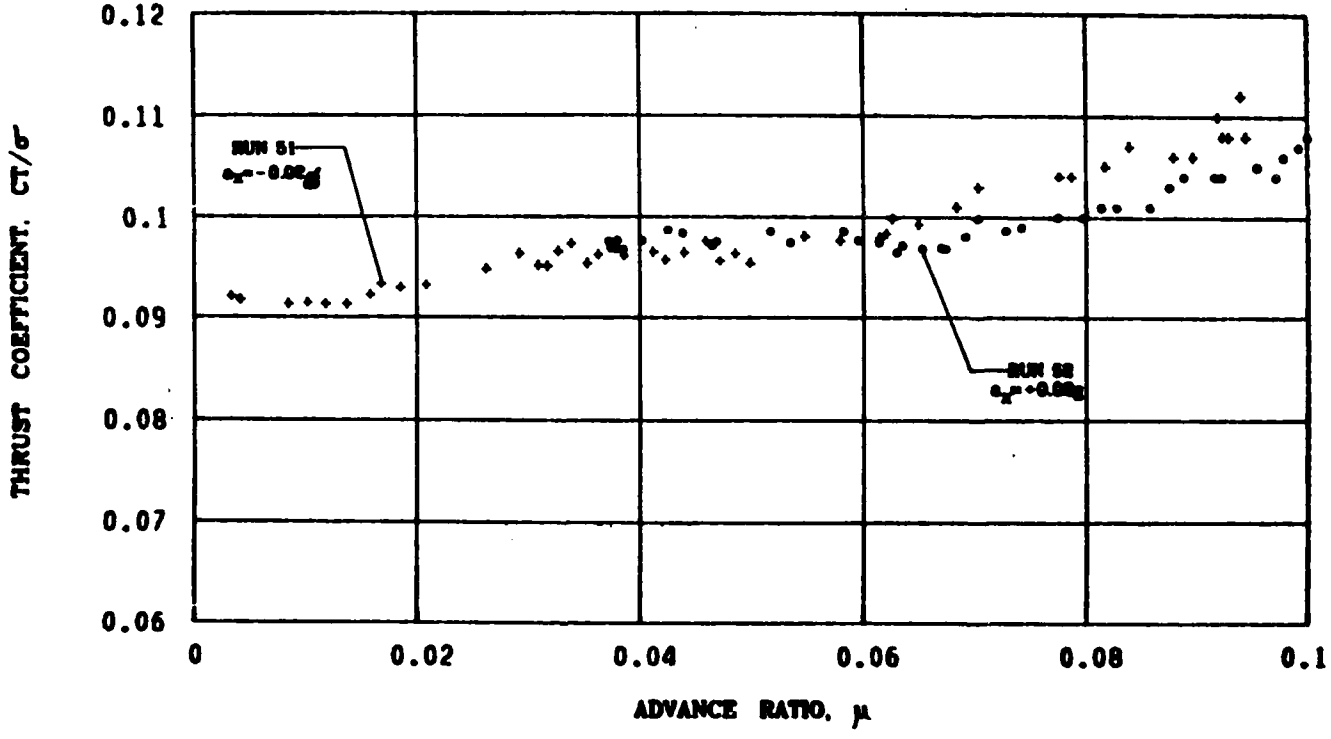

Figure A-9. Continued.

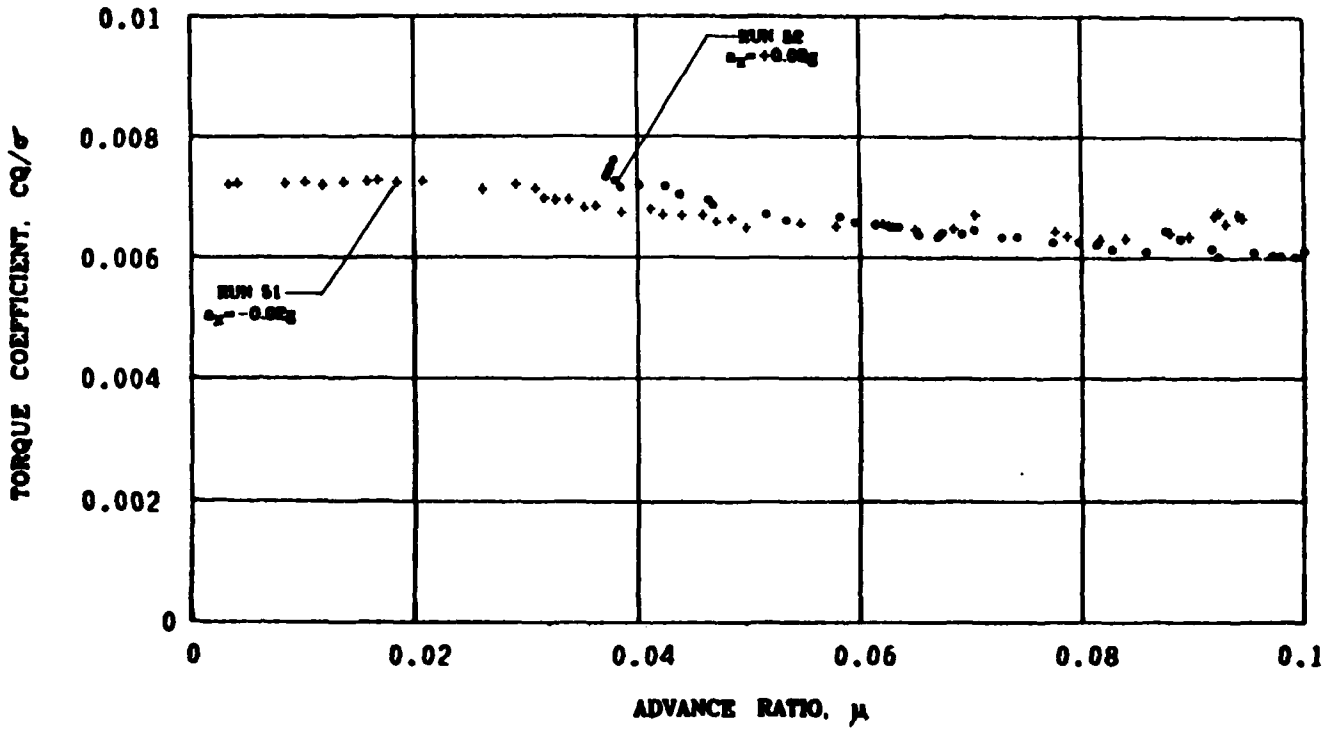

Figure A-9. Continued.

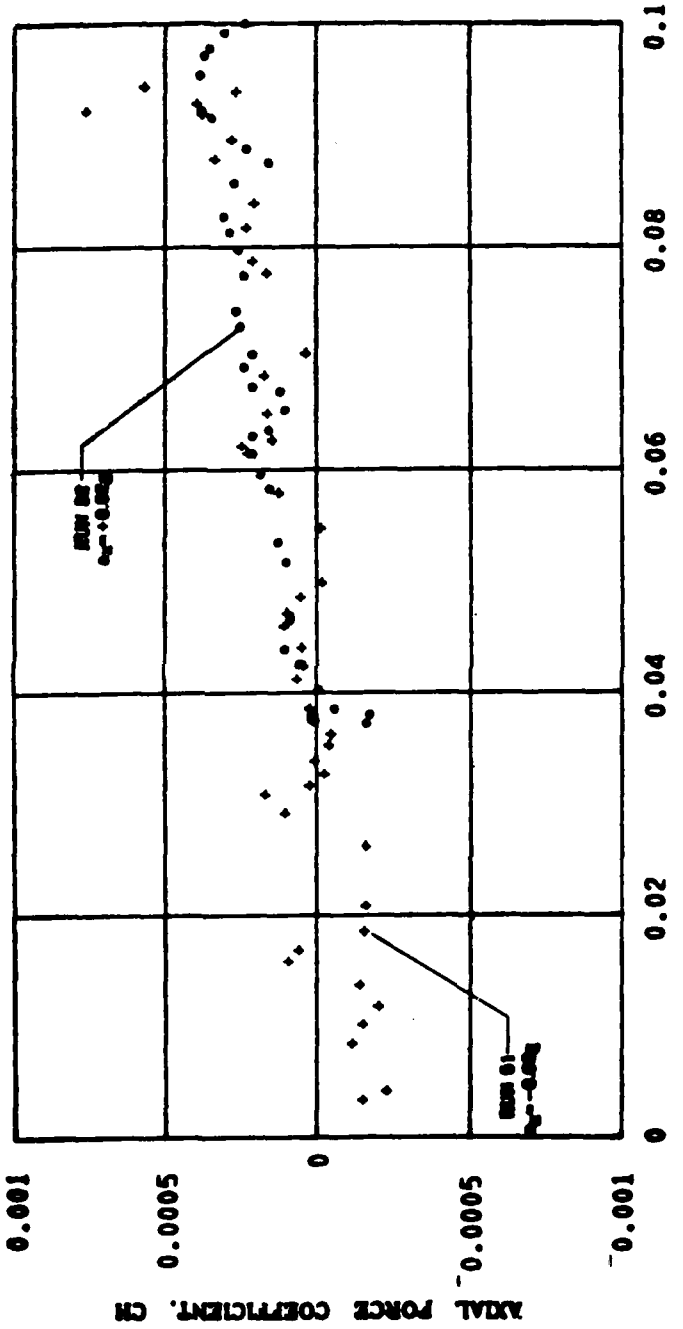

Figure A-9. Continued.

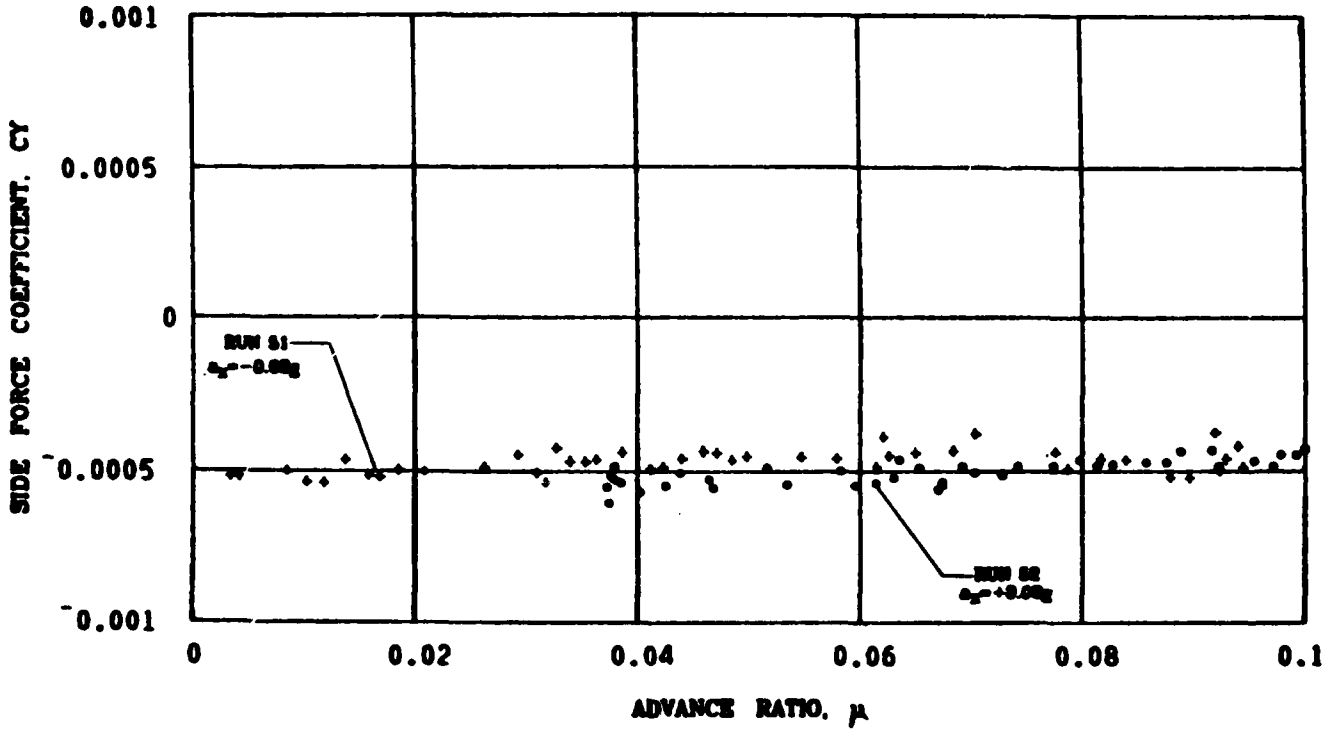

Figure A-9. Continued.

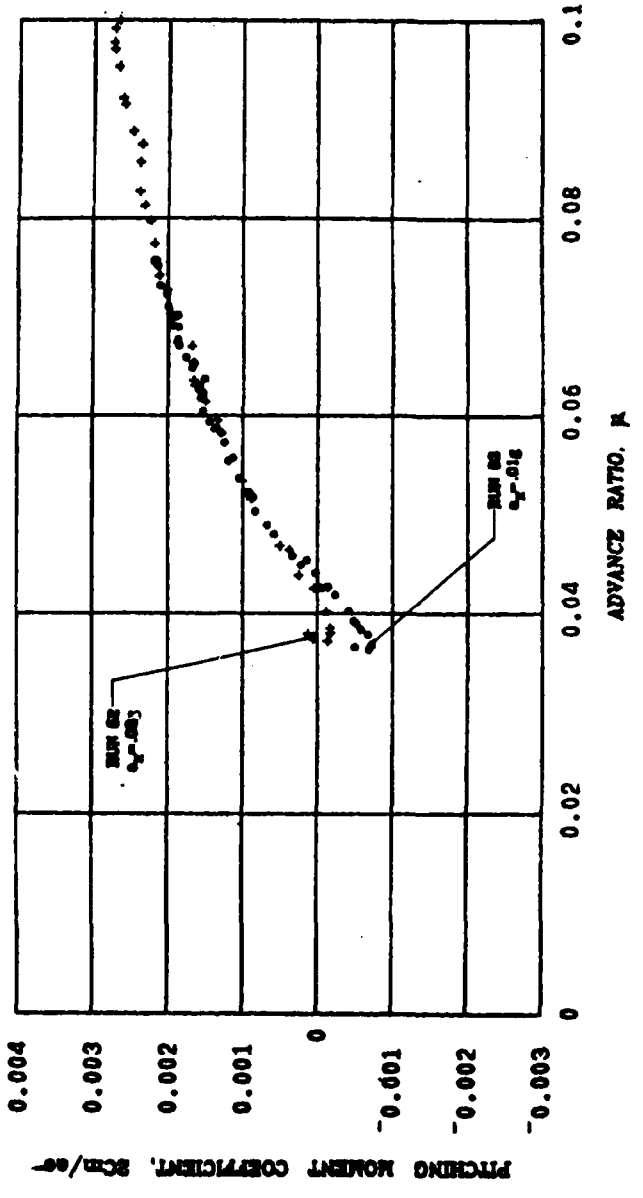

Figure A-10. Comparison of Rotor Force and Moment Variations with Advance Ratio and Translational Acceleration, $\theta_c = 9.8^o$, $\bar{h} = 0.45$, $a_x = 0.01g$, $0.02g$.

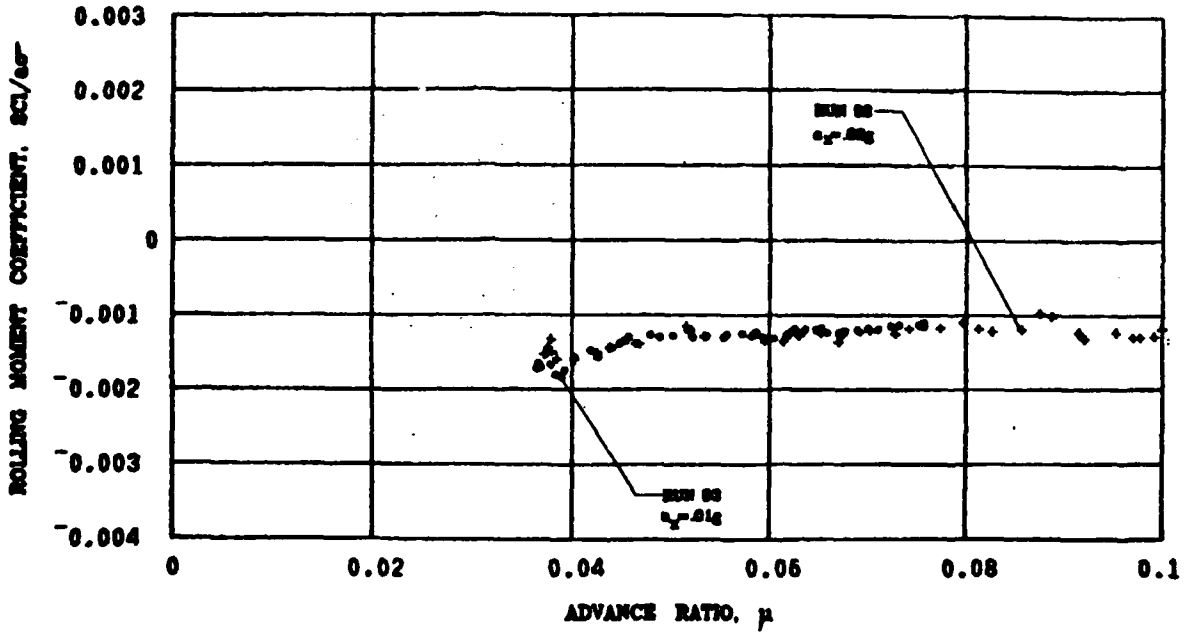

Figure A-10. Continued.

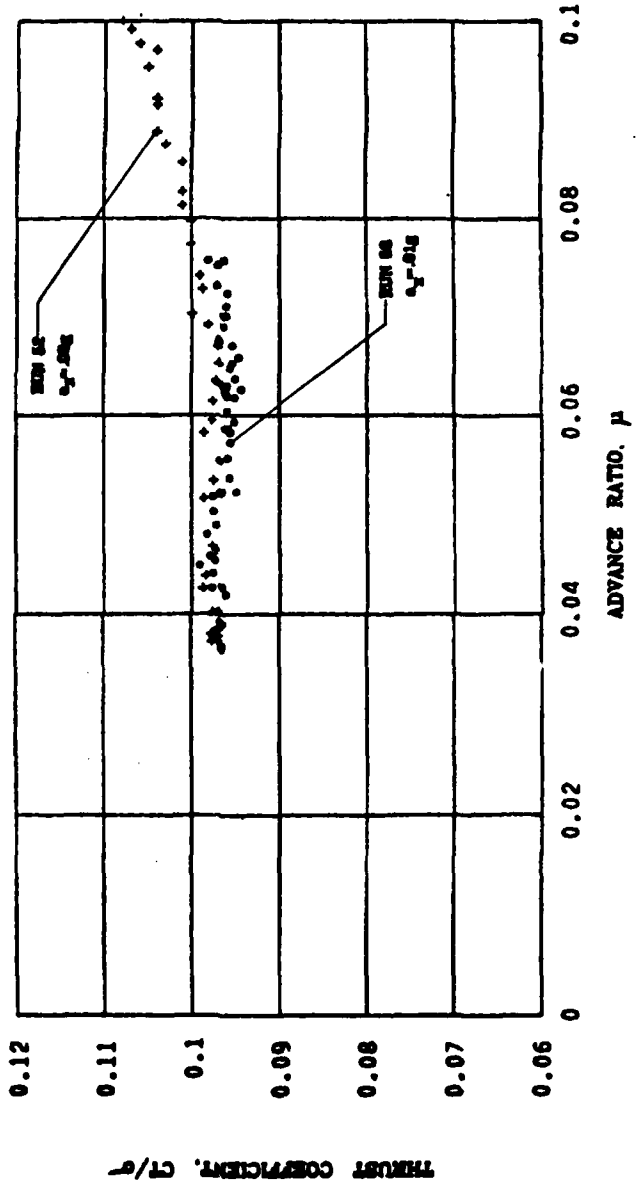

Figure A-10. Continued.

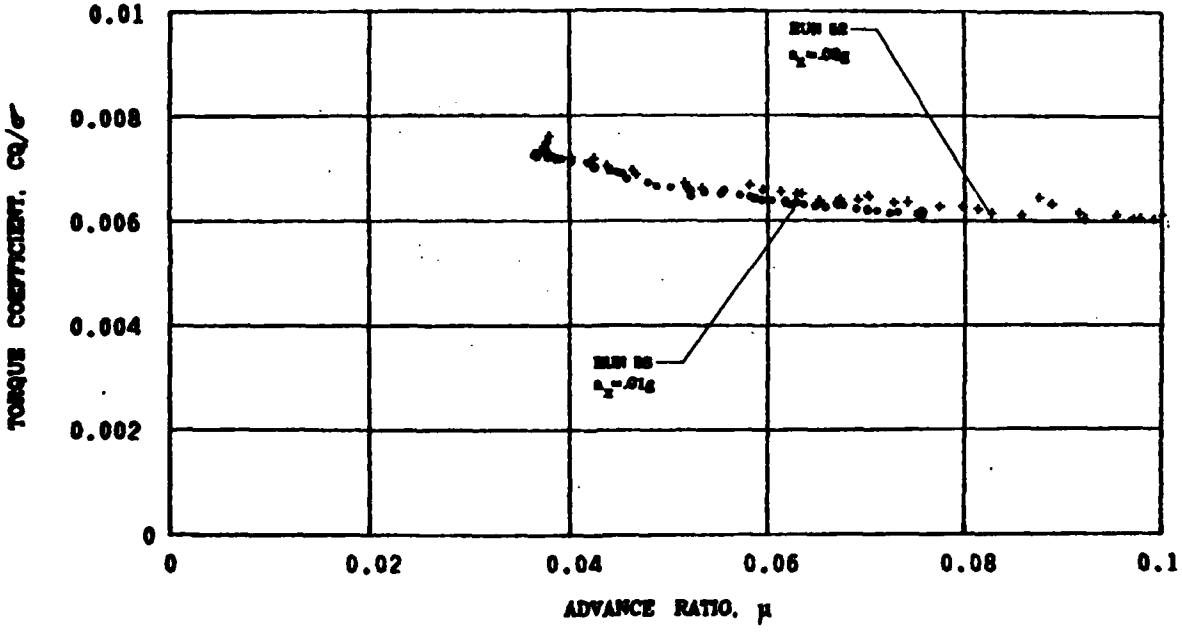

Figure A-10. Continued.

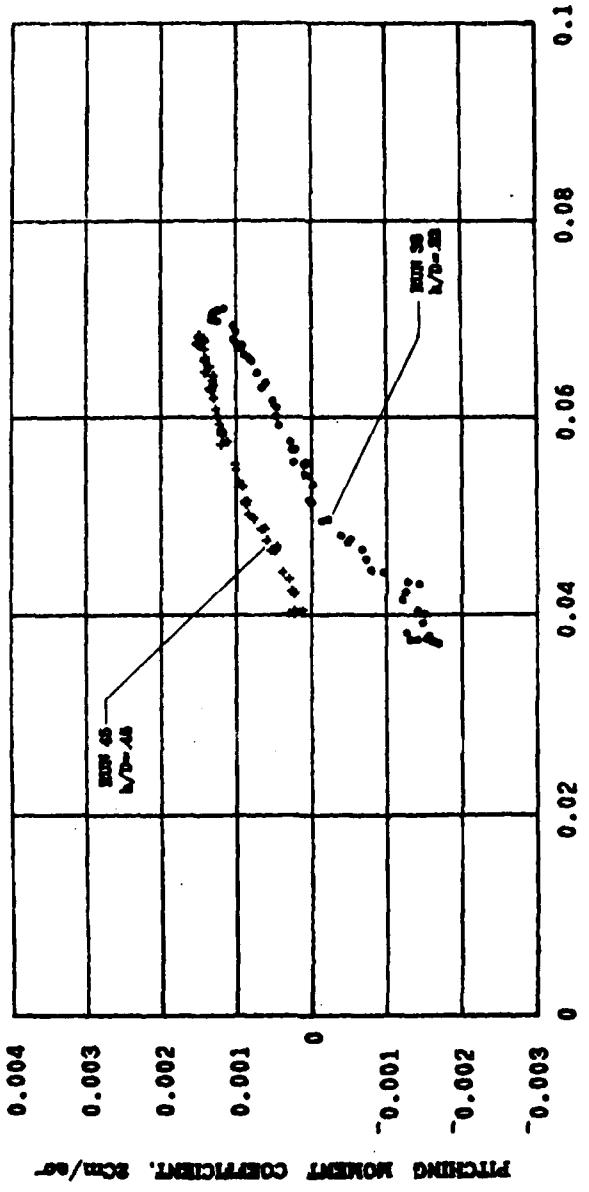

Figure A-11. Variation in Rotor Force and Moment Coefficients with Advance Ratio and Height-to-Diameter Ratio, $\theta_c = 8.4^0$, $a_x = 0.01g$.

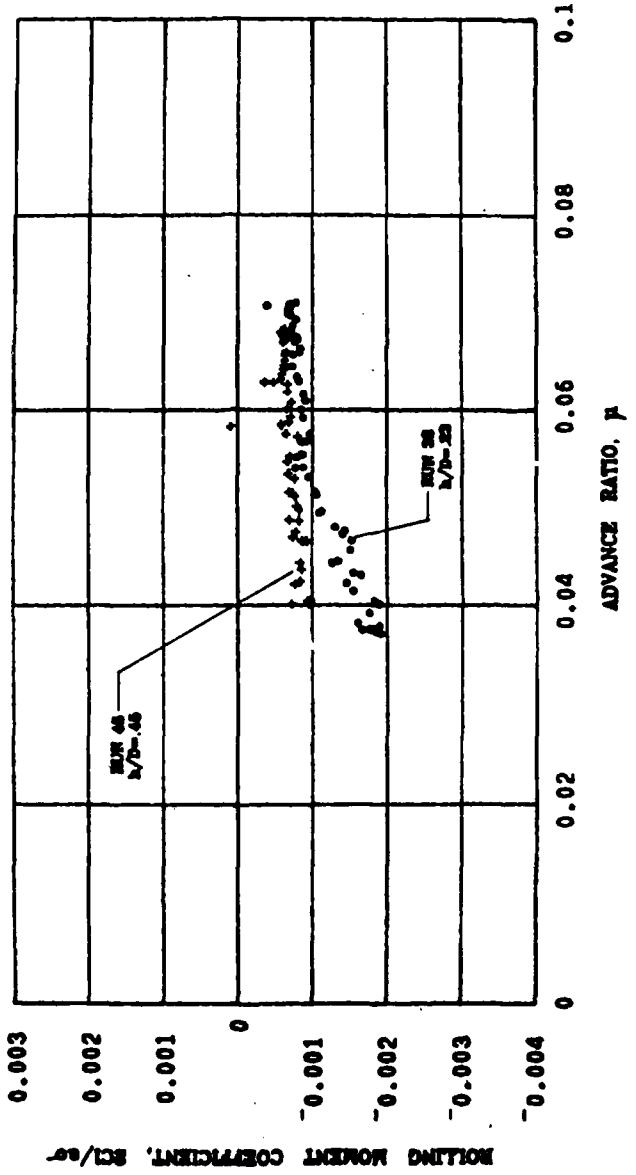

Figure A-11. Continued.

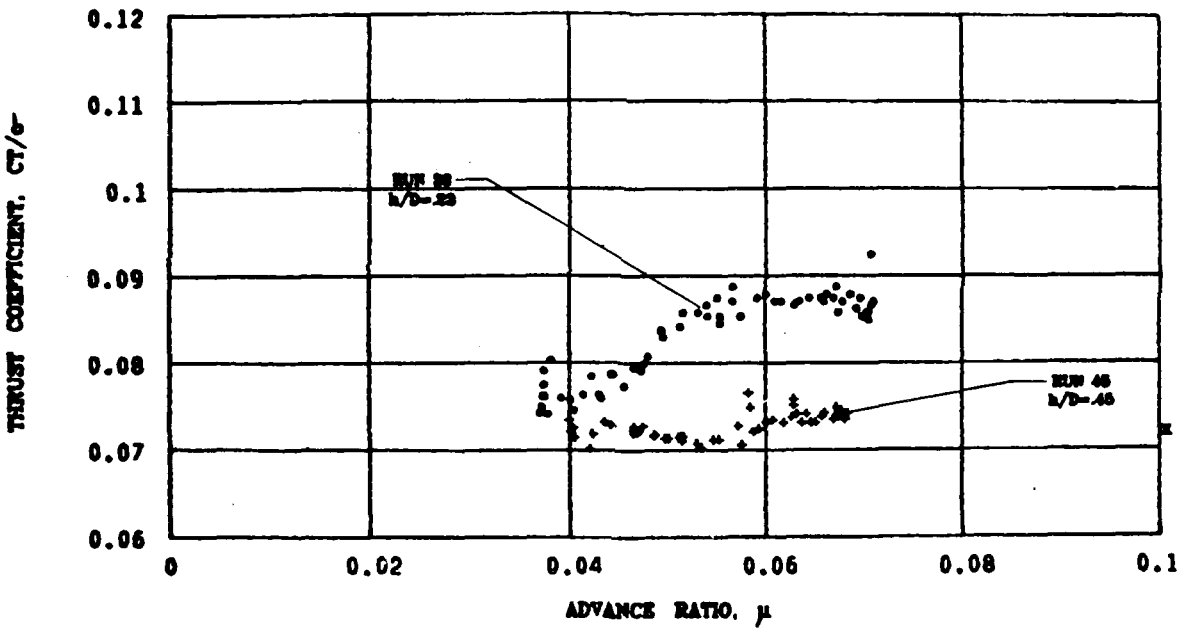

Figure A-11. Continued.

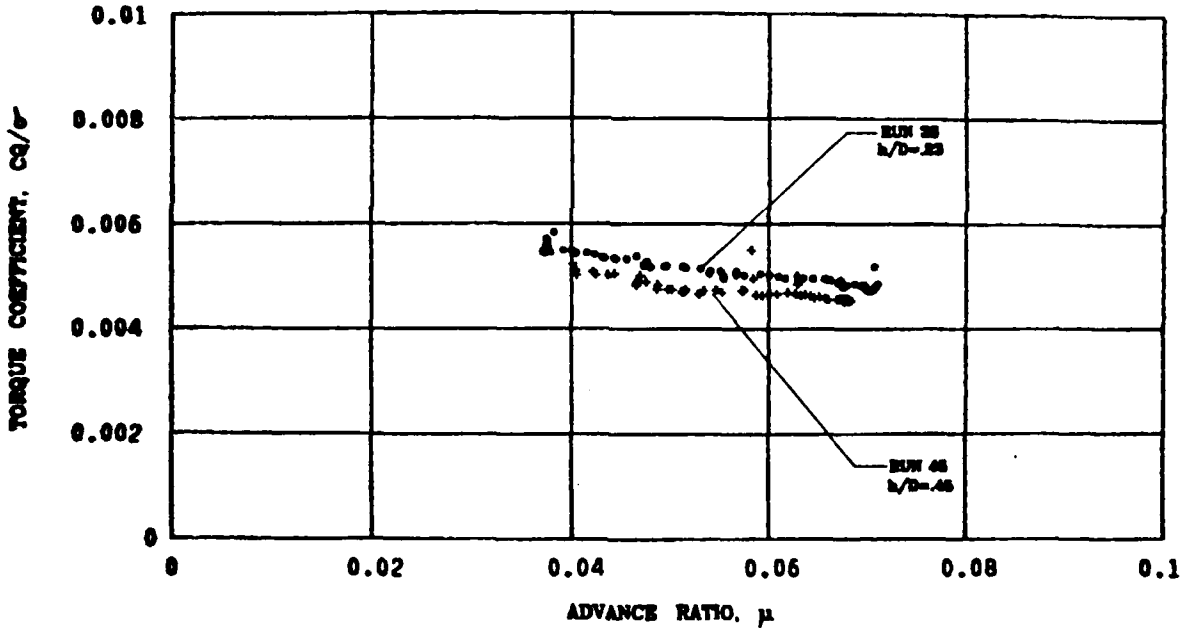

Figure A-11. Continued.

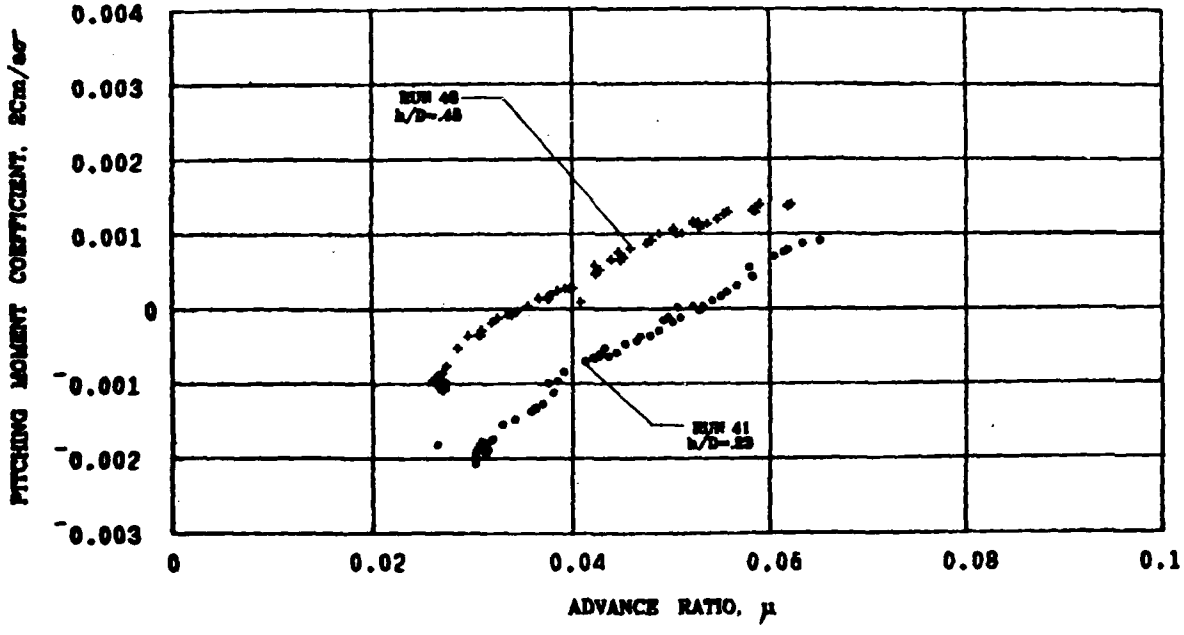

Figure A-12. Variation in Rotor Force and Moment Coefficients with Advance Ratio and Height-to-Diameter Ratio, $\theta_c = 9.8^0$, $a_x = -0.01g$.

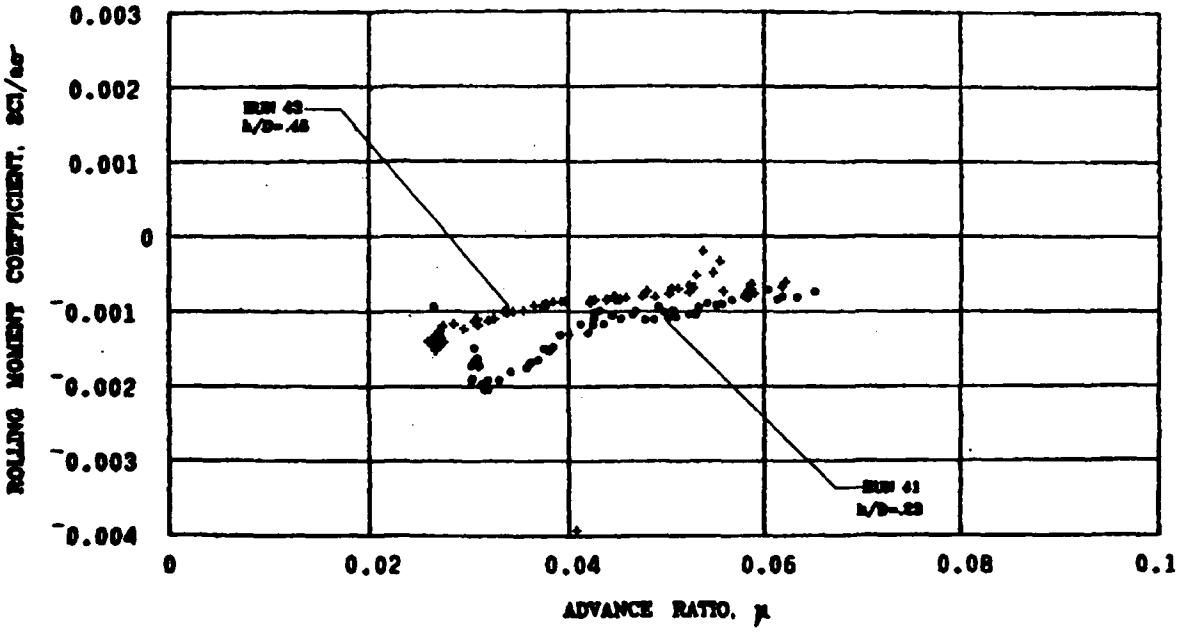

Figure A-12. Continued.

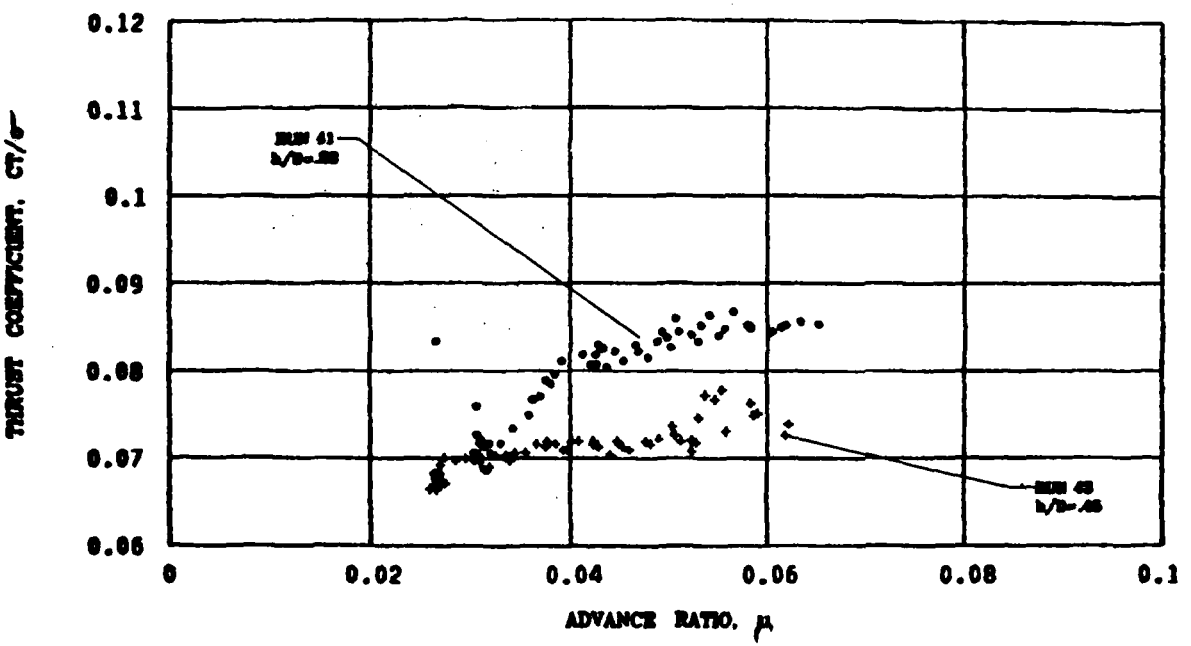

Figure A-12. Continued.

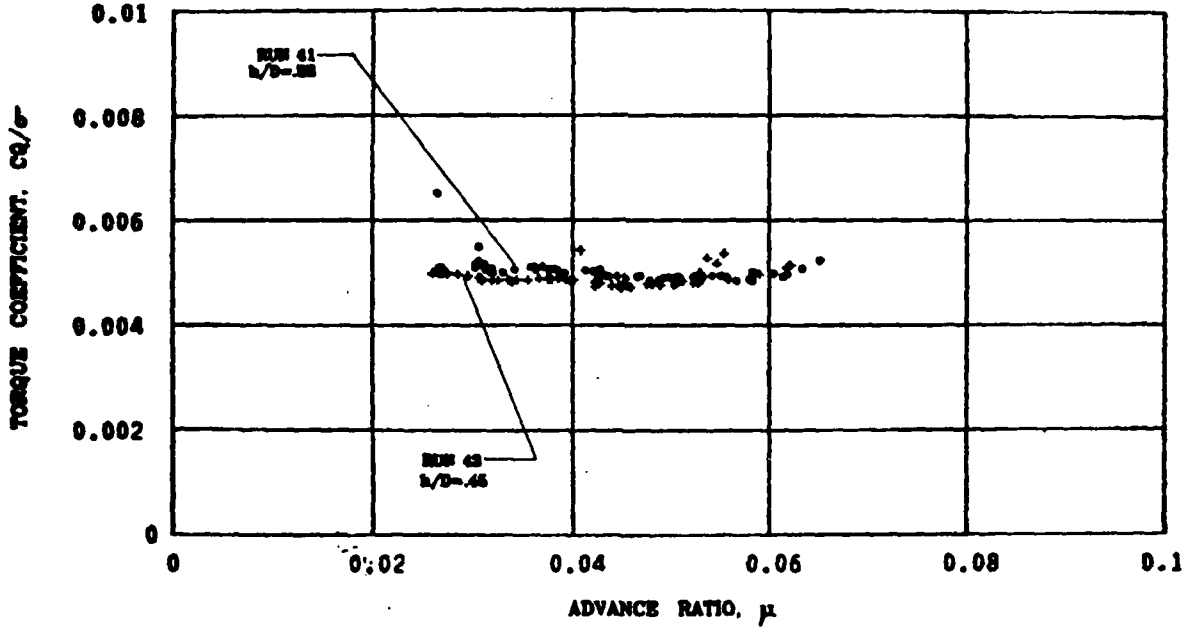

Figure A-12. Continued.

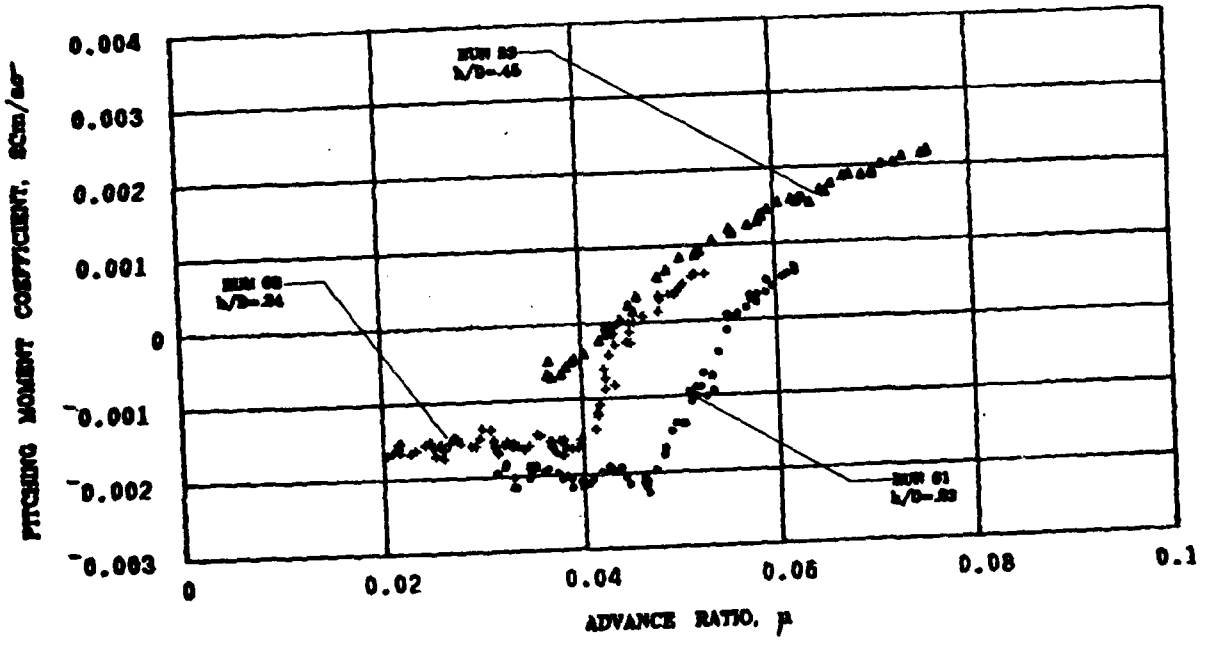

Figure A-13. Variation in Rotor Force and Moment Coefficients with Advance Ratio and Height-to-Diameter Ratio, $\theta_c = 9.8^o$, $a_x = 0.01g$.

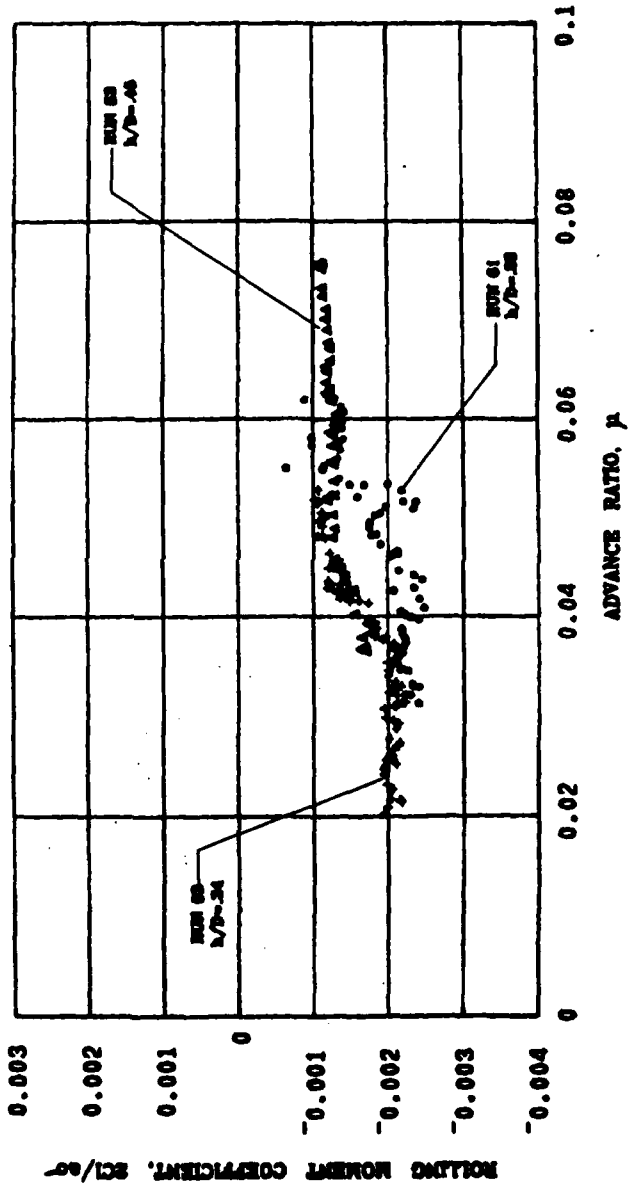

Figure A-13. Continued.

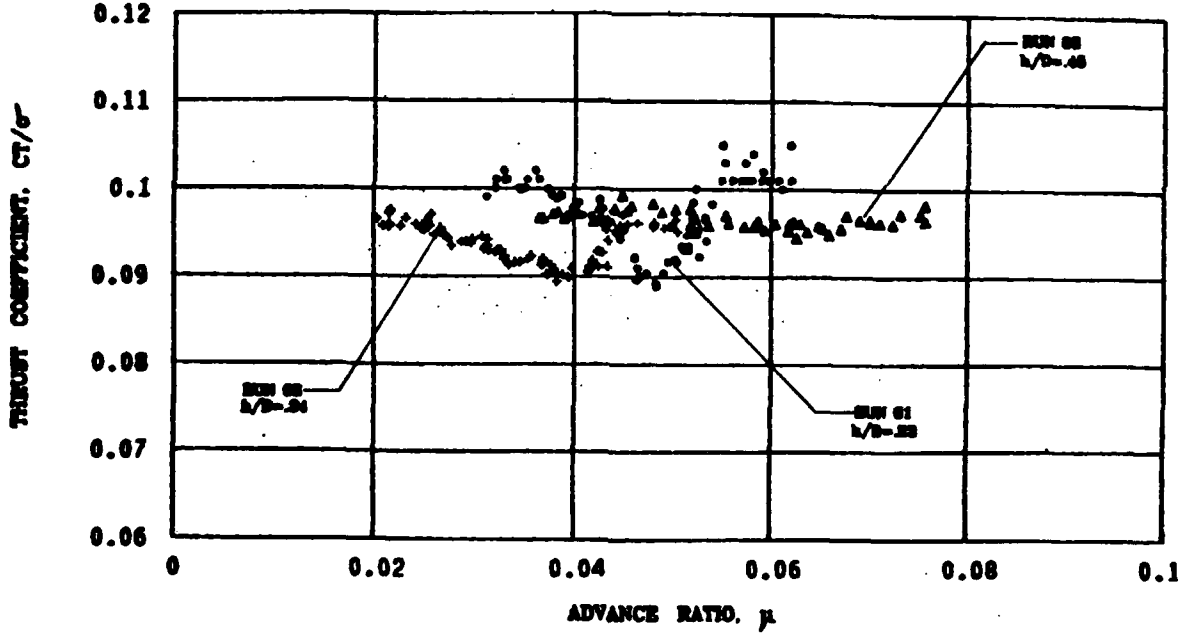

Figure A-13. Continued.

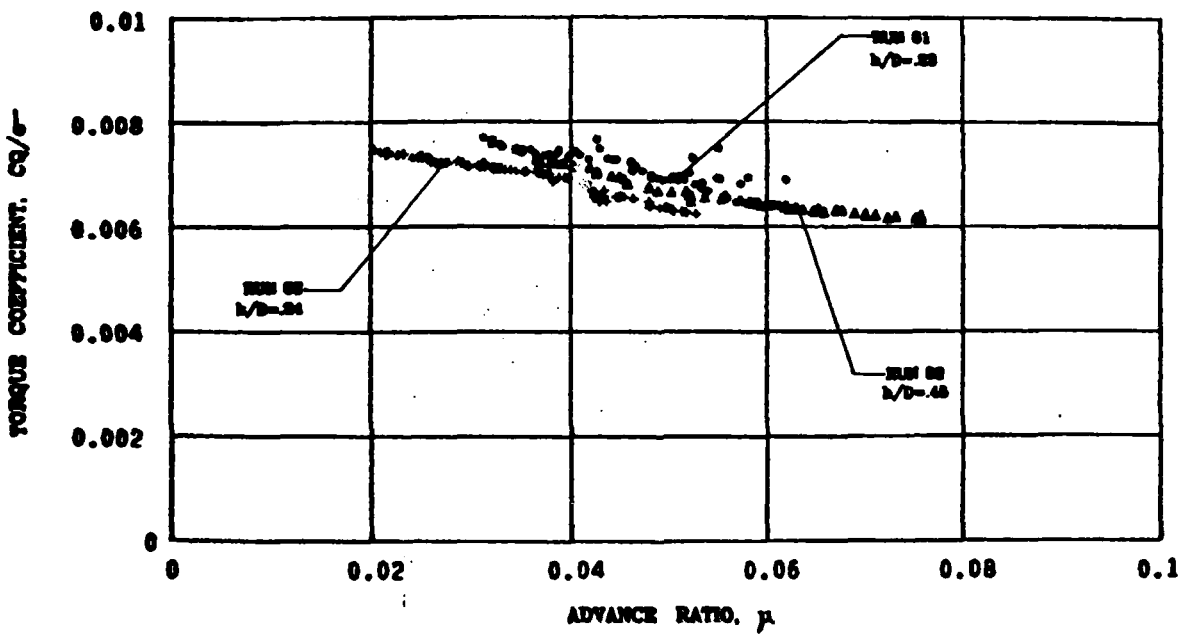

Figure A-13. Continued.

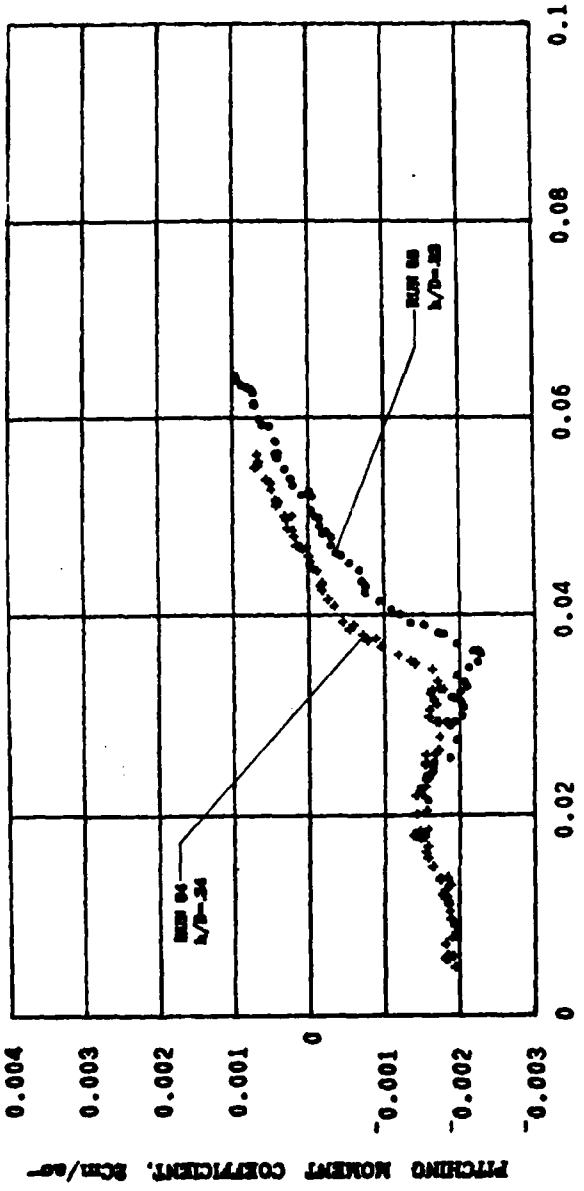

Figure A-14. Variation in Rotor Force and Moment Coefficient with Advance Ratio and Height-to-Diameter Ratio, $\theta_c = 9.8^{o}$, $a_x = -0.01g$.

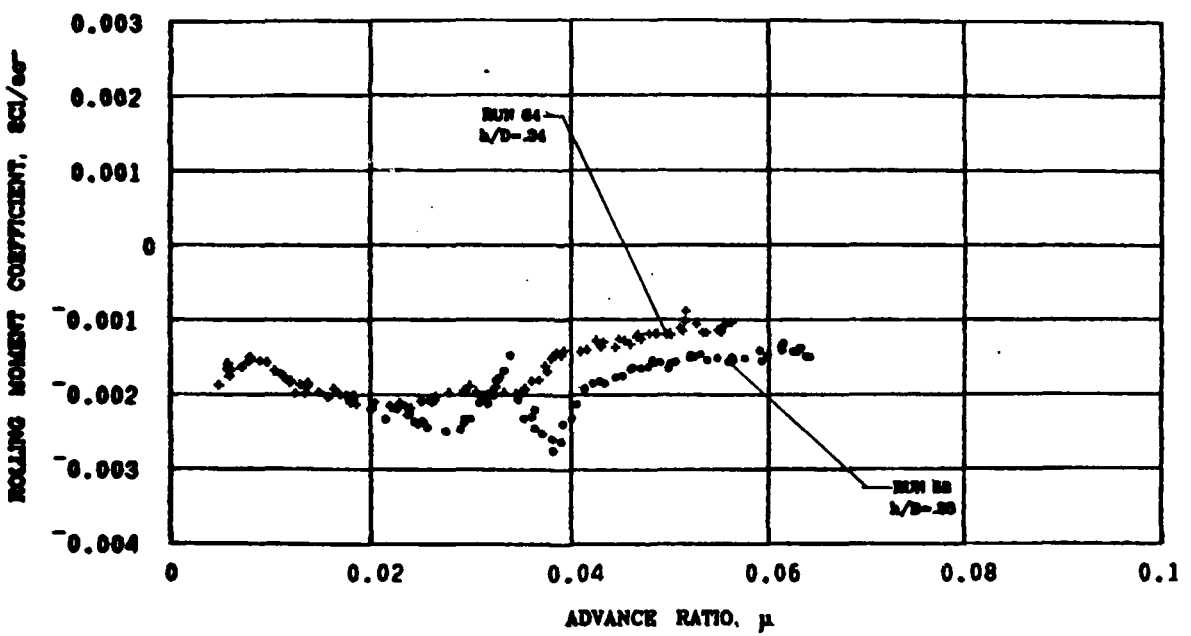

Figure A-14. Continued.

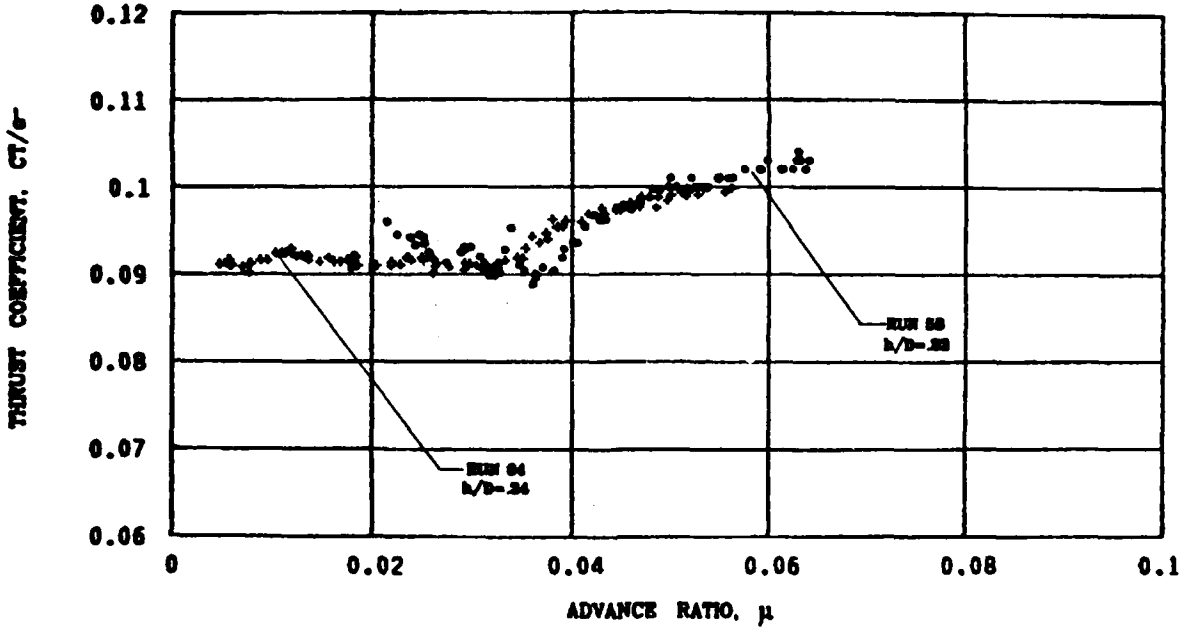

Figure A-14. Continued.

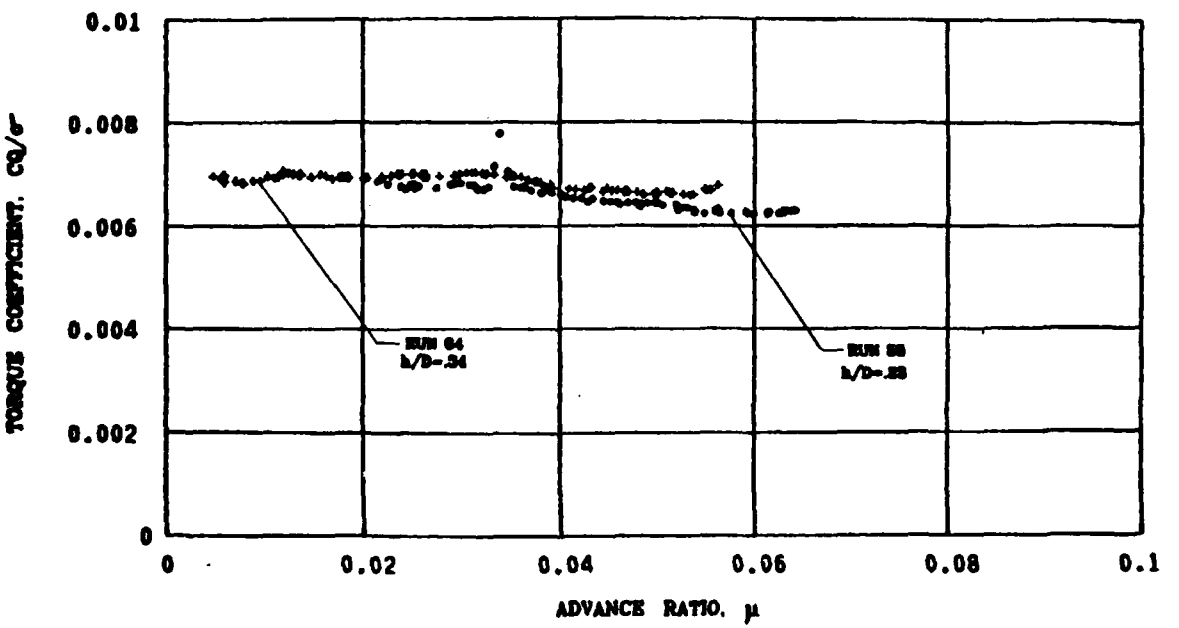

Figure A-14. Continued.


DATE
FILME
8